# Tracing Carbon Through Lotic Food Webs Using Amino Acid Stable Isotope Analysis

By



Emily R. Arsenault
B.A., Colby College, 2014
M.A., University of Kansas, 2017

Submitted to the graduate degree program in Ecology and Evolutionary Biology and the Graduate Faculty of the University of Kansas in partial fulfillment of the requirements for the degree of Doctor of Philosophy.

---

Chair: James H. Thorp

---

Amy J. Burgin

---

Benjamin A. Sikes

---

W. Leo Smith

---

Marina B. Suarez

Date Defended: 25 June 2021

The dissertation committee for Emily R. Arsenault certifies that this is the approved version of the following dissertation:

# Tracing Carbon Through Lotic Food Webs Using Amino Acid Stable Isotope Analysis

Chair: James H. Thorp

Date Approved: 25 June 2021

## Abstract

Understanding the flow of carbon in ecosystems is important for the conservation and management of diverse organisms and environments. In lotic systems, quantifying the trophic basis of production on which entire food webs rely is a primary research goal because flowing waters are characterized by complex and often cryptic energy pathways. Carbon compound-specific stable isotope analysis of individual amino acids (CSIA-AA) is an emerging tool that allows researchers to obtain more accurate and detailed estimates of basal resource assimilation by consumers. In this dissertation, I first contributed a review of best practices for carbon CSIA-AA to be used by new and current users of the method to lower the barrier of entry into its use and encourage further collaboration. As part of this review, I analyzed a wide variety of potential food resources for freshwater systems. I found that carbon amino acid isotope values ($\delta^{13}C_{AA}$) of broad taxonomic groups of terrestrial plants and aquatic algae were conserved across broad spatiotemporal scales, suggesting that these data can be used by others conducting CSIA-AA studies in similar environments. Second, I conducted a laboratory experiment to investigate whether fungal $\delta^{13}C_{AA}$ differed based on the amino acid contents of their media substrates and found evidence for direct uptake of certain essential amino acids by fungi. This finding has implications for the way that researchers incorporate and interpret the role of fungi as a pathway for allochthonous carbon into food webs. Third, I carried out a cross-continental assessment of basal resources supporting fish consumers in streams located in three ecoregions of the understudied temperate steppe biome using CSIA-AA. I found that autochthonous resources provided consistent support for fish production across a wide variety of low-order stream sites, independent of riparian canopy coverage and across a range of hydrogeomorphic conditions, which contributes to our understanding of stream headwaters at the global scale.

**Acknowledgments**

Many mentors, family members, and friends have supported me as I pursued this degree. I would like to thank my Ph.D. adviser, Dr. Jim Thorp for investing in me over the six total years I spent in his lab since starting at the University of Kansas as a masters student. I appreciate the freedom that you granted me to develop my own research ideas and for the funding that you acquired to support me as a graduate student. I am grateful for the friendships I have formed with past and present graduate students, postdocs, and technicians of the Thorp Lab, especially Mica Rumbach, Mike Thai, Dr. Rachel Bowes, Nic Kotlinski, Dr. Caleb Robbins, Jake Lutchen, and Greg Mathews. I would also like to thank the undergraduate students who I have worked with over the years: Tracy Funk, Rianon Wallace-Demby, Nikki Pelkey, Katelyn Milbrandt, and Tamara Tyner. Working with you all has been a highlight of my graduate career.

I would like to thank my fantastic Ph.D. committee for the time and advice they have offered over the years. Dr. Ben Sikes, you have been on my team since 2015 when I had my first RAC meeting for my masters degree. Thank you so much for your consistent support, expert knowledge in SEM and statistics, and for your leadership on my committee. Dr. Amy Burgin, your mentorship has been a huge benefit to me over my time as a graduate student. You welcomed me as a guest into your lab, which has provided a great place for me to build community and think through the perspective of ecosystem ecology. Dr. Leo Smith, you have gone out of your way to be a supportive committee member during high-stress times, and I really appreciated that. Our chats after Ichthyology are some of my fondest memories in KU EEB. And Dr. Marina Suarez: thank you so much for joining my committee in the last year of my Ph.D. I appreciate your willingness to step in and provide support during my final stretch.

I would like to acknowledge my coauthors to versions of Chapter 1 (J. H. Thorp, M. J. Polito, C. J. Robbins, J. H. Liew, W. K. Dodds, F. Tromboni, and H. Bennadji), Chapter 2 (J. H. Liew and J. R. Hopkins), and Chapter 3 (J. H. Thorp, M. J. Polito, A. Maasri, W. K. Dodds, M. Pyron, B. Mendsaihan, M. Minder, A. Otgonganbat, S. Altangerel, F. Tromboni, H. Bennadji, and S. Chandra) that have been submitted to scientific journals for publication. I would also like to acknowledge others who have assisted with field or lab work or provided data or code, including R. C. Shields, C. C. Artz, G. S. Mathews, M. Thai, R. E. Bowes, J. Robbins, B. Boldgiv, J. J. Costello, B. Erdenee, A. Schechner, N. Kotlinski, J. Knock, and M. Hernandez. Special thanks to Jia Huan Liew for being a fantastic mentor to me in manuscript preparation. I would also like to acknowledge the sources of funding that have supported this work: National Science Foundation MacroSystems Biology #1442595, Val H. and Marilyn S. Smith Research Award, Association for Women Geoscientists, Kansas Biological Survey, KU Ecology and Evolutionary Biology, and the KU College of Liberal Arts and Sciences.

I am grateful for the collaborations I have gained from being a part of the NSF MACRO team. Working with all of you has been such an important part of my personal and professional development. I know that my experiences with MACRO will continue to impact me for the rest of my career, whether directly from continued collaboration or through teamwork and research skills that I have learned from you over the years. Special thanks to Anne Schechner, Dr. Mario Minder, Dr. Mark Pyron, Boloroo Erdenee, Amka Otgonganbat, Soko Altangerel, Dr. Robert Shields, Caleb Artz, and John Costello for becoming some of my closest friends over our many years and field seasons together. I would also like to thank Dr. Alain Maasri and Dr. Flavia Tromboni, who have been amazing leaders on the MACRO team.

I would also like to thank a few mentors who supported me in science even before I began as a graduate student at KU. Very special thanks to Dr. Sharon Douglas and Dr. Robert Marra at the Connecticut Agricultural Experiment Station for giving me my first opportunity in science and for supporting my every career step after that. I am also so grateful for my undergraduate mentors at Colby College, including Dr. Russ Cole, Dr. Cathy Bevier, and Dr. Denise Bruesewitz. Working with you on the Belgrade Lakes was my introduction to aquatic ecology. In addition to past mentors, I am so grateful for the mentorship of my new postdoctoral adviser, Dr. Holly Ewing, who helped me to prepare for my dissertation defense presentation. I could not be more excited to learn from you in my new role.

Finally, I would like to thank my family and friends for their endless support. Mom, this accomplishment of mine is an accomplishment of yours, too. From figuring out the college application process, to making the last grammatical edits on the final version of my dissertation, we did it all together! Eric, even though you are younger than me, you are a wiser Ph.D. student; thank you for sharing your advice. And Luke, MSW, I am so excited that we got to share our graduations together this spring. I would like to thank Grandma, Charlie, Grandpa, Dad, Sarah, Ben, and my other family members for all of your tremendous support. And of course, my Lawrence family, Dr. Kaila Colyott, Riley Ross, Dr. Alex Erwin, Kaylee Herzog, Dr. Stephen Baca, and so many other graduate students in EEB, thank you for everything! Special thanks to Kaila, who has been paving the way for me to succeed as a researcher, teacher, and person since the day we met. Last but not least, thank you to my fiancé Dave. This dissertation very truly could not have been finished without your love and support. Thank you for being a constant cheerleader for me, for doing way more than your fair share of the chores throughout this crazy time, and for making sure that I still got outside every now and then.

## Table of Contents

## List of Figures

## List of Tables

## Introduction

Food webs integrate biotic and abiotic components of ecosystems, which makes them useful for elucidating ecosystem-level processes like nutrient cycling and energy flow (Peterson and Fry 1987). A central research theme in lotic ecology concerns whether autochthonous carbon, produced in-stream, or allochthonous carbon, originating from an external (terrestrial) environment, is more important for supporting the food web base. Over the last several decades, researchers have put forth a series of conceptual models to serve as theoretical foundations that describe broad patterns and processes generalizable to all river networks. A major goal for these models and others has been to predict the trophic basis of production for metazoan communities located at different points along a river network (e.g., the river continuum concept, Vannote et al. 1980; the flood pulse concept, Junk et al. 1989; the riverine productivity model, Thorp and Delong 1994, 2002; and the riverine ecosystem synthesis, Thorp et al. 2006, 2008).

However, despite theoretical developments and a large literature of empirical studies and meta-analyses, there is still disagreement about which models best describe carbon sources or trophic structure in river food webs. One major reason for these discrepancies is that studies addressing food web ecology may be impacted by certain shortcomings in the methods used to identify food sources or trophic position (e.g., gut contents and bulk-tissue stable isotope analysis). However, new developments in the stable isotope analysis of specific compounds (i.e., lipids and proteins) have improved the accuracy and reliability of our food source estimations, providing researchers with the tools necessary to better address these fundamental questions in lotic ecology. Compound-specific stable isotope analysis of individual amino acids (CSIA-AA) provides accurate and reliable estimates of basal resource use and trophic position, even for small consumer sample sizes (Liew et al. 2019) and across large spatiotemporal scales (Gómez et al. 2018; Chapter 1).

Another possible reason why models of river food webs have not found generalizable meaning is that certain types of rivers (e.g., terminal basin rivers or grassland rivers) have generally been understudied relative to others (e.g., temperate rivers in forested watersheds). Here, I contribute a global-scale study of the basal carbon sources of temperate steppe headwater stream food webs of North America (United States) and Asia (Mongolia), with focus at the local, valley (functional process zone; FPZ; Thorp et al. 2006, 2008), and ecoregion scales. The overarching research goal for my dissertation is to characterize the trophic base of production for fish food webs of temperate steppe streams.

In the first chapter of my dissertation, I present a critical examination of the use of carbon CSIA-AA for its ability to trace basal resources through ecosystems at large spatiotemporal scales. Past studies have confirmed the usefulness of CSIA-AA in ecological studies of marine and freshwater systems, but there is not yet a clear consensus about best practices for this new technique, which can lead to misconceptions by new users or lack of comparability among studies. In Chapter 1, I present a guide for the use of carbon CSIA-AA to help synthesize common practices in the methodology. I evaluated practices from previously published studies, from sample collection to data analysis, while also providing recommendations to address some of the assumptions and limitations associated with the method. I also analyzed an original food source dataset characterizing isotope signatures of common basal resources to consumers in freshwater ecosystems. Analyses of this contributed dataset suggested that the carbon amino acid isotope profiles of essential amino acids were conserved within resource groups despite differences in sample senescence and geographic location of collection, suggesting that the food source data I present may also be used by other researchers studying similar ecological systems.

In the second chapter of my dissertation, I address a lingering methodological constraint to the interpretation of CSIA-AA data for lotic ecosystems, where heterotrophic microorganisms may

contribute to the consumer resource pool. In previous studies, fungi cultured in amino acid-free media have been used as proxies to represent the fungal resource signature in studies of natural environments. However, in natural systems fungi may gain energetic benefits by taking up substrate amino acids directly rather than synthesizing them *de novo* (Bianchi et al. 2019). This means that $\delta^{13}C_{AA}$ profiles of fungi can be either fungal or autotrophic in origin, based on differential fractionation occurring in *de novo* biosynthesis versus direct amino acid uptake, respectively. I found that fungi did take up some essential amino acids directly from their substrates in the laboratory when amino acids were provided in relatively higher absolute amounts. This suggests that fungi are likely to reflect the $\delta^{13}C_{AA}$ profiles of ultimate carbon sources *in situ*, especially during early colonization of detrital matter. This is an important finding for studies that aim to quantify allochthony in natural ecosystems, but further study is needed to characterize $\delta^{13}C_{AA}$ profiles of fungi on natural (non-media) substrates.

In the third chapter of my dissertation, I used lessons and outcomes from Chapter 1 and Chapter 2 to quantify the trophic basis of production for fish consumers across 50 low-order temperate steppe stream sites spanning two continents. As a secondary goal, I also assessed potential local-scale and valley-scale influences on the trophic basis of production at these sites (Chapter 3). Results provide strong evidence for the consistent support of autochthonous algal resources for fish food webs in low-order streams of two globally significant stretches of the temperate steppe biome. This finding held true across study sites, despite site variability in local-scale canopy cover and valley-scale hydrogeomorphology. The results of this study contribute additional support for recent studies that have begun to reveal the importance of algae for fueling food webs in a variety of freshwater systems (McNeely et al. 2007, Hayden et al. 2016, Thorp and Bowes 2017, Liew et al. 2019).

# Chapter 1: Best Practices for Analyzing Consumer Resource Use with Carbon Stable Isotope Analysis of Amino Acids


## Abstract

Use of compound-specific stable isotope analysis of amino acids (CSIA-AA) is expanding in food web studies. In particular, carbon stable isotope values ($\delta^{13}C$) of individual amino acids provide the ability to estimate resource assimilation by metazoan consumers living in systems where resource contributions are complex or cryptic, such as in aquatic or subterranean food webs. Past studies have confirmed the value of carbon CSIA-AA, but a clear consensus about best practices is lacking. Here, we present a guide for both new and current users of carbon CSIA-AA to help standardize common practices in methodology, from sample collection to data interpretation, while also providing recommendations to address the assumptions and limitations associated with this method. We also analyze an original CSIA-AA ($\delta^{13}C_{AA}$) dataset ($n$=42) comprising common basal resources to consumers of freshwater ecosystems, finding that $\delta^{13}C_{AA}$ values of essential amino acids are conserved within source groups despite differences in sample senescence and geographic location. This demonstrates that the diagnostic ability of carbon CSIA-AA for distinguishing resource samples is robust to spatial confounding. Understanding the flow of carbon in ecosystems is important for the conservation and management of diverse systems and organisms, and carbon CSIA-AA provides an important tool for quantifying these pathways over large spatiotemporal scales. We recommend more detailed reporting of methodology and continued data sharing to improve successful use of carbon CSIA-AA as a tool in ecological studies and other applications.

## Introduction

Food web ecologists have gained important insights into energy flow and ecosystem function from widespread analyses of stable isotope signatures of primary producers and their metazoan consumers over the last few decades. Approaches using isotopic tools have been built upon the concept that "you are what you eat (plus a few per mil)" (Deniro and Epstein 1976). That is, the predictable fractionation of some stable isotope values, bulk tissue carbon ($\delta^{13}C$) and nitrogen ($\delta^{15}N$) in particular, makes it possible to trace food source assimilation from the isotopic signature of consumers. While bulk tissue stable isotope analysis (BSIA) is an accessible and versatile tool, many complex food web pathways cannot be completely resolved with BSIA alone due to the common problems of high spatial and temporal variability in isotope signatures of source samples (Tieszen et al. 1983, Finlay et al. 1999), substantial overlap in signatures of separate food sources, and their inability to represent the isotopic composition as assimilated by organisms (Dodds et al. 2014).

Some of these complexities can be directly addressed by measuring the stable isotope values of individual compounds, a method commonly referred to as compound-specific stable isotope analysis (CSIA). While individual compounds have been examined using stable isotope analysis as early as the 1960s (e.g., Abelson and Hoering 1961), CSIA has gained popularity in recent years with the development of gas chromatograph-combustion-isotope-ratio mass spectrometer (GC-C-IRMS) systems (Evershed et al. 2007). The advantage of CSIA is its ability to quantify the stable isotope value for each monomer in a compound (i.e., fatty acid building blocks of lipids or amino acid building blocks of proteins), while BSIA only provides an average signature of all biomolecular fractions. Thus, the ability to use $\delta^{13}C$ values measured using BSIA as a trophic biomarker may be obscured by the different $\delta^{13}C$ values characterizing various

macromolecular components (i.e., carbohydrate, lipid, and protein fractions; Elliott Smith et al. 2018). This difference gives CSIA the potential to provide more detailed information about energy flow, resource use, and trophic structure in food web studies (Whiteman et al. 2019). This newly gained specificity from CSIA approaches has contributed to advances in many disciplines, including archaeology, geology, food science, and ecology (Lichtfouse 2000, Twining et al. 2020).

Compound-specific stable isotope analysis of individual amino acids (CSIA-AA) has emerged as an effective strategy for estimating the relative importance of diverse food resources to consumer diets (e.g., CSIA-AA of carbon; $\delta^{13}C_{AA}$) and as a tool to more accurately quantify trophic position of consumers (e.g., CSIA-AA of nitrogen; $\delta^{15}N_{AA}$; Fantle et al. 1999, Fogel and Tuross 2003). CSIA-AA is useful across a wide range of applications and systems because protein (composed of amino acid monomers) accounts for a large fraction (~50%) of most consumer tissue (Whiteman et al. 2019). Each amino acid can have a unique isotopic signature because biosynthetic pathways and the number of fractionation steps for each amino acid are different (Ohkouchi et al. 2015, Takizawa et al. 2020). Methodological approaches for the analysis and interpretation of $\delta^{15}N_{AA}$ values have been studied and largely clarified (Ohkouchi et al. 2017, Takizawa et al. 2020). In comparison, methodological assessments and approaches for analysis and interpretation in the use of estimating food sources using $\delta^{13}C_{AA}$ values are lacking, despite the significant potential of this approach for refining the study of energy flow in food webs.

The biochemical underpinning for the use of $\delta^{13}C_{AA}$ values to estimate resource assimilation lies in the fact that amino acids fall into three categories based on whether or not metazoan consumers can synthesize their carbon backbones *de novo*. These categories are

essential amino acids (EAAs), nonessential amino acids (NEAAs), and conditionally essential amino acids (CEAAs). The biochemical properties of each group have important implications for how we trace carbon through food webs (Larsen et al. 2013). While most primary producers, bacteria, and fungi can synthesize all amino acids *de novo*, metazoan consumers typically synthesize only NEAAs, which means that they can only acquire EAAs from the food they eat. Additionally, the carbon skeletons of EAAs do not undergo significant modification as they move between trophic levels (Takizawa et al. 2020), which means that trophic discrimination factors for EAAs are negligible (i.e., the difference in stable isotope values between consumers and their diets). The biochemical characteristics of EAAs make them very effective tracers of basal (ultimate) dietary carbon sources in various ecosystems. This concept underlies the isotope "fingerprinting" approach (Larsen et al. 2009, McMahon et al. 2010, Larsen et al. 2013, Larsen et al. 2015, McMahon et al. 2016). In contrast, NEAAs typically show trophic discrimination ranging from -10 to 10 ‰, as a result of fractionation occurring in reactions associated with *de novo* synthesis or trophic discrimination (Takizawa et al. 2020). Metazoans have not completely lost the ability to synthesize CEAAs *de novo*, but they are more likely to obtain them through their diet than true NEAAs, especially when physiologically stressed (Morris et al. 2017).

Previous studies employing $\delta^{13}C_{AA}$ have demonstrated the ability of the method to convey reliable consumer resource assimilation estimates even with a low number of sample replicates (e.g., Elliott Smith et al. 2018, Liew et al. 2019). Aside from the financial benefit of reduced sample size requirements, this information can be especially important for researchers working with threatened species (e.g., Liew et al. 2019), rare archaeological samples (e.g., Jarman et al. 2017), or across large spatial scales. Additionally, $\delta^{13}C_{AA}$ values can help researchers to determine resource use of consumers with omnivorous or otherwise complex or

cryptic food source use such as freshwater fishes (Thorp and Bowes 2017, Bowes et al. 2020), migrating birds (Gómez et al. 2018), kelp forest consumers (Elliott Smith et al. 2018), and even subterranean populations of invertebrates (Saccò et al. 2019) and a cave fish (Liew et al. 2019).

Nevertheless, obtaining CSIA-AA data involves the following sequential combination of many complex decisions and analytical steps: sample collection and preservation, sample analysis and quality control, data processing and statistical analysis of mixing model outputs. Each step of this sequence could benefit from further clarification and standardization across studies because they can each introduce error that may confound data interpretation. While the resolution gained by the availability of a relatively large number of tracers greatly improves the accuracy of resource estimation, it also complicates the way researchers can properly analyze these data, leading to potential challenges in interpretability and comparability.

Our paper has two principal purposes. First, we analyze the potential limitations and assumptions of carbon CSIA-AA techniques and present a guide on best practices for new or current users of this novel tool. Second, we contribute a library of food source data for use in food web studies of freshwater ecosystems to build upon available literature values (e.g., Larsen et al. 2013, Thorp and Bowes 2017, Liew et al. 2019; Supplemental Table A-1). Together, this review and analysis: (1) identifies assumptions and biases in carbon CSIA-AA research; (2) synthesizes the current state of the literature on method development and best practices for carbon CSIA-AA studies; (3) presents original data from case studies that test critical assumptions of the effects of sample purity and environment on CSIA-AA data; and (4) offers suggestions for best practices, important caveats for limitations to interpretation, and recommendations for future studies needed to address methodological knowledge gaps.

## Sample Collection and Preservation

The first step in conducting a CSIA-AA study is to identify and collect consumer and source samples for analysis. While individual research questions drive selection of consumer samples, $\delta^{13}C_{AA}$ values from source samples may have the potential to be aggregated and shared across individual studies and ecosystems. Such aggregation is not always appropriate for BSIA studies. This data aggregation and sharing could provide an opportunity for researchers to save time and cost, while also fostering collaborative opportunities. Therefore, it is critical that researchers identifying and collecting source samples make informed and transparent decisions, and clearly document these decisions in their published results, when identifying and collecting source samples. Important decision-making steps in designing a library of source samples for subsequent analyses include: (i) identifying which source groups (i.e., $C_3$ plants, $C_4$ plants, algae, fungi, etc.) may be potential basal trophic components, (ii) deciding whether samples should be collected *in situ* (as either fresh or senesced material) or cultured in the lab, (iii) selecting the geographic location(s) and season(s) in which sampling should occur; and (iv) identifying an appropriate plan for sample preservation.

### *Identifying Basal Resource Groups*

Users of carbon CSIA-AA should determine the number and types of basal food source groups important in their system of study. For studies taking place in relatively constrained systems with low diversity of potential resources, such as in controlled feeding experiments, decisions about specific samples to collect and analyze can be straightforward. In contrast, in community-level studies characterized by sites spanning large spatiotemporal scales, determining the breadth of basal resources potentially important to target consumers may be more

challenging. In particular, resources representing some functional groups (e.g., heterotrophic microorganisms) are often left absent from resource libraries because of sampling difficulties. This may be problematic because the absence of potential basal resources like fungi and bacteria could affect interpretation of mixing model outputs, particularly in freshwater ecosystems where resources of terrestrial origin move to consumers via the microbial loop (Phillips et al. 2014).

Characterizing fungi is particularly challenging because, unlike primary producers, heterotrophic fungi can both synthesize amino acids *de novo* and absorb amino acids from their environment for direct use. Thus, the amino acid isotope profiles of fungi may differ depending upon their sources of nutrition. For example, pure cultures of *Saccharomyces cerevisiae* (baker's yeast) supplemented with amino acids exhibited different $\delta^{13}C_{AA}$ profiles relative to those of control yeasts grown in amino acid-free media (Chapter 2). While previous representations of fungal $\delta^{13}C_{AA}$ fingerprints using commercially available yeast (Thorp and Bowes 2017), or fungi cultured in amino acid-free media (Larsen et al. 2013) are useful for researchers estimating diet broadly, existing fungal $\delta^{13}C_{AA}$ profile data may be confounding when tracing ultimate carbon sources (i.e., primary producers) that enter consumer food webs via fungal pathways (e.g., when quantifying allochthony in freshwaters). Further research should be conducted to determine the degree to which $\delta^{13}C_{AA}$ profiles of fungi reflect those of their substrates to more accurately trace carbon flow through detrital pathways.

### *Effect of Environmental Conditioning on Resource Samples (Case Study)*

When employing BSIA methods, researchers typically collect potential dietary and/or basal resources *in situ* for the most accurate representation of tracers (e.g., decomposing leaves within a stream rather than fresh leaves). However, source samples in CSIA-AA studies are

derived from fresh tissue, or pure laboratory cultures, to reveal patterns of isotopic signatures of major source groups in some studies (e.g., Scott et al. 2006, Larsen et al. 2013, Thorp and Bowes 2017). To our knowledge, no research has been conducted to determine how $\delta^{13}C_{AA}$ values of terrestrial plants may vary based on their degree of senescence. However, this knowledge is important to ensure that $\delta^{13}C_{AA}$ profiles of resource samples such as leaf litter do not differ from fresh plant material. Therefore, to test the assumption that $\delta^{13}C_{AA}$ values are unaffected by their degree of senescence, we collected samples of attached fresh and senesced needles from a single pine tree (*Pinus* sp., Lawrence, KS, USA). Needles were rinsed in distilled water, dried at 60ºC for 48 hours, and homogenized into a fine powder using a Wig-L-Bug mixer/amalgamator. We sent *Pinus* samples to the Louisiana State University Stable Isotope Ecology Laboratory for carbon CSIA-AA (for more detailed methods see Supplemental Methods A-1).

Next, we compared $\delta^{13}C_{AA}$ values of five common EAA between fresh and senesced material to determine whether they could still be reliably identified as representing the same source group regardless of their degree of senescence. While sample size was small ($n$=6) due to high cost of analysis, 95% confidence intervals indicated overlap between the $\delta^{13}C_{AA}$ values of fresh and senesced needles for all five EAA, indicating no evidence for a difference in carbon CSIA-AA signatures between fresh and senesced needles (Figure 1-1). However, variability around the mean differed among amino acids, with valine having the highest variance and phenylalanine having the lowest variance in fresh samples, and leucine and valine showing the highest and lowest variance in senesced samples, respectively. This result provides additional support for the robust diagnostic ability of $\delta^{13}C_{AA}$ fingerprinting independent of environmental conditioning, consistent with observations by Larsen et al. (2015) in a marine diatom.

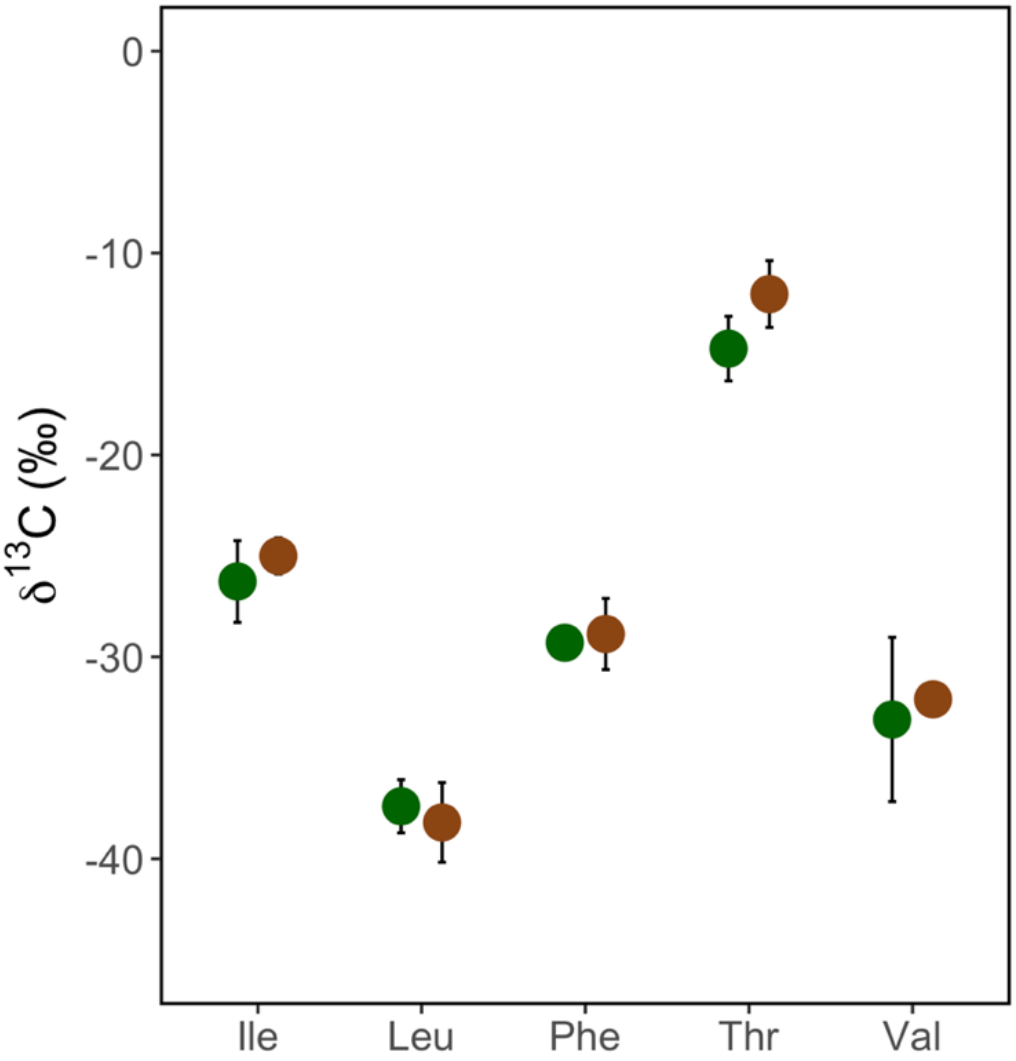


**Figure 1-1.** Non-normalized carbon isotope values of essential amino acids ($\delta^{13}C_{AA}$) for isoleucine (Ile), leucine (Leu), phenylalanine (Phe), threonine (Thr), and valine (Val) for fresh (green) and senesced (brown) needle samples from a single *Pinus* sp. individual. Error bars indicate 95% confidence intervals. Where no error bar is visible, the error was less than the size of the point.

***Effect of Locality on Resource Samples***

Another major benefit of CSIA-AA is the constancy of resource $\delta^{13}C_{AA}$ profiles despite differences in geographic location and environmental condition (Larsen et al. 2013, Larsen et al. 2015), both of which influence resource $\delta^{13}C_{AA}$ values when analyzed using traditional BSIA methods. This difference is a result of an important biochemical difference between the $\delta^{13}C_{AA}$ values of bulk-tissue and individual amino acids in the step of primary producer metabolism at which $\delta^{13}C$ fractionation occurs (Larsen et al. 2013). While bulk $\delta^{13}C$ values are influenced by the isotopic fractionation occurring through the catalyzation of rubisco in the carbon fixation of $CO_2$ during photosynthesis, carbon isotope fractionation in individual amino acids happens further downstream of these chemical processes within the plant cell, as amino acids are synthesized through various pathways that all occur after the Calvin Cycle (Miflin and Lea 1977). Therefore, taxon-specific fractionation occurring during amino acid biosynthesis should influence differences among $\delta^{13}C_{AA}$ values of taxonomically distinct basal resource samples to a greater degree than changes in environmental conditions (Larsen et al. 2015). The latter assumption benefits researchers working at large spatial and temporal scales (e.g., Larsen et al. 2013, Gómez et al. 2018), or those working in the fields of anthropology, archaeology, and paleoecology who may need to refine estimates of resource contributions by supplementing samples of ancient dietary components with modern resource samples (e.g., Jarman et al. 2017). Additionally, this relative lack of variation in $\delta^{13}C_{AA}$ values by environmental origin can reduce research costs by allowing researchers to expand the breadth of their sample coverage by using published resource $\delta^{13}C_{AA}$ values (but see *Sample analysis and quality control* below).

***Effect of Locality on Resource Samples (Case Study)***

Previous research has tested related effects of season, environmental condition, and geography on CSIA-AA resource $\delta^{13}C_{AA}$ values. Larsen et al. (2009) found no categorical differences in $\delta^{13}C_{AA}$ values among plants grown in boreal, mangrove, or greenhouse conditions. Additionally, Larsen et al. (2015) assessed effects of various growth conditions on a laboratory population of marine diatoms. They found no effects of pH, irradiance, salinity, temperature, or UV light on $\delta^{13}C_{AA}$ signatures of a cultured diatom. While the range of $\delta^{13}C_{AA}$ values differed by amino acid, these differences could not be explained by treatment (Larsen et al. 2015). To further investigate the effect of geographic location across wider spatial extents, we collected fresh, attached leaves from stream-side willow trees (*Salix* spp.) growing in a wide variety of geographic locations: the western desert and eastern grassland regions of Mongolia, and the Great Basin, Rocky Mountain, and Great Plains regions of the western United States. *Salix* spp. are common features of riparian zones globally and represent a potentially relevant terrestrially derived food source for freshwater consumers. All leaves were dried or pressed except for *Salix* samples collected from the U.S. Great Plains, which were preserved in 75% ethanol (Chua et al. 2020; see *Effect of preservation method* below), and rinsed and dried upon return to the laboratory (for more detailed methods see Supplemental Methods A-1).

We visualized patterns of normalized EAA $\delta^{13}C_{AA}$ values ($\delta^{13}C_{EAA}$) for this collection of *Salix* leaves ($n$=15), along with normalized $\delta^{13}C_{EAA}$ values ($n$=168) aggregated by Liew et al. (2019) and originating from research by Fogel and Tuross (2003), Scott et al. (2006), Larsen et al. (2013), Paolini et al. (2015), Jarman et al. (2017), Thorp and Bowes (2017), and Liew et al. (2019) in a principal component analysis (PCA; Figure 1-2). In the aggregated dataset, aquatic sources were represented by macrophytes, algae, and cyanobacteria, and terrestrial sources

included trees, grasses, shrubs, peat, and leaf litter with both $C_3$ and $C_4$ photosynthetic pathways. When visualizing all *Salix* samples in the context of other basal resource samples collected as part of a larger food source library and representing aquatic and terrestrial groups, individual samples showed subtle differences that could stem from local conditions or species identity within the genus. However, despite subtle differences, *Salix* samples collected from all regions still fell within a relatively tight cluster within other terrestrial sources (
Figure **1-2**). This result supports conclusions from Larsen et al. (2009, 2013), suggesting that normalized $\delta^{13}C_{EAA}$ fingerprints are generally conserved within a broad taxonomic group. This is an encouraging finding for those conducting studies over wide geographic ranges, especially because sample size is often limited by the high cost of CSIA-AA sample analyses. Still, more research is needed to determine how the inclusion of additional taxonomic groups collected across a range of spatial scales could influence source separation.

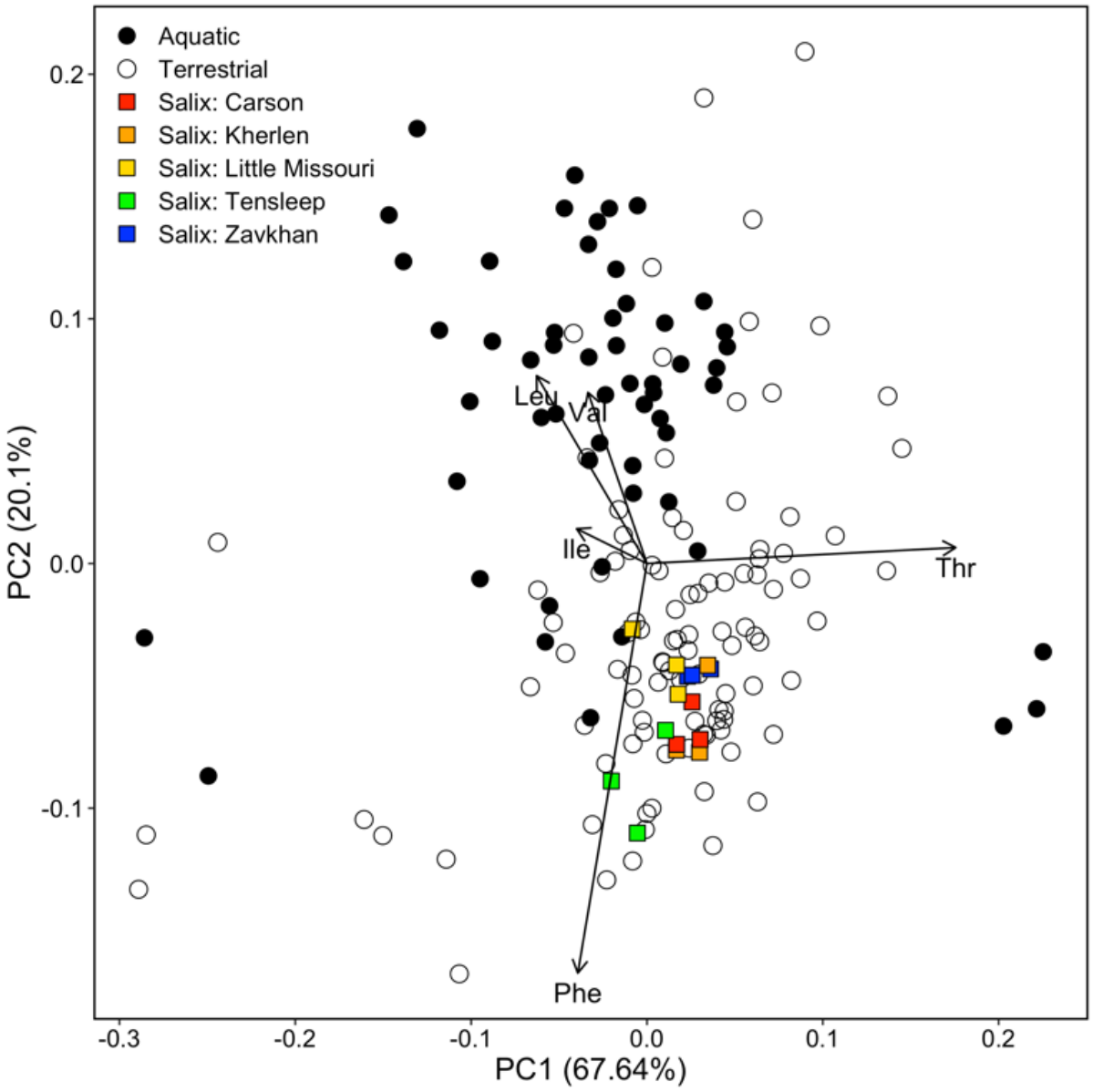


**Figure 1-2.** Principal component analysis based on normalized amino acid isotope signatures of carbon ($\delta^{13}C_{AA}$) for five essential amino acids: isoleucine (Ile), leucine (Leu), phenylalanine (Phe), threonine (Thr), and valine (Val) of *Salix* spp. collected *in situ* from the riparian zones of five rivers in Mongolia and the United States. Points represent aggregated data from literature sources ($n$=168; Fogel and Tuross 2003, Scott et al. 2006, Larsen et al. 2013, Paolini et al. 2015, Jarman et al. 2017, Thorp and Bowes 2017, and Liew et al. 2019), with black points indicating

resources of aquatic origin and white points indicating resources of terrestrial origin. Colored squares represent *Salix* spp. as primary data collected as part of the present study (*n*=15). *Salix* spp. samples are contextualized within this larger resource library as indicated in the figure legend, with the Kherlen and Zavkhan Rivers representing Mongolia, and the Carson, Little Missouri, and Tensleep Rivers representing United States sites.

***Effect of Preservation Method***

An additional consideration when collecting samples for CSIA-AA studies is the effect of preservation method on $\delta^{13}C_{AA}$ values, especially when working with historic samples (e.g., museum collections) or when collecting samples *in situ* in remote field settings. Previous studies employing CSIA-AA have used a variety of preservation methods, including ethanol (e.g., Arsenault 2017), formalin (e.g., Thorp and Bowes 2017), and salt (e.g., Liew et al. 2019) under the assumption that these preservatives would have little to no effect on $\delta^{13}C_{AA}$ values. In a recent review, Whiteman et al. (2019) identified a critical knowledge gap regarding these preservation effects and recommended that researchers lyophilize samples or store them at -20°C or below. However, these methods of sample storage are prohibitively difficult in some cases, such as when working at remote field sites. A more recent study by Chua et al. (2020) indicated that preservation by 70% ethanol or 10% formalin had no significant effect on $\delta^{13}C_{AA}$ and $\delta^{15}N_{AA}$ values over an eight-week period, which is an encouraging finding for the expansion of the use of CSIA-AA in a variety of studies requiring sample preservation. In this study, we found that the normalized $\delta^{13}C_{EAA}$ values of a *Salix* leaf sample (collected from the Little Missouri River) that was preserved in 75% ethanol prior to drying still clustered tightly with *Salix* samples that were pressed and dried (

Figure **1-2**). Still, whether or not preservatives are used, CSIA-AA samples should always be stored in pre-combusted (400-500°C for at least 8 hours) or acid-washed glass containers to avoid potential contamination of samples by organic residues on sample containers (Whiteman et al. 2019).

In summary, evidence from samples from our study suggested that $\delta^{13}C_{EAA}$ values remained consistent within source groups, despite differences in sample purity (comparing fresh and senesced *Pinus* needles) or geographic location (comparing signatures of *Salix* leaves collected in five distinct geographic locations differing in environmental condition). We recommend future studies of freshwater periphytic algae to quantify potential differences in $\delta^{13}C_{AA}$ values resulting from diffusion across the boundary layer owing to differences in water velocity, as has been investigated for bulk-tissue work (Finlay et al. 1999). Overall, results provide strong support of previous studies that suggest the powerful potential to share source data across CSIA-AA studies, which is not possible with BSIA. We recommend sustained transparency in reporting of collection methods, location of origin, and preservation method for source data to further a culture of open science and data sharing that will also facilitate the continued expansion of existing food source libraries. As these source libraries expand, thereby increasing analytical power, carbon CSIA-AA studies will continue to provide increasingly accurate estimates of resource assimilation.

**Sample Analysis and Quality Control**

Sample analysis for carbon CSIA-AA involves a series of processing steps that have not yet been universally standardized among different analytical laboratories (Rieley 1994, Docherty et al. 2001, Corr et al. 2007, Hunkeler et al. 2008). Major analytical steps for CSIA-AA include

isolating the protein fraction of a sample, freeing individual amino acids via acid hydrolysis, purifying samples using Dowex column cation-exchange (for plants, algae, soils, samples collected on GF/C filters, and any other samples containing compounds that can interfere with GC separation; Amelung and Zhang 2001, He et al. 2011), derivatizing amino acids to increase their volatility for GC-C-IRMS analysis, and standardizing and normalizing raw isotope values to correct for drift and contamination by derivatization reagents (Walsh et al. 2014). Each step of this process can be performed with some variations, and universal standardized protocols do not currently exist.

A particular challenge inhibiting standardization of CSIA-AA analytical procedures across laboratories is the fact that the critical derivatization step also introduces additional C atoms to the sample reaction prior to GC-C-IRMS, leading to artificial fractionation that alters the integrity of the isotope value of the sample material (Takizawa et al. 2020). This causes variability in isotope signature among analytical laboratories and even among different replicates of a single sample (Glaser and Amelung 2002, Corr et al. 2007). This and other sources of uncertainty (e.g., instrumental error) are accounted for with a series of quality control steps downstream of sample analysis (e.g., application of correction factors), requiring a tremendous amount of individual expertise and time (Dunn et al. 2011). Difficulties in standardizing quality control steps can lead to lower analytical reproducibility for CSIA-AA as compared to BSIA. For example, Popp et al. (2007) reported an analytical error of 1.0–4.4‰ for $\delta^{15}N_{AA}$ analysis, which is high relative to the analytical error of 0.2‰ reported for bulk tissue $\delta^{15}N$ analysis (Boecklen et al. 2011).

To address reproducibility issues, Whiteman et al. (2019) recommended prioritizing the development of standard methods for derivatization and methylation steps in particular, because

both steps are key sources of error. In many cases, CSIA-AA data cannot be reliably compared among different laboratories at present because of these methodological differences (Yarnes and Herszage 2017), so some studies compensate by applying correction factors to combined datasets from multiple laboratories (Arthur et al. 2014, Jarman et al. 2017). However, these differences are not always unidirectional (Yarnes and Herzage 2017). Alternatively, simulated datasets that incorporate analytical error from inter-laboratory comparisons have also shown promise as a tool for addressing inter-laboratory comparability (Arthur et al. 2014, Gómez et al. 2018, Liew et al. 2019). We recommend that analytical experts in different laboratories conducting CSIA-AA follow the suggestion of Roberts et al. (2018) to conduct a systematic inter-laboratory survey of calibrated mixtures to address the issue of comparability more directly.

With CSIA-AA applications on the rise, the need to improve inter-laboratory data comparisons is urgent. While normalization or calibration of $\delta^{13}C_{AA}$ values can account for some baseline variability in absolute values generated by different laboratories, improved analytical standardization would allow for more direct, quantitative comparisons of non-normalized $\delta^{13}C_{AA}$ values. For example, the ability to seamlessly share primary resource data sets (see *Sample collection and preservation*) would make CSIA-AA more accessible to all researchers, and this continued collaboration would help improve the robustness of statistical models currently limited due to sample size constraints. While some analytical decisions are outside of the scope of expertise of many researchers employing CSIA-AA approaches (i.e., for those sending out samples to an external analytical laboratory for analysis), transparent communication between researchers and analytical labs is essential to ensure data quality and interpretability. In the case where samples are being analyzed by external laboratories, we recommend working with contractors to gather and review data from internal standards (e.g., norleucine). In addition, we

recommend including a few external standards with samples upon submission. This is especially important for those researchers new to CSIA-AA or forming a new collaboration with any analytical lab, as labs are often willing to analyze test samples before a researcher commits to working with them on an entire project. For instance, homogenized samples of commercial proteins (e.g., fish, shrimp, chicken, eggs, and soy) are inexpensive to obtain and straightforward to analyze for CSIA-AA because of their high amino acid content.

## Data Processing and Analysis

Analyzing $\delta^{13}C_{AA}$ values with the goal of estimating basal resource use in metazoans involves a complex series of steps that currently lacks a set of unified best practices. These steps include (i) amino acid selection, (ii) visualization and categorization of basal resource groups, (iii) data normalization, (iv) parameterization of mixing models; and (v) statistical analysis of mixing model outputs. In this section, we outline each of these points of decision-making and review common approaches to increase transparency and accessibility to CSIA-AA data analysis.

### *Selecting Appropriate Amino Acid Tracers*

First, carbon CSIA-AA approaches require careful selection of amino acids of interest, where researchers should choose between incorporating EAA, NEAA, or CEAA for downstream analyses. Conservative approaches to CSIA-AA diet studies employ only EAA tracers, because EAAs cannot be synthesized *de novo* by metazoans and therefore must come from the consumer diet (Payne and Loomis 2006). However, some researchers have also employed NEAAs as dietary tracers in instances where the use of EAAs alone does not provide sufficient information for effective separation of isotopic signals of potential food sources. For example, NEAAs have

been included when more possible food sources exist than EAA tracers (Thorp and Bowes 2017). In a recent study, Liew et al. (2019) compared four AA tracer selection strategies: (1) all amino acids (EAAs and NEAAs); (2) only amino acids with data available for at least 95% of samples; (3) all EAAs; and (4) only EAAs with data available for at least 95% of samples. Amino acid selection strategies 2 and 4 maximized sample replication over amino acid tracer type, and amino acid selection strategies 1 and 3 prioritized amino acid tracer type. Results from this study suggest that selection strategy 3 provided the most robust and reliable estimate of resource use, emphasizing the importance of considering biochemical properties of amino acid tracers.

Although the focus on EAA tracers for food source estimation is the currently accepted approach, we note that the assumption that EAAs directly reflect the consumer diet may be oversimplified. Previous studies have refined our understanding of this critical assumption, suggesting that symbiotic intestinal bacteria contribute additional EAA to the diet of metazoan consumers in some cases (e.g., Newsome et al. 2011). Here, $\delta^{13}C_{AA}$ values are more likely to reflect an intermediate $\delta^{13}C$ value that integrates the overall diet and the protein component of the diet, because EAA may be obtained from either symbiotic bacteria or dietary protein (Ayayee et al. 2016). Alternatively, in cases where symbiotic intestinal bacteria are not significant contributors of EAAs, we would expect $\delta^{13}C_{EAA}$ values to more specifically reflect the protein fraction of the diet only, rather than the bulk diet, because that C would be primarily originating from the protein fraction of the diet (Newsome et al. 2011, Newsome et al. 2020). In controlled feeding studies with known food sources, researchers can estimate potential bacterial contributions by subtracting consumer $\delta^{13}C_{EAA}$ values from diet $\delta^{13}C_{EAA}$ values. A difference of

zero (i.e., the diet and consumer $\delta^{13}C_{EAA}$ values are the same) indicates that these amino acids are being routed directly to consumer growth from the protein fraction of the diet.

However, Whiteman et al. (2019) reviewed 10 controlled feeding studies and found that while EAA are more likely than NEAA to have near 0‰ differences between consumers and diet $\delta^{13}C_{AA}$ values, there can be considerable variation. They suggest the role of the gut microbiome in host protein homeostasis as a principal cause of variation (Whiteman et al. 2019), though variable metabolic routing, and insufficient characterizations of variation in dietary $\delta^{13}C_{AA}$ values are also likely to contribute to the observed variation. The potential influence of gut microbes suggests that in some situations EAAs may be less conservative tracers than was commonly assumed. Further research should continue to investigate mechanisms of trophic discrimination of $\delta^{13}C_{EAA}$, especially because of the importance of accurate information regarding trophic discrimination in Bayesian mixing models (Phillips et al. 2014). For now, we recommend following McMahon et al. (2010, 2016) by including a small, non-zero value for trophic discrimination (e.g., 0.1 ± 0.1 ‰) in parameterization of Bayesian mixing models, given that trophic discrimination between diet and consumer is not likely to be exactly zero in all consumers studied.

### *Visualizing and Separating Resource Samples*

Another critical step in the analysis of carbon CSIA-AA data is the visualization and separation of resource samples, for use as "fingerprints" that can later be used as training datasets for classification or to inform consumer mixing models (Larsen et al. 2013). We summarized the common approaches taken in this step by conducting a comprehensive literature search of original research articles employing the method between 2010-2020 (Supplemental Table A-2).

First, the $\delta^{13}C_{AA}$ values (commonly EAAs or all amino acids) of putative basal carbon resources are typically visualized in a principal component analysis (PCA) to preliminarily determine their likely resource categories. Next, the probability of membership of specific samples into isotopically and functionally distinct basal carbon resource groups (e.g., aquatic vs. terrestrial, seagrasses vs. algae, etc.) can be calculated using linear discriminant analysis (LDA) with a leave-one-out cross validation approach. Importantly, users should adhere to the requirements for sample size necessary to meet the assumptions of LDA by ensuring that the minimum sample size for each potential basal source group is at least equal to the number of amino acid tracers used plus one (Tabachnick and Fidell 2013, Elliott Smith et al. 2020). Alternatively, distance-based canonical analysis of principal coordinates (CAP) may be used in place of LDA when analyses are limited by smaller sample sizes (Elliott Smith et al. 2018). Once statistically different resource groups are identified in this LDA classification step, these resource groups can be used as inputs to Bayesian mixing models (as summarized means and variances or individual data points), or to train LDA models for classifying consumers based on basal resource use.

### *Normalization of Carbon Amino Acid Isotope Data*

In many instances, users should normalize $\delta^{13}C_{AA}$ values prior to mixing model input, or even for visualization in PCA. Normalization is especially necessary when using aggregated source data collected from various geographic regions (Larsen et al. 2015). The goal of this normalization procedure is to remove baseline variability by normalizing to the intermolecular variability between amino acids in a tissue (Larsen et al. 2020). The most common method of normalization is to mean-center $\delta^{13}C_{EAA}$ values, where the mean of all $\delta^{13}C_{EAA}$ values of a source

sample is subtracted from each $\delta^{13}C_{EAA}$ value within that sample (e.g., Arthur et al. 2014, Liew et al. 2019, Larsen et al. 2020):

$$\delta^{13}C_{n,ij}=\delta^{13}C_{ij}-\frac{\sum_{k=1}^{P}\delta^{13}C_{kj}}{P},$$

where $\delta^{13}C_{n,ij}$ is the normalized $\delta^{13}C$ value of the *i*th amino acid of the *j*th observation (sample), and $\delta^{13}C_{ij}$ is the raw signature of the *i*th amino acid of the *j*th observation, from which the mean of all $\delta^{13}C$ values (*P*) for one sample is subtracted (equation from Liew et al. 2019).

Because all amino acids are reported in the same unit of measurement, this normalization method of mean-centering does not distort CSIA-AA data. Rather, normalization serves as a way to represent the taxonomic uniqueness of specific resource groups by factoring out the effects of environmental variability on baseline $\delta^{13}C_{AA}$ values, which can be significant across time (Honch et al. 2012) and space (Larsen et al. 2020). Normalization reduces overlap among different resource samples and improves the interpretability of subsequent mixing model outputs, which are greatly influenced by source uncertainty. However, some studies using CSIA-AA do not mention normalization specifically. Moreover, the statistical definition of data normalization is inherently vague, referring to a variety of methods for transforming data to enable statistical comparisons across levels of a dataset. We therefore recommend the clear reporting of normalization techniques along with reproducible software scripts given the important mathematical implications for interpreting research findings.

***Estimating Resource Use Using Carbon Amino Acid Isotope Data***

While some researchers use LDA classification as a method to infer consumer resource use, many also analyze $\delta^{13}C_{AA}$ values using stable isotope mixing models (e.g., Thorp and Bowes 2017, Gómez et al. 2018, and Liew et al. 2019; Supplemental Table A-2). The difference between the two approaches is that LDA predicts the probability of resource use, while mixing models can quantify the relative contributions of multiple food sources (Larsen et al. 2009). Both approaches can also be used complimentarily, where amino acids with the highest absolute LDA coefficients are shortlisted for use as inputs to mixing models, given their utility as informative tracers for differentiating between potential food sources (Larsen et al. 2009, Gómez et al. 2018, Popatov et al. 2019). Bayesian methods are more widely used for mixing models in CSIA-AA studies because they mathematically account for variability in source and consumer stable isotope values and trophic discrimination (Stock and Semmens 2016). Although Bayesian methods are generally robust to large dimensionality, users of Bayesian mixing models must still avoid the use of these models for underdetermined systems (i.e., number of sources > number of tracers + 1; Boeklen et al. 2011, Stock and Semmens 2016). This is because under-determined models are less accurate and prone to uncertainty, thereby biasing results toward the uninformative Bayesian priors (Brett 2014, Stock and Semmens 2016, Brett et al. 2017). A few different Bayesian mixing models have been used in previous CSIA-AA studies, including FRUITS (Fernandes et al. 2014), MixSIAR (Moore and Semmens 2008), and the R package *simmr* (Parnell 2019). These models have subtle differences in their underlying algorithms, but choice of specific mixing model software is a primarily matter of user needs and preferences (Stock and Semmens 2016).

Regardless of choice of Bayesian mixing model platform, users should be prepared to contextualize model outputs based on likely feeding tendencies of consumers of interest. This is because the concept of isotopic routing suggests that different diet components may be differentially routed to catabolic or anabolic (i.e., tissue growth) processes based on availability (Boecklen et al. 2011, Newsome et al. 2011). While mixing models assume that foods are broken down into their atomic building blocks upon ingestion and then reassembled into molecules to form body tissues (Parnell et al. 2010), direct routing of amino acids to biosynthesis of certain tissues is a more biologically realistic scenario. The intact carbon skeletons of amino acid macromolecules and carbon-based molecules that are assembled *de novo* have different stable isotope values due to different levels of isotope fractionation, so mixing models can misestimate dietary contributions, especially in omnivores that may meet their dietary needs by consuming a variety of macromolecules in relatively even proportions (Wolf et al. 2009, Newsome et al. 2011). The ability to set informative priors (based on knowledge of natural history, gut contents, or BSIA data) is a unique feature of Bayesian methods that may help to increase accuracy of model outputs based on knowledge of likely basal resource use (Stock and Semmens 2016).

### *Statistical Analysis of Mixing Model Outputs*

Results from mixing models can be directly interpreted if a researcher's goal is to simply quantify resource use in a consumer or consumers of interest. However, it is also possible to address questions about community niches and ecosystem function through the additional downstream analyses of mixing model outputs. Methods for describing the community isotopic niche are well-developed in BSIA studies, with opportunities to quantify community structure and niche breadth using metrics presented by Layman et al. (2007) and variations of the standard

ellipse area (SEAc; Jackson et al. 2011). However, these analyses cannot always be directly applied to CSIA-AA data, which tends to be limited by small sample sizes and a large number of tracers (Boyd et al. 2006, Ellis et al. 2014). However, Bowes et al. (2017) presented a method to describe niche space using multidimensional data that can be directly applied to CSIA-AA data. In addition, MANOVA of Euclidean distances has also been used to test patterns in CSIA-AA data, because it is robust to small sample sizes and deviations from normality (Boyd et al. 2006, Ellis et al. 2014). Finally, resource contributions drawn from posterior distributions of Bayesian mixing models can be used to conduct robust analyses of niche space (Newsome et al. 2012). Most recently, James et al. (2020) and Lesser et al. (2020) established methods for hypervolume analysis of communities using stable isotope mixing model outputs, which can be similarly applied to mixing model outputs for CSIA-AA data.

Data analysis pipelines cannot realistically be standardized among research groups, because different biological questions will necessitate different statistical approaches. However, we recommend increased transparency in methodological decisions at all points in the CSIA-AA process by uploading reproducible code with manuscripts.

**Conclusions and Future Studies**

The expanding use of compound-specific stable isotope analysis of amino acids (CSIA-AA) of carbon provides benefits to researchers working to understand food source use in complex systems. When compared to traditional bulk-tissue analyses, CSIA-AA can provide more detailed estimates of diet components based on more specific dietary tracers (i.e., a $\delta^{13}C$ signature for each amino acid in a tissue sample), and CSIA-AA signatures are also more resistant to confounding from spatial variability (Larsen et al. 2013; e.g., Gómez et al. 2018).

However, CSIA-AA studies are also more difficult to standardize and compare analytically and statistically, due to the many individual decisions during these processes (Figure 1-3). To address this limitation, we have synthesized these processes and points of potential inconsistency with the objective to improve the accessibility of CSIA-AA methodology for new and current users.

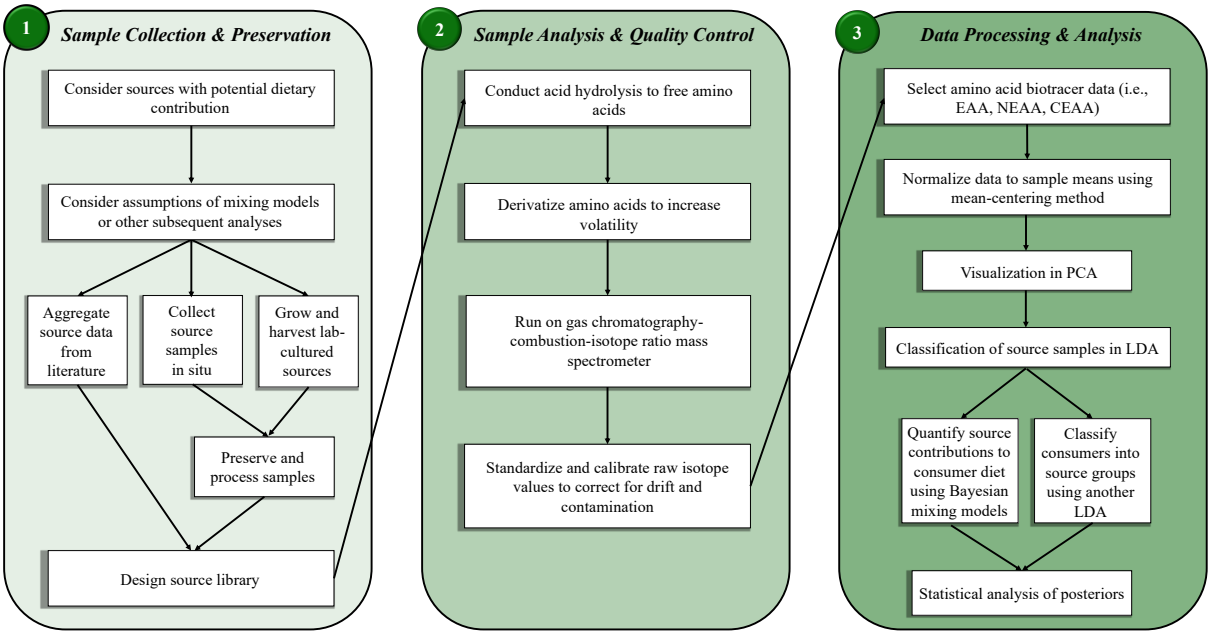


**Figure 1-3.** Condensed summary of best practices for each step described for the analysis of carbon amino acid, compound specific stable isotope data, from sample collection to statistical analysis.

Here, we also contribute an original resource library for use in CSIA-AA studies in freshwaters (Supplemental Table A-1). These data can inform mixing models designed for similar ecosystems. We found that a diverse set of basal carbon sources were statistically distinguishable into major phylogenetic groups by CSIA-AA. Additionally, in case studies

presented herein, we did not find evidence for biologically meaningful between-sample differences within basal carbon source groups (based on differences in sample quality, geographic location of origin, or preservation method). This is a highly encouraging finding that suggests that these source data may be used by other researchers studying similar systems, a major benefit of CSIA-AA methods compared to traditional bulk-tissue isotope studies.

Current limitations of CSIA-AA of carbon are primarily a result of its novelty and should continue to decrease as more researchers continue to employ and develop the method over time and technology improves. As future research continues, we recommend further study on the conservation of $\delta^{13}C_{AA}$ fingerprints within functional groups of benthic algae and heterotrophic food sources like bacteria and fungi, and continued comparison of field-collected food sources to cultures and other sources used as proxies for natural basal resources. We stress the importance of detail in methods reporting (especially in terms of normalization decisions and mixing model parameterization) and suggest that users of CSIA-AA follow the trend of transparency in scientific publication by uploading reproducible code along with new publications so that data analysis steps can be clearly communicated across lab groups, scientific fields, and systems of study. We note that documentation of methodology such that other researchers could repeat the work is one basic yardstick of a scientific publication's value, and reporting these decision steps is necessary for reproducibility.

**References**

Abelson, P. H., and T. C. Hoering. 1961. Carbon isotope fractionation in the formation of amino acids by photosynthetic organisms. Proceedings of the National. Academy of Sciences USA 47:623–632.

Amelung, W., and X. Zhang. 2001. Determination of amino acid enantiomers in soils. Soil Biology and Biochemistry 33:553–562.

Arsenault, E. R. 2017. Basal carbon sources supporting fish food webs in terminal basin rivers Masters thesis. Univ. of Kansas.

Arthur, K. E., S. Kelez, T. Larsen, A. A. Choy, and B. N. Popp. 2014. Tracing the biosynthetic source of essential amino acids in marine turtles using $\delta^{13}C$ fingerprints. Ecology 95:1285–1293.

Ayayee, P. A., T. Larsen, and Z. Sabree. 2016. Symbiotic essential amino acids provisioning in the American cockroach, *Periplaneta americana* (Linnaeus) under various dietary conditions. PeerJ 4:e2046.

Boecklen, W. J., C. T. Yarnes, B. A. Cook, and A. C. James. 2011. On the use of stable isotopes in trophic ecology. Annual Review of Ecology, Evolution, and Systematics 42:411–440.

Bowes, R. E., J. H. Thorp, and D. C. Reuman. 2017. Multidimensional metrics of niche space for use with diverse analytical techniques. Scientific Reports 7:41599.

Bowes, R. E., J. H. Thorp, and M. D. Delong. 2020. Reweaving river food webs through time. Freshwater Biology 65:390–402.

Boyd, T. J., C. L. Osburn, K. J. Johnson, K. B. Birgl, and R. B. Coffin. 2006. Compound-specific isotopic analysis coupled with multivariate statistics to source-apportion hydrocarbon mixtures. Environmental Science and Technology 40:1916–1924.

Brett, M. T. 2014. Resource polygon geometry predicts Bayesian stable isotope mixing model bias. Marine Ecology Progress Series 514:1–12.

Brett, M. T., S. E. Bunn, S. Chandra, and others. 2017. How important are terrestrial organic carbon inputs for secondary production in freshwater ecosystems?. Freshwater Biology 62:833–853.

Chua, K. W. J., J. H. Liew, K. H. Shin, and D. C. J. Yeo. 2020. Effects of ethanol preservation and formalin fixation on amino acid stable isotope analysis ($\delta^{13}C$ and $\delta^{15}N$) and its ecological applications. Limnology and Oceanography: Methods 18:77–88.

Corr, L. T., R. Berstan, and R. P. Evershed. 2007. Optimisation of derivatisation procedures for the determination of delta13C values of amino acids by gas chromatography/combustion/isotope ratio mass spectrometry. Rapid Communications in Mass Spectrometry 21:3759–3771.

DeNiro M., and S. Epstein. 1976. You are what you eat (plus a few per mil): the carbon isotope cycle in food chains. Geological Society of America 8:834–35. (Abstract)

Docherty, G., V. Jones, R. P. Evershed. 2001. Practical and theoretical considerations in the gas chromatography/combustion/isotope ratio mass spectrometry delta(13)C analysis of small polyfunctional compounds. Rapid Communications in Mass Spectrometry 15:730–738.

Dodds, W. K., S. M. Collins, S. K. Hamilton, and others. 2014. You are not always what we think you eat: selective assimilation across multiple whole-stream isotopic tracer studies. Ecology 95:2757–2767.

Dunn, P. J. H., N. V. Honch, and R. P. Evershed. 2011. Comparison of liquid chromatography–isotope ratio mass spectrometry (LC/IRMS) and gas chromatography–combustion–isotope ratio mass spectrometry (GC/C/IRMS) for the determination of collagen amino

acid $\delta^{13}C$ values for palaeodietary and palaeoecological reconstruction. Rapid Communications in Mass Spectrometry 25:2995–3011.

Elliott Smith, E. A., C. Harrod, and S. D. Newsome. 2018. The importance of kelp to an intertidal ecosystem varies by trophic level: insights from amino acid $\delta^{13}C$ analysis. Ecosphere 9:e02516.

Elliott Smith, E. A., C. Harrod, F. Docmac, and S. D. Newsome. 2021. Intraspecific variation and energy channel coupling within a Chilean kelp forest. Ecology 102:e03198.

Ellis, G. S., G. Herbert, and D. Hollander. 2014. Reconstructing carbon sources in a dynamic estuarine ecosystem using oyster amino acid $\delta^{13}C$ values from shell and tissue. Journal of Shellfish Research 33:217–225.

Hunkeler, D., R. U. Meckenstock, B. Sherwood Lollar, T. C. Schmidt, J. T. Wilson, T. Schmidt, and J. Wilson. 2008. A guide for assessing biodegradation and source identification of organic ground water contaminants using compound specific isotope analysis (CSIA). Office of Research and Development, National Risk Management Research Laboratory, US Environmental Protection Agency.

Evershed, R. P., I. D. Bull, L. T. Corr, and others. 2007. Compound-specific stable isotope analysis in ecology and paleoecology. *Stable isotopes in ecology and environmental science* 480.

Fantle, M. S., A. I. Dittel, S. M. Schwalm, C. E. Epifanio, M. L. Fogel. 1999. A food web analysis of the juvenile blue crab, *Callinectes sapidus*, using stable isotopes in whole animals and individual amino acids. Oecologia 120:416–26.

Fernandes, R., A. R. Millard, M. Brabec, M.-J. Nadeau, and P. Grootes. 2014. Food Reconstruction Using Isotopic Transferred Signals (FRUITS): A Bayesian model for diet reconstruction. PLoS ONE 9:e87436.

Finlay, J. C., M. E. Power, and G. Cabana. 1999. Effects of water velocity on algal carbon isotope ratios: Implications for river food web studies. Limnology and Oceanography 44:1198–1203.

Fogel, M. L., N. Tuross. 2003. Extending the limits of paleodietary studies of humans with compound specific carbon isotope analysis of amino acids. Journal of Archaeological Science 30:535–45.

Glaser, B., and W. Amelung. 2002. Determination of $^{13}C$ natural abundance of amino acid enantiomers in soil: methodological considerations and first results. Rapid Communications in Mass Spectrometry 16:891–898.

Gómez, C., T. Larsen, B. Popp, K. A. Hobson, and C. D. Cadena. 2018. Assessing seasonal changes in animal diets with stable-isotope analysis of amino acids: a migratory boreal songbird switches diet over its annual cycle. Oecologia 187:1–13.

Honch, J., S. O. McCullagh, and R. E. M. Hedges. 2012. Variation of bone collagen amino acid $\delta^{13}C$ values in archaeological humans and fauna with different dietary regimes: developing frameworks of dietary discrimination. Americal Journal of Physical Anthropology 148:495–511.

He, H., H. Lü, W. Zhang, S. Hou, and X. Zhang 2011. A liquid chromatographic/mass spectrometric method to evaluate $^{13}C$ and $^{15}N$ incorporation into soil amino acids. Journal of Soils and Sediments 11:731–740.

Jackson A. L., R. Inger, A. C. Parnell, and S. Bearhop. 2011. Comparing isotopic niche widths among and within communities: SIBER – Stable Isotope Bayesian Ellipses in R. Journal of Animal Ecology 80:595–602.

James, W. R., J. S. Lesser, S. Y. Litvin, and J. A. Nelson. 2020. Assessment of food web recovery following restoration using resource niche metrics. Science of the Total Environment 711:134801.

Jarman, C. L., T. Larsen, T. Hunt, and others. 2017. Diet of the prehistoric population of Rapa Nui (Easter Island, Chile) shows environmental adaptation and resilience. American Journal of Physical Anthropology 164:343–361.

Larsen, T., D. E. Taylor, M. B. Leigh, D. M. O'Brien. 2009. Stable isotope fingerprinting: a novel method for identifying plant, fungal, or bacterial origins of amino acids. Ecology 90:3526–3535.

Larsen, T., M. Ventura, N. Andersen, D. M. O'Brien, U. Piatkowski, and M. D. McCarthy. 2013. Tracing carbon sources through aquatic and terrestrial food webs using amino acid stable isotope fingerprinting. PLoS ONE 8:e73441.

Larsen, T., L. T. Bach, R. Salvatteci, Y. V. Wang, N. Andersen, M. Ventura, M. D. McCarthy. 2015. Assessing the potential of amino acid $^{13}C$ patterns as a carbon source tracer in marine sediments: effects of algal growth conditions and sedimentary diagenesis. Biogeosciences Discussions 12:4979–4992.

Larsen, T., T. Hansen, and J. Dierking. 2020. Characterizing niche differentiation among marine consumers with amino acid $\delta^{13}C$ fingerprinting. Ecology and Evolution 10:7768–7782.

Layman, C. A., D. A. Arrington, C. G. Montaña, and D. M. Post. 2007. Can stable isotope ratios provide for community-wide measures of trophic structure? Ecology 88:42–48.

Lesser, J. S., W. R. James, C. D. Stallings, R. M. Wilson, and J. A. Nelson. 2020. Trophic niche size and overlap decreases with increasing ecosystem productivity. Oikos 129:1303–1313.

Liew, J. H., K. W. J. Chua, E. R. Arsenault, J. H. Thorp, A. Suvarnaraksha, A. Amirrudin, and D. C. J. Yeo. 2019. Quantifying terrestrial carbon in freshwater food webs using amino acid isotope analysis: Case study with an endemic cavefish. Methods in Ecology and Evolution 10:1594–1605.

Lichtfouse, E. 2000. Compound-specific isotope analysis. Application to archaelogy, biomedical sciences, biosynthesis, environment, extraterrestrial chemistry, food science, forensic science, humic substances, microbiology, organic geochemistry, soil science and sport. Rapid Communications in Mass Spectrometry 14:1337–1344.

McMahon, K. W., M. L. Fogel, T. S. Elsdon, S. R. Thorrold. 2010. Carbon isotope fractionation of amino acids in fish muscle reflects biosynthesis and isotopic routing from dietary protein. Journal of Animal Ecology 79:1132–1141.

McMahon, K. W., S. R. Thorrold, L. A. Houghton, and M. L. Berumen. 2016. Tracing carbon flow through coral reef food webs using a compound-specific stable isotope approach. Oecologia 180:809–821.

Miflin B. J., and P. J. Lea. Amino acid metabolism. Annual Review of Plant Physiology 282:299–329.

Moore, J. W., and B. X. Semmens. 2008. Incorporating uncertainty and prior information into stable isotope mixing models. Ecology Letters 11:470–480.

Morris, C. R., J. Hamilton-Reeves, R. G. Martindale, M. Sarav, and J. B. O. Gautier. 2017. Acquired amino acid deficiencies: A focus on arginine and glutamine. Nutrition in Clinical Practice 32:30S–47S.

Newsome, S.D., M. L. Fogel, L. Kelly, and C. Martínez del Rio. 2011. Contributions of direct incorporation from diet and microbial amino acids to protein synthesis in Nile tilapia. Functional Ecology 25:1051–1062.

Newsome, S. D., J. D. Yeakel, P. V. Wheatley, and M. Tinker. 2012. Tools for quantifying isotopic niche space and dietary variation at the individual and population level. Journal of Mammalogy 93:329–341.

Newsome, S. D., K. L. Feeser, C. J. Bradley, C. Wolf, C. Takacs-Vesbach, and M. L. Fogel. 2020. Isotopic and genetic methods reveal the role of the gut microbiome in mammalian host essential amino acid metabolism. Proceedings of the Royal Society B 287:20192995.

Ohkouchi, N., Y. Chikaraishi, H. G. Close, and others. 2017. Advances in the application of amino acid nitrogen isotopic analysis in ecological and biogeochemical studies. Organic Geochemistry 113:150–174.

Ohkouchi, N., N. O. Ogawa, Y. Chikaraishi, H. Tanaka, and E. Wada. 2015. Biochemical and physiological bases for the use of carbon and nitrogen isotopes in environmental and ecological studies. Progress in Earth and Planetary Science 2:1.

Paolini, M., L. Ziller, K. H. Laursen, S. Husted, and F. Camin. 2015. Compound-Specific $\delta^{15}N$ and $\delta^{13}C$ analyses of amino acids for potential discrimination between organically and conventionally grown wheat. Journal of Agricultural and Food Chemistry 63:5841–5850.

Parnell, A. C., R. Inger, S. Bearhop, and A. L. Jackson. 2010. Source partitioning using stable isotopes: coping with too much variation. PLoS ONE 5:e9672.

Parnell, A. 2019. Simmr: A Stable Isotope Mixing Model. R package version 0.4.1. https://CRAN.R-project.org/package=simmr

Payne, S. H., and W. F. Loomis. 2006. Retention and loss of amino acid biosynthetic pathways based on analysis of whole-genome sequences. Eukaryotic Cell 5:272–276.

Phillips, D. L., R. Inger, S. Bearhop, A. L. Jackson, J. W. Moore, A. C. Parnell, B. X. Semmens, and E. J. Ward. 2014. Best practices for use of stable isotope mixing models in food-web studies. Canadian Journal of Zoology 92:823–835.

Potapov, A. M., A. V. Tiunov, and S. Scheu. 2019. Uncovering trophic positions and food resources of soil animals using bulk natural stable isotope composition. Biological Reviews 94:37–59.

Popp, B. N., B. S. Graham, R. J. Olson, C. C. S. Hannides, M. J. Lott, G. A. López-Ibarra, F. Galván-Magaña, and B. Fry. 2007. Insight into the trophic ecology of yellowfin tuna, *Thunnus albacares*, from compound-specific nitrogen isotope analysis of protenacious amino acids. Terrestrial Ecology 1:173–190.

Rieley, G. 1994. Derivatization of organic compounds prior to gas chromatographic-combustion-isotope ratio mass spectrometric analysis: identification of isotope fractionation processes. Analyst 119:915–919.

Roberts, P., R. Fernandes, O. E. Craig, T. Larsen, A. Lucquin, J. Swift, and J. Zech. 2018. Calling all archaeologists: guidelines for terminology, methodology, data handling, and reporting when undertaking and reviewing stable isotope applications in archaeology. Rapid Communications in Mass Spectrometry 32:361–372.

Saccò, M., A. J. Blyth, W. F. Humphreys, A. Kuhl, D. Mazumder, C. Smith, and K. Grice. 2019. Elucidating stygofaunal trophic web interactions via isotopic ecology. PLoS ONE 14: e0223982.

Scott, J. H., D. M. O'Brien, D. Emerson, H. Sun, G. D. McDonald, A. Salgado, and M. L. Fogel. 2006. An examination of the carbon isotope effects associated with amino acid biosynthesis. Astrobiology 6:867–880.

Stock, B. C., and B. X. Semmens. 2016. Unifying error structures in commonly used biotracer mixing models. Ecology 97:2562–2569.

Tabachnick, B. G., and L. S. Fidell. 2013. Using multivariate statistics. 6th ed. Pearson Education.

Takizawa, Y., Y. Takano, B. Choi, P. S. Dharampal, S. A. Steffan, N. O. Ogawa, N. Ohkouchi, and Y. Chikaraishi. 2020. A new insight into isotopic fractionation associated with decarboxylation in organisms: implications for amino acid isotope approaches in biogeoscience. Progress in Earth and Planetary Science 7:50.

Thorp, J. H., and R. E. Bowes. 2017. Carbon sources in riverine food webs: new evidence from amino acid isotope techniques. Ecosystems 20:1029–1041.

Tieszen, L. L., T. W. Boutton, K. G. Tesdahl, and N. A. Slade. 1983. Fractionation and turnover of stable carbon isotopes in animal tissues: implications for $\delta^{13}C$ analysis of diet. Oecologia 57:32–37.

Twining, C. W., S. J. Taipale, L. Ruess, A. Bec, D. Martin-Creuzburg, and M. J. Kainz. 2020 Stable isotopes of fatty acids: current and future perspectives for advancing trophic ecology. Philosophical Transactions of the Royal Society B 375:20190641.

Walsh, R. G., S. He, and C. T. Yarnes. 2014. Compound-specific $\delta^{13}C$ and $\delta^{15}N$ analysis of amino acids: a rapid, chloroformate-based method for ecological studies. Rapid Communications in Mass Spectrometry 28:96–108.

Whiteman, J., E. E. Smith, A. Besser, and S. Newsome. 2019. A guide to using compound-specific stable isotope analysis to study the fates of molecules in organisms and ecosystems. Diversity 11:8.

Wolf, N., S. A. Carleton, and C. M. del Rio. 2009. Ten years of experimental animal isotopic ecology. Functional Ecology 23:17–26.

Yarnes, C. T., and J. Herszage. 2017. The relative influence of derivatization and normalization procedures on the compound specific stable isotope analysis of nitrogen in amino acids. Rapid Communications in Mass Spectrometry 31:693.

# Chapter 2: Substrate Composition Influences Carbon Amino Acid Isotope Signatures of Fungi: Implications for Tracing Resource use in Freshwater Food Webs


## Abstract

As decomposers, fungi form critical links between recalcitrant, terrestrially derived food sources and metazoan consumers in freshwater food webs. Despite their functional importance, contributions of fungi to consumers may be misestimated in amino acid isotope fingerprinting studies. This is because, unlike other freshwater food sources, fungi are capable of both synthesizing amino acids *de novo* and taking up amino acids from their environment for direct use. While fungi cultured in amino acid-free media have been used to represent the fungal resource signature in studies of natural environments, fungi living *in situ* may gain energetic benefits by taking up substrate amino acids directly. Consequently, the degree to which carbon essential amino acid isotope profiles ($\delta^{13}C_{EAA}$) of fungi may reflect those of their environmental substrates (i.e., primary producers) may be highly variable. The objective of this laboratory experiment was to determine the effect of substrate amino acid availability on carbon amino acid isotope profiles ($\delta^{13}C_{AA}$) of baker's yeast (*Saccharomyces cerevisiae*). We hypothesized that increasing substrate amino acid availability would cause yeast $\delta^{13}C_{AA}$ profiles to be more similar to substrate $\delta^{13}C_{AA}$ profiles, and therefore less similar to $\delta^{13}C_{AA}$ profiles characteristic of *de novo* amino acid synthesis. We found that the $\delta^{13}C_{AA}$ profiles of yeasts grown in substrates containing amino acids were significantly different from those grown in amino acid-free controls. Importantly, our observations suggest that yeast utilized two essential amino acids (Leu and Val) directly from media substrates when available. We conclude that fungal $\delta^{13}C_{AA}$ profiles may

closely reflect those of their substrates in some instances, such as during seasons where initial colonization of organic matter occurs.

## Introduction

Fungi link recalcitrant, terrestrially derived food sources and metazoan consumers in freshwater food webs (Moore et al. 2004). These links are especially important for food webs that have demonstrated reliance on detritus entering freshwater ecosystems as a terrestrial subsidy (Polis et al. 1997, Vanni et al. 2004). Upon its entry into aquatic systems, terrestrial (allochthonous) detrital material is not immediately palatable for consumption by freshwater organisms because it is composed of complex structural polysaccharides that have low nutritional value and are difficult to digest (Kaushik and Hynes 1971, Mann 1988). However, the nutritional quality (e.g., lower C:N ratio) of detrital matter improves as it is conditioned by mechanical, chemical, and biological processes within the water column (Webster and Benfield 1986). In particular, microbial biofilms composed of mostly fungi (>90%; Hieber and Gessner 2002, Grossart et al. 2019) colonize and decompose detrital matter. During decomposition, fungi resynthesize and recompose detritus (Steffan and Dharampal 2019), thereby increasing the bioavailability and palatability of allochthonous carbon to detritivorous consumers (Mackay and Kalff 1973, Cummins 1974, Danger et al. 2012). Therefore, by acting as the "peanut butter on a cracker" (Cummins 1974), fungi provide a key pathway through which allochthonous resources are introduced into freshwater food webs (France 2011).

Accurate quantification of the role of fungi in freshwater food webs is challenging due to difficulties in collecting and separating fungal-based biofilm from their detrital substrates in situ (Ohkouchi et al. 2015). Recent studies have demonstrated that amino acid specific stable isotope

analysis of carbon can resolve estimates of dietary sources that might otherwise be obscured using traditional bulk-tissue approaches (Larsen et al. 2013, Whiteman et al. 2019). In particular, carbon stable isotope profiles of essential amino acids ($\delta^{13}C_{EAA}$) can discriminate among terrestrial plants, fungi, and bacteria (Larsen et al. 2009, 2013) on the basis of their diverse, taxonomically unique biosynthetic pathways (Scott et al. 2006). These $\delta^{13}C_{EAA}$ profiles can then be used to trace basal resource assimilation of metazoan consumers because trophic discrimination (i.e., the difference in stable isotope values between consumers and their diets) for $\delta^{13}C_{EAA}$ is minimal (Takizawa et al. 2020).

However, analyses of fungal (and heterotrophic bacterial) $\delta^{13}C_{AA}$ may be more complex than previously supposed. This is because fungi can synthesize all 20 amino acids (henceforth referred to as AAs) de novo (Payne and Loomis 2006), but they can also take up AAs from their substrates directly (Hanscho et al. 2012, Takizawa et al. 2020). The former is typical in primary producers, while the latter is commonly associated with heterotrophs. Fungi are believed to gain an energetic advantage by taking up AAs available within environmental substrates for direct use rather than synthesizing them de novo (Bianchi et al. 2019). The relative importance of either of these pathways is likely to influence fungal $\delta^{13}C_{AA}$ profiles, reflecting substrate $\delta^{13}C_{AA}$ when fungi predominantly take up AAs from external sources, but not when they are primarily synthesizing AAs de novo. This trend is likely to be most apparent in fungal $\delta^{13}C$ profiles of essential AAs ($\delta^{13}C_{EAA}$) given previous observations of their negligible trophic discrimination (Takizawa et al. 2020).

The objective of the present study was to investigate the effects of substrate AA availability as one possible determinant of the relative importance of direct AA uptake and de novo AA synthesis in fungi. Here, we determined whether baker's yeast (*Saccharomyces*

*cerevisiae*) grown on media with available AAs would have different $\delta^{13}C_{AA}$ profiles than yeasts grown on AA-free media (i.e., relying only on de novo AA biosynthesis). We conducted a laboratory experiment comparing $\delta^{13}C_{AA}$ of yeasts grown on media substrates that varied in AA content. To contextualize results, we also measured the C:N ratios and bulk tissue stable isotope values of cultured yeast carbon ($\delta^{13}C$) and nitrogen ($\delta^{15}N$). We hypothesized that yeast $\delta^{13}C_{AA}$, especially for essential AAs, would be more similar to substrate $\delta^{13}C_{AA}$ with increasing substrate AA content, given the potential energetic advantage (Bianchi et al. 2019). Findings from our study will help ascertain the utility of fungal $\delta^{13}C_{AA}$ as an indicator of the functional role of fungus as a pathway for allochthonous resources in freshwater food webs.

## Methods

### *Media Preparation and Laboratory Culturing of Yeast*

We plated a pure culture of baker's yeast (*Saccharomyces cerevisiae*) onto media with differing absolute amounts of seven AAs. All media contained BactoAgar medium (20 g/L) supplemented with AA-free yeast nitrogen base (6.7 g/L, Formedium CYN0401) and glucose (20 g/L). Depending on AA treatment, media was then spiked with AA mixtures of varying amounts of L-asparagine (Asn), L-glutamine (Gln), L-isoleucine (Ile), L-leucine (Leu), L-threonine (Thr), L-phenylalanine (Phe), and L-valine (Val; Formedium) to designate *Control*, *Low*, *Reference*, and *High* treatment plates (Table 2-1). Specifically, *Reference* plates were supplemented with AAs in amounts specified in supplemented minimal media recipes given in Amberg et al. (2005) and Curran and Bugeja (2006). *High* and *Low* treatments were supplemented with AAs in absolute amounts of ± 50% of the *Reference* media recipe, respectively. Amino acid-free *Control*

plates were also included in the study so that we could measure baseline $\delta^{13}C_{AA}$ under conditions necessitating ~100% de novo synthesis of AAs by cultured fungi.

**Table 2-1.** Amino acid concentrations (mg/L) for four media substrate treatments: amino acid-free *Control* media (*n*=5), media with *Low* amino acid availability (*n*=5), media with *Reference* amino acid availability (amounts for supplemented minimal media; Amberg et al. 2005 and Curran and Bugeja 2006; *n*=5), and media with *High* amino acid availability (*n*=5). All plates contained equal amounts of yeast nitrogen base, agar, and glucose and differed only in the concentrations of their amino acid supplements, which included L-asparagine (L-Asx), L-glutamine (L-Glx), L-isoleucine (L-Ile), L-leucine (L-Leu), L-threonine (L-Thr), L-phenylalanine (L-Phe), and L-valine (L-Val).

| Treatment | L-Asx | L-Glx | L-Ile | L-Leu | L-Thr | L-Phe | L-Val |
|---|---|---|---|---|---|---|---|
| *Control* | 0 | 0 | 0 | 0 | 0 | 0 | 0 |
| *Low* | 50 | 50 | 15 | 50 | 100 | 25 | 75 |
| *Reference* | 100 | 100 | 30 | 100 | 200 | 50 | 150 |
| *High* | 150 | 150 | 45 | 150 | 300 | 75 | 225 |

Media ingredients were combined in 1 L of DI water and autoclaved at 20 psi for 20 min at 121ºC. Amino acids Asn and Thr were added after autoclaving, under sterile conditions, as recommended in Curran and Bugeja (2006). After media was prepared, we plated yeast in a sterile hood using a lawn plating method. Yeast culture plates were arranged in random order in an incubator and held at 35°C for 10 days, during which they were monitored for growth and contamination daily. After incubation, yeast cultures were harvested and dried for 48 hr at 60ºC. To obtain enough sample material for isotope analysis, each replicate sample (*n*=5 for each of

four treatments) represented a pooled sample from yeast cultured on three plates from the same treatment, all of which were plated at the same time and stored together. Dried yeast samples were homogenized using a Wig-L-Bug mixer/amalgamator, weighed into quantities of 20–40 mg, and placed in pre-combusted glass vials for elemental and isotopic analyses.

All yeast samples ($n$=20) were sent to the Louisiana State University Stable Isotope Ecology Laboratory, where they were analyzed for amino acid compound specific stable isotope analysis of carbon ($\delta^{13}C_{AA}$), as well as %C, %N, C:N ratio, and bulk-tissue stable isotope analysis of carbon ($\delta^{13}C$) and nitrogen ($\delta^{15}N$). To characterize the $\delta^{13}C_{AA}$ profile of media substrates, AAs used to supplement growth media (Asn, Gln, Ile, Leu, Thr, Phe, and Val) were also individually analyzed for $\delta^{13}C$ ($\delta^{13}C_{Substrate}$).

### *Elemental and Isotopic Analyses*

For elemental analysis and bulk-tissue stable isotope analyses of carbon and nitrogen, samples were weighed into tin capsules and flash-combusted using a Costech ECS4010 elemental analyzer coupled to a Thermo-Fisher Delta Plus XP continuous-flow stable isotope ratio mass spectrometer. Stable isotope values were then normalized using a two-point system with glutamic acid reference material (USGS-40 and USGS-41). Sample precision was examined by comparing the standard deviation of repeated reference materials (USGS-40 and USGS-41) and an internal laboratory standard. Stable isotope values are expressed in standard delta ($\delta$) per mil (‰) notation according to the following equation: $\delta X = [(R_{sample}/R_{standard})\text{-}1] \times 1000$, where X is either $^{13}C$ or $^{15}N$, and R is the corresponding ratio of either $^{13}C/^{12}C$ or $^{15}N/^{14}N$. The $R_{standard}$ values were represented by Vienna Pee Dee Belemnite (VPDB) for $\delta^{13}C$ and atmospheric $N_2$ for

$\delta^{15}N$. Analytical precision based on USGS-40 and USGS-41 ranged from 0.04–0.09‰ for $\delta^{13}C$ and 0.19–0.22‰ for $\delta^{15}N$.

Carbon AA isotope values were also obtained for 20 yeast samples, using the methyl chloroformate derivatization method described by Walsh et al. (2014). Briefly, samples were acid hydrolyzed, derivatized with methyl chloroformate, and injected in duplicate onto a gas chromatography/combustion/isotope ratio mass spectrometer (GC/C/IRMS) system. Prior to GC/C/IRMS, yeast samples were column purified using a Dowex 50WX8-400 cation exchange resin. Raw isotope values of samples were corrected based on norleucine and individual L-amino acid standards of known isotopic composition, which were included with all sample runs. Isotope values are expressed in delta (δ) per mil (‰) notation according to the formula above, as calculated for each AA in the sample tissue. Amino acids Ala, Asp (converted from Asn during acid hydrolysis), Glu (converted from Gln during acid hydrolysis), Gly, Ile, Leu, Pro, Thr, and Val were recovered for all samples, with a mean analytical error of 0.42‰ for all AAs in samples and 0.51‰ for all AAs in reference materials.

### *Statistical Analysis*

To compare C:N ratios, as well as bulk-tissue stable isotope values of carbon ($\delta^{13}C$) and nitrogen ($\delta^{15}N$) among media treatments (*Control*, *Low*, *Reference*, and *High*), we used one-way ANOVAs with Tukey HSD post-hoc tests. Normality was checked prior to ANOVA by visualizing Q-Q plots. Tests resulting in p-values$<0.05$ were considered statistically significant.

To test for differences in yeast $\delta^{13}C_{AA}$ profiles with varying levels of substrate AA, we used a MANOVA, followed by separate ANOVAs for each AA (Asp, Glu, Ile, Leu, Phe, Thr,

and Val) to determine differences among experimental treatments. Finally, we assessed individual pairwise differences between treatments for each AA using Tukey HSD tests.

We used a principal component analysis (PCA) to visualize differences in $\delta^{13}C_{EAA}$ profiles of yeasts exposed to different treatments. We did not normalize (mean-center) values prior to analysis, because all samples were grown on a common media and under constant environmental conditions. Next, we tested whether yeast $\delta^{13}C_{EAA}$ profiles were statistically distinguishable among treatment groups (*Low*, *Reference*, *High*, and AA-free *Control*) with linear discriminant analysis (LDA) using the *MASS* package in R (Venables and Ripley 2002), based on non-normalized $\delta^{13}C_{EAA}$ values. We used a leave-one-out cross validation approach to determine the accuracy with which yeast samples correctly classified into their respective treatments.

To determine whether yeasts were absorbing AAs directly from their substrates, we calculated the difference between $\delta^{13}C_{Substrate}$ and $\delta^{13}C_{EAA}$ profiles of consumers (fungi), separately for each experimental treatment (*Control*, *Low*, *Reference*, and *High*). If essential AAs were routed to growth through direct uptake, we would expect that $\Delta^{13}C_{EAA}$ ($\delta^{13}C_{EAA}$ consumer – $\delta^{13}C_{EAA}$ diet) would be approximately equal to zero because, unlike for AAs categorized as non-essential, minimal trophic discrimination is expected (Takizawa et al. 2020). Alternatively, deviations from zero for $\Delta^{13}C_{EAA}$ may suggest some combination of de novo synthesis and direct uptake for essential AAs. For nonessential AAs that undergo more variable trophic discrimination, even if direct absorption of AAs from the substrate had occurred, deviations from zero for $\Delta^{13}C$ might still be observed. Therefore, we based our interpretations of AA uptake on $\Delta^{13}C_{EAA}$ exclusively. For the purpose of comparison, $\Delta^{13}C_{EAA}$ was also quantified for *Control* yeasts even though no AAs were present in the substrate. In this case, deviations observed

between $\delta^{13}C_{EAA}$ profiles of *Control* yeasts and $\delta^{13}C_{Substrate}$ are reflective of baseline differences between $\delta^{13}C$ values of fungal AAs that were synthesized de novo, and $\delta^{13}C$ values of AA supplements. To quantify deviation from zero in $\Delta^{13}C_{AA}$ between yeasts and their substrates, we conducted one-sample t-tests for each AA, for each experimental treatment group. All data analyses were conducted in R version 3.6.3 (R Core Team 2020).

## Results

### *Elemental and Bulk Tissue Isotope Analyses ($\delta^{13}C$ and $\delta^{15}N$)*

Yeast C:N ratios differed among media treatments of varying AA concentrations (*Control*, *Low*, *Reference*, and *High*; $F_{3,16}$=12.72, p<0.001), with the highest C:N ratio found in *Control* yeasts grown in AA-free media (6.6±0.1; p<0.001), and the lowest C:N ratio in yeasts grown in *High* treatment conditions (5.8±0.2; p<0.001), but *Control* yeasts did not differ significantly from *Low* or *Reference* treatments (Supplemental Table B-1). We observed significant differences in yeast bulk-tissue $\delta^{13}C$ among treatments ($F_{3,16}$=6.69, p=0.004), with the AA-free *Control* treatment having a higher $\delta^{13}C$ value compared to the *High* (p=0.023) and *Reference* (p=0.003) treatments. The highest variation in bulk $\delta^{13}C$ was observed for yeasts grown under *Control* (-8.6‰ to -7.7‰) and *Low* (-9.5‰ to -8.3‰) treatment conditions, and the lowest variation in $\delta^{13}C$ occurred in the yeast grown in *High* treatment media (-9.3‰ to -9.1‰). However, there were no significant differences in $\delta^{15}N$ among yeast samples from different treatments ($F_{3,16}$=1.55, p=0.24).

***Carbon Amino Acid Isotope Analyses ($\delta^{13}C_{AA}$)***

Yeast $\delta^{13}C_{AA}$ profiles varied among treatments (Asp, Glu, Ile, Leu, Phe, Thr, and Val; Pillai=2.593, $F_{3,16}$=10.91, $p<0.001$). These differences were due to inter-treatment variations between all AAs except for Phe and Thr (Figure 2-1). Pairwise differences indicated that yeast $\delta^{13}C_{AA}$ of Asp, Glu, and Val were significantly higher in *Control* versus *High* treatments ($p<0.05$), while $\delta^{13}C_{AA}$ of Ile and Leu were significantly lower in *Control* versus *High* treatments ($p<0.05$). Significant pairwise differences ($p<0.05$) between *Control* and *Reference* treatments were observed for Asp, Glu, Leu, and Val, with all AA but Val having higher $\delta^{13}C_{AA}$ values in the Control treatment. Lastly, yeast $\delta^{13}C_{AA}$ was significantly higher in *Control* than *Low* treatments for Asp, Ile, and Val. Statistical significance was generally not observed between yeasts from *Control* and *Low* treatments, or between yeasts from *Reference* and *High* treatments, except for in Asp and Val, and additionally in Ile for *Control* and *Low* yeasts (Supplemental Table B-2).

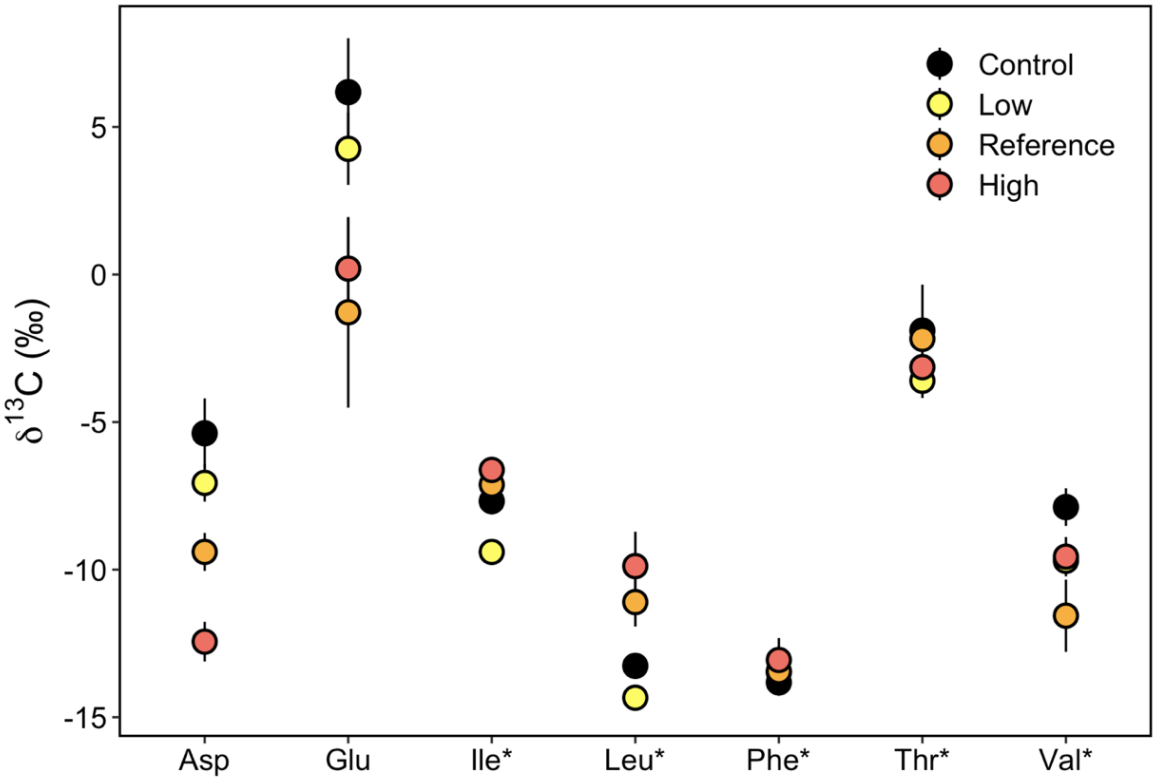


**Figure 2-1.** Carbon amino acid isotope profiles ($\delta^{13}C_{AA}$) of yeast samples grown in *Control* (amino acid-free), *Low*, *Reference*, and *High* amino acid availability treatments. These treatments contained different amounts of aspartic acid (Asp), glutamic acid (Glu), isoleucine (Ile), leucine (Leu), phenylalanine (Phe), threonine (Thr), and valine (Val). Asterisks (*) indicate essential amino acids.

Yeast $\delta^{13}C_{EAA}$ profiles from the AA-free *Control* treatment group were visually distinct from yeast $\delta^{13}C_{EAA}$ profiles of *Reference* and *High* treatment groups in PCA, with PC1 and PC2 explaining 55.5% and 26.8% of the total variance among groups, respectively (Figure 2-2). Separation by treatment group was best explained by Ile (2.30), followed by Val (-1.78), Leu (1.33), Phe (-0.68), while Thr explained the least variation among yeasts of different treatment

groups (0.18), based on the absolute values of the coefficients of the first linear discriminant (LD1). Overall classification accuracy of yeast samples based on $\delta^{13}C_{EAA}$ values in LDA was 80%. Within treatments, yeasts in *Control* and *Low* treatments classified with 100% accuracy, while *Reference* and *High* samples classified with 60% accuracy.

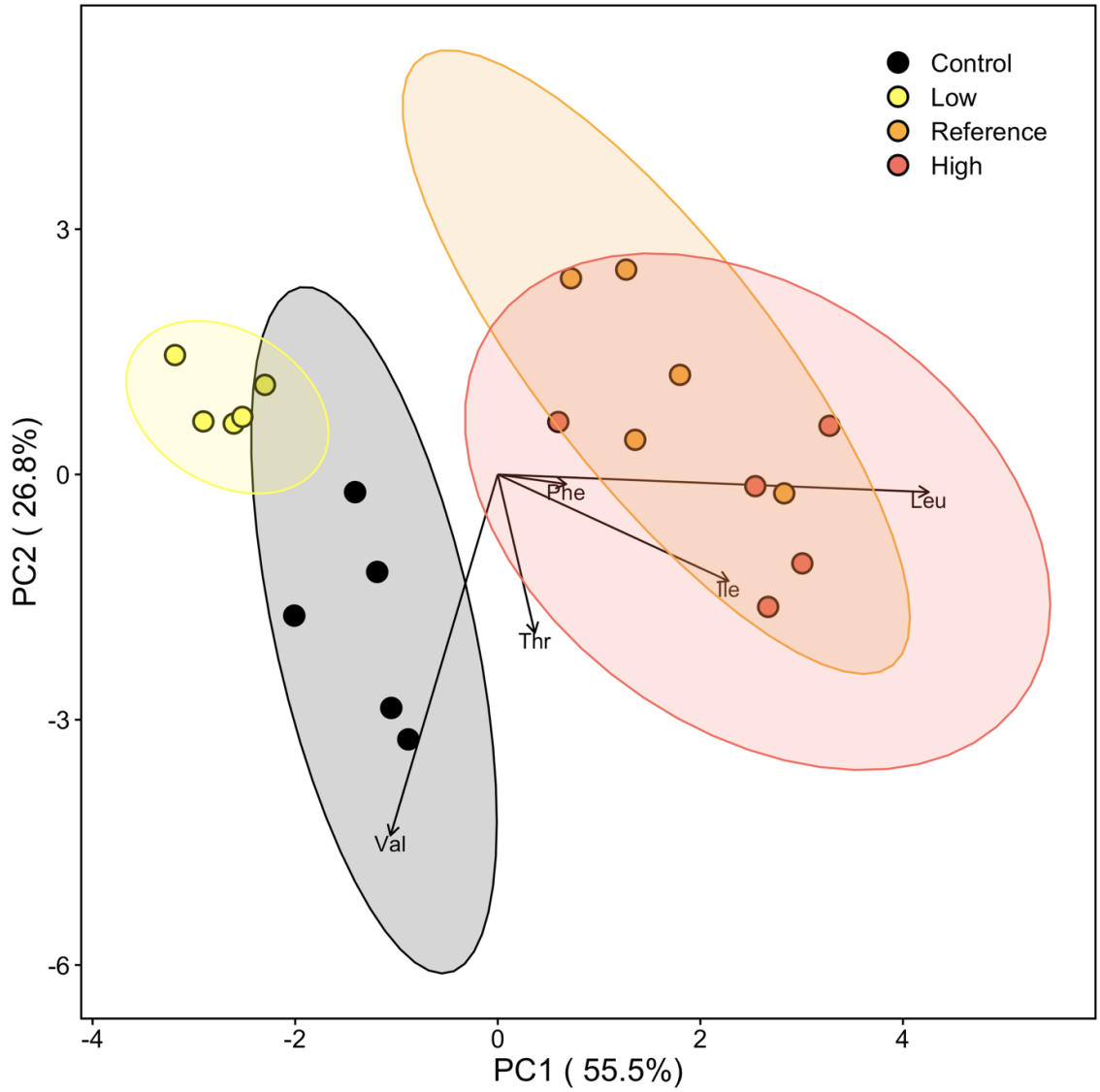


**Figure 2-2.** Principal component analysis using carbon isotope profiles of essential amino acids ($\delta^{13}C_{EAA}$) to group yeast samples grown under four different experimental conditions (*Low*,

*Reference*, and *High,* and amino acid-free *Control*). (Isoleucine (Ile), leucine (Leu), phenylalanine (Phe), threonine (Thr), and valine (Val)). Observations are plotted with 95% data ellipses.

As a general trend, yeasts had higher $\delta^{13}C_{AA}$ values than their substrates, but some yeast $\delta^{13}C_{AA}$ values were lower relative to the substrate for Leu and Phe (Supplemental Table B-1). Differences in $\delta^{13}C_{AA}$ values between diet (substrate) and consumer (yeast) were variable by treatment and AA (Figure 2-3). In yeast from the *Reference* treatment, $\Delta^{13}C_{EAA}$ of both Leu and Val did not differ significantly from zero ($t_4$=0.36, p=0.737; $t_4$=-0.35, p=0.742). Additionally, in *High* treatment yeasts, $\Delta^{13}C_{EAA}$ of Leu did not differ significantly from zero ($t_4$=2.60, p=0.060). Furthermore, results also suggested a convergence toward a $\Delta^{13}C_{EAA}$ value of zero for Phe, when comparing *Reference* and *High* treatment yeasts to yeasts grown in AA-free conditions (*Control*). Amino acids Ile and Thr exhibited similar $\Delta^{13}C_{EAA}$ regardless of substrate AA availability. Conversely, for nonessential AAs Asp and Glu, which can undergo trophic discrimination when moving from diet to consumer, $\Delta^{13}C_{EAA}$ showed the highest deviation from zero for all experimental treatments.

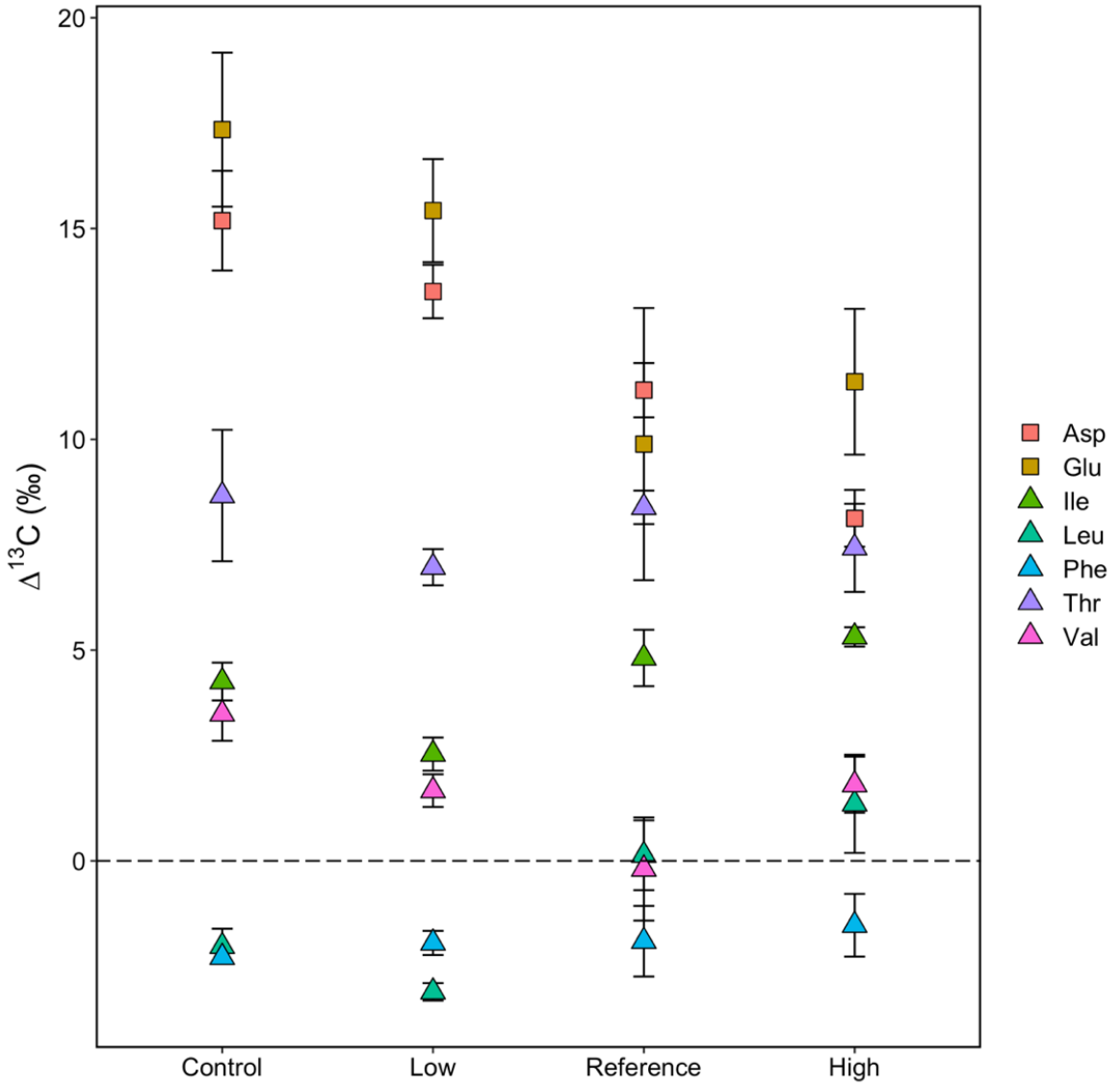


**Figure 2-3.** Mean ± SD $\Delta^{13}C$ ($\delta^{13}C_{Yeast} - \delta^{13}C_{Substrate}$) showing differences in yeast (*Saccharomyces cerevisiae*) $\delta^{13}C_{AA}$ profiles relative to the known substrate $\delta^{13}C_{AA}$ profile for four experimental treatments: amino acid-free *Control*, and treatments supplemented with *Low*, *Reference*, and High amounts of seven amino acids (Asp = aspartic acid, Glu = glutamic acid, Ile = isoleucine, Leu = leucine, Phe = phenylalanine, Thr = threonine, and Val = valine). The dashed line indicates the threshold at which $\Delta^{13}C = 0$. For comparative purposes, $\delta^{13}C_{AA}$ values of *Control* yeasts were also differentiated with $\delta^{13}C_{AA}$ of amino acid supplements ($\delta^{13}C_{Substrate}$). even though no amino acids were present in the substrate. Deviations from $\delta^{13}C_{Substrate}$ here

would therefore be reflective of baseline differences between $\delta^{13}C$ values of fungal AAs that were synthesized de novo, and $\delta^{13}C$ values of AA supplements.

**Discussion**

We observed that baker's yeast (*Saccharomyces cerevisiae*) from the same original culture but exposed to media substrates of differing AA compositions were characterized by different $\delta^{13}C_{AA}$ profiles. Specifically, yeasts could take up some AAs directly from their substrates, which caused their $\delta^{13}C_{AA}$ profiles to shift relative to yeasts grown in AA-free substrates that necessitated ~100% de novo synthesis of AAs. This finding supports our hypothesis that yeast $\delta^{13}C_{EAA}$ of essential AAs would be more similar to substrate $\delta^{13}C_{EAA}$ with increasing substrate AA content because of an increase in direct uptake of available AAs and a subsequent decrease in de novo biosynthesis. This trend was particularly apparent for the essential AAs Leu, Phe, and Val. These results have important implications for the accurate representation and interpretation of fungal resource pathways in basal diet tracing studies using carbon compound-specific stable isotope analysis of individual AAs.

As a whole, yeasts exposed to different amounts of extracellular AAs were distinguishable based on their $\delta^{13}C_{AA}$ values. Differences in $\delta^{13}C_{EAA}$ profiles were especially apparent when comparing yeasts grown in *Reference* and *High* conditions to yeasts grown in AA-free (*Control*) conditions or *Low* amounts of AAs. Notably, we observed higher overlap between $\delta^{13}C_{EAA}$ profiles of *Reference* and *High* treatment yeasts, which may indicate a potential limit to AA uptake by yeast as driven by substrate AA content. Differences in bulk $\delta^{13}C$ among treatments were likely driven by these differences among $\delta^{13}C_{AA}$ profiles because all other media ingredients were given in the same amounts across treatments and all yeasts were plated from the

same initial strain. The high variability in bulk $\delta^{13}C$ in *Control* and *Low* yeasts when compared to *Reference* and *High* treatment yeasts can likely be attributed to the less predictable effects of fractionation during de novo AA synthesis. Additionally, yeasts grown with AA supplements had lower bulk $\delta^{13}C$ compared to *Control* yeasts, with $\delta^{13}C$ decreasing with increasing substrate AA content, which could mean that yeasts exposed to AA-supplemented substrates had entered a later growth phase than *Control* yeasts (Henn et al. 2002).

When comparing $\Delta^{13}C_{AA}$ values between yeast and substrate, we observed that $\delta^{13}C_{AA}$ values of yeast and $\delta^{13}C_{AA}$ values of the substrate in the *Control* treatments (AA-free media) were isotopically distinct because $\delta^{13}C_{AA}$ profiles of *Control* yeast were presumably reflective of de novo synthesized AAs exclusively. This distinction was apparent for *Low* yeasts as well, where having only small amounts of AAs available in the substrate may similarly necessitate de novo AA synthesis. However, yeast $\delta^{13}C_{AA}$ profiles began to converge with substrate $\delta^{13}C_{AA}$ profiles in treatments characterized by higher AA content (*Reference* and *High* treatments), especially for two essential AAs (Leu and Val). While mechanistic differences are unclear, we note that Leu and Val share a common precursor molecule (3-methyl-2-oxobutanoate) in the *S. cerevisiae* AA biosynthetic pathway, where pyruvate is metabolized to Val or Leu (Jones and Fink 1982). Additionally, Leu has been previously identified as a particularly costly AA to produce energetically (Barton et al. 2010), which may cause yeasts to prioritize its uptake when multiple essential AAs are available.

In natural environments, the availability of extracellular AAs in detritus is influenced by the AA composition of parent plant matter (Rice 1982, Rice and Hanson 1984). While Bowen (1987) noted that relative concentrations of AAs stayed fairly consistent among detritus of different origin (Supplemental Table B-3), there can be considerable variation in absolute AA

content among primary producer samples based on differences in protein content (Boyd 1973). Therefore, variation in absolute AA content, which we focused on in the present study, is likely the more important driver of differences in AA uptake rates related to availability. In natural systems, the absolute AA content of detritus is influenced by season (Johnson and Pregitzer 2007) and stage of decomposition (Boyd 1970), which is influenced by litter quality (Krishna and Mohan 2017). For example, the AA content of salt marsh detritus was exhausted of most free AAs within a span of about two weeks (Lee and Bushsbaum unpublished, Valiela and Rietsma 1984, Buchsbaum et al. 1991). Because of the variability that has previously been observed in the AA content of natural substrates, we hypothesize that direct uptake of AAs by fungi is likely to occur in nature, especially on detrital substrates that are relatively immature and/or high in protein. However, additional study is needed to quantify the time period over which absorbed environmental AAs are retained in fungi to understand how long fungal $\delta^{13}C_{AA}$ profiles are likely to reflect those of their substrate after direct uptake.

The ability of fungi to directly take up AAs from extracellular substrates under conditions of high AA availability has important implications for tracing the assimilation of basal resources. This finding may be particularly relevant to studies that identify the ultimate carbon resources (i.e., primary producers) that contribute to consumer diet, such as in determining whether the trophic basis of production is autochthonous (aquatic) or allochthonous (terrestrial) in origin for freshwaters (i.e., quantifying allochthony). In AA isotope fingerprinting studies where fungi have been cultured in AA-free media (e.g., Larsen et al. 2009, 2013), $\delta^{13}C_{AA}$ values of fungi represent ~100% de novo synthesis of AAs. Commercially available yeast has also been used as a proxy for a natural fungal fingerprint (e.g., Thorp & Bowes 2017), in which case growth conditions are entirely unknown. However, our findings suggest that in the case where fungi

represent a pathway for the movement of basal resources, fungal $\delta^{13}C_{AA}$ profiles should reflect those of their primary producer substrates, enabling users to trace the energetic contributions of ultimate (basal) carbon directly from freshwater consumers.

**Conclusions and Recommendations**

Fungi link carbon sources of terrestrial (allochthonous) origin to aquatic food webs. However, quantifying consumer assimilation of basal resources through fungal pathways is complex because fungi have the potential to both biosynthesize all AAs and to absorb AAs directly from their extracellular substrates (Payne and Loomis 2006, Jones and Fink 1982). We found that the ability of yeasts (*S. cerevisiae*) to directly take up essential AAs from their environments drove changes in $\delta^{13}C_{AA}$ profiles, particularly when AAs were available in higher amounts. Because variability in natural substrate $\delta^{13}C_{AA}$ profiles is common, we conclude that fungal $\delta^{13}C_{AA}$ profiles may closely reflect those of their substrates in some instances, such as during seasons where initial colonization of organic matter occurs. This suggests that, particularly for essential AAs, $\delta^{13}C_{AA}$ of animal consumers of fungal-colonized detritus can be reliably traced back to their ultimate (autotrophic) sources of carbon rather than being confounded by unique fungal AA profiles that reflect de novo biosynthesis. We recommend further study on the timing of retention of absorbed environmental AA to understand how long fungal $\delta^{13}C_{AA}$ profiles reflect those of their substrate after direct uptake. We also recommend characterization of detrital AA content to further contextualize the results of this study.

**References**

Amberg D. C., D. J. Burke, and J. N. Strathern. 2005. Methods in yeast genetics. Cold Spring Harbor Laboratory Press, Cold Spring Harbor, NY.

Barton, M. D., D. Delneri, S. G. Oliver, M. Rattray, and C. M. Bergman. 2010. Evolutionary systems biology of amino acid biosynthetic cost in yeast. PLoS ONE 5:e11935.

Bianchi, F., J. S. van't Klooster, S. J. Ruiz, and B. Poolman. 2019. Regulation of amino acid transport in *Saccharomyces cerevisiae*. Microbiology and Molecular Biology Reviews 83:e00024–19.

Bowen, S. H. 1987. Composition and nutritional value of detritus, p. 192-216. In D. J. W. Moriarty and R. S. V. Pullin (eds.) Detritus and microbial ecology in aquaculture. ICLARM Conference Proceedings 14, 420 p. International Center for Living Aquatic Resources Management, Manila, Philippines.

Bowen, S. H. 1980. Detrital nonprotein amino acids are the key to rapid growth of Tilapia in Lake Valencia, Venezuela. Science 207:1216–1218.

Boyd, C. E. 1970. Amino acid, protein, and caloric content of vascular aquatic macrophytes. Ecology 51:902–906.

Boyd, C. E. 1973. Amino acid composition of freshwater algae. Archiv für Hydrobiologie 72:1–9.

Buchsbaum, R., I. Valiela, T. Swain, M. Dzierzeski, and S. Allen. 1991. Available and refractory nitrogen in detritus of coastal vascular plants and macroalgae. Marine Ecology Progress Series 72:131–143.

Cummins, K. W. 1974. Structure and function of stream ecosystems. BioScience 24:631–641.

Curran, B. P., and V. Bugeja. 2006. Basic investigations in *Saccharomyces cerevisiae*. In *Yeast Protocol* (p. 1-13). Humana Press, Totowa, NJ.

Danger, M., J. Cornut, A. Elger, and E. Chauvet. 2012. Effects of burial on leaf litter quality, microbial conditioning and palatability to three shredder taxa. Freshwater Biology 57:1017–1030.

De la Cruz, A. A., and W. E. Poe. 1975. Amino acids in salt marsh detritus. Limnology and Oceanography 20:124–127.

France, R. 2011. Leaves as "crackers," biofilm as "peanut butter": Exploratory use of stable isotopes as evidence for microbial pathways in detrital food webs. Oceanological and Hydrobiological Studies 40:110.

Grossart, H. P., S. Van den Wyngaert, M. Kagami, C. Wurzbacher, M. Cunliffe, and K. Rojas-Jimenez. 2019. Fungi in aquatic ecosystems. Nature Reviews Microbiology 17:339–354.

Hanscho, M., D. E. Ruckerbauer, N. Chauhan, H. F. Hofbauer, S. Krahulec, B. Nidetzky, S. D. Kohlwein, J. Zanghellini, and K. Natter. 2012. Nutritional requirements of the BY series of *Saccharomyces cerevisiae* strains for optimum growth. FEMS Yeast Research 12:796–808.

Henn, M. R., G. Gleixner, and I. H. Chapela. 2002. Growth-dependent stable carbon isotope fractionation by Basidiomycete fungi: $\delta^{13}C$ pattern and physiological process. Applied and Environmental Microbiology 68:4956-4964.

Hieber, M., M. O. and Gessner. 2002. Contribution of stream detritivores, fungi, and bacteria to leaf breakdown based on biomass estimates. Ecology 83:1026–1038.

Johnson, R. M., and K. S. Pregitzer. 2007. Concentration of sugars, phenolic acids, and amino acids in forest soils exposed to elevated atmospheric $CO_2$ and $O_3$. Soil Biology and Biochemistry 39:3159–3166.

Jones, E. W., and G. R. Fink. 1982. Regulation of amino acid and nucleotide biosynthesis in yeast. The molecular biology of the yeast *Saccharomyces* 2:181–299.

Kaushik, N. K., and H. B. N. Hynes. 1971. The fate of the dead leaves that fall into streams. Archiv für Hydrobiologie 68:465–515.

Krishna, M. P., and M. Mohan. 2017. Litter decomposition in forest ecosystems: a review. Energy, Ecology and Environment 2:236–249.

Larsen, T., D. L. Taylor, M. B. Leigh, and D. M. O'Brien. 2009. Stable isotope fingerprinting: a novel method for identifying plant, fungal, or bacterial origins of amino acids. Ecology 90:3526–3535.

Larsen, T., M. Ventura, N. Andersen, D. M. O'Brien, U. Piatkowski, and M. D. McCarthy. 2013. Tracing carbon sources through aquatic and terrestrial food webs using amino acid stable isotope fingerprinting. PLoS ONE 8:e73441.

Larsen, T., L. T. Bach, R. Salvatteci, Y. V. Wang, N. Andersen, M. Ventura, and M. D. McCarthy. 2015. Assessing the potential of amino acid $^{13}C$ patterns as a carbon source tracer in marine sediments: effects of algal growth conditions and sedimentary diagenesis. Biogeoscience 12:4979–4992.

Liew, J. H., K. W. J. Chua, E. R. Arsenault, J. H. Thorp, A. Suvarnaraksha, A. Amirrudin, and D. C. J. Yeo. 2019. Quantifying terrestrial carbon in freshwater food webs using amino acid isotope analysis: Case study with an endemic cavefish. Methods in Ecology and Evolution 10:1594–1605.

Mackay, R. J., and J. Kalff. 1973. Ecology of two related species of caddis fly larvae in the organic substrates of a woodland stream. Ecology 54:499–511.

Mann, K. H. 1988. Production and use of detritus in various freshwater, estuarine and coastal marine systems. Limnology and Oceanography 33:910–930.

Moore, J. C., E. L. Berlow, D. C. Coleman, P. C. de Ruiter, Q. Dong, A. Hastings, N. C. Johnson, et al. 2004. Detritus, trophic dynamics and biodiversity. Ecology Letters 7:584–600.

Ohkouchi, N., N. O. Ogawa, Y. Chikaraishi, H. Tanaka, and E. Wada. 2015. Biochemical and physiological bases for the use of carbon and nitrogen isotopes in environmental and ecological studies. Progress in Earth and Planetary Science 2:1.

Payne, S. H., and W. F. Loomis. 2006. Retention and loss of amino acid biosynthetic pathways based on analysis of whole-genome sequences. Eukaryotic Cell 5:272–276.

Polis, G. A., W. B. Anderson, and R. D. Holt. 1997. Toward an integration of landscape and food web ecology: the dynamic of spatially subsidized food webs. Annual Review of Ecology and Systematics 28:289–316.

R Core Team. 2020. R: A language and environment for statistical computing. R Foundation for Statistical Computing, Vienna, Austria. https://www.R-project.org/

Rice, D. L. 1982. The detritus nitrogen problems: New observations and perspectives from organic geochemistry. Marine Ecology Progress Series 9:153–162.

Rice, D. L., and R. B. Hanson. 1984. A kinetic model for detritus nitrogen: The role of the associated microflora in nitrogen accumulation. Bulletin of Marine Science 35:326–340.

Scott, J. H., D. M. O'Brien, D. Emerson, H. Sun, G. D. McDonald, A. Salgado, and M. L. Fogel. 2006. An examination of the carbon isotope effects associated with amino acid biosynthesis. Astrobiology 6:867–880.

Sigleo, A. C., P. E. Hare, and G. R. Helz. 1983. The amino acid composition of estuarine colloidal material. Estuarine, Coastal and Shelf Science 17:87–96.

Steffan, S. A., and P. S. Dharampal. 2019. Undead food-webs: integrating microbes into the food-chain. Food Webs 18:e00111.

Takizawa, Y., Y. Takano, B. Choi, P. S. Dharampal, S. A. Steffan, N. O. Ogawa, N. Ohkouchi, and Y. Chikaraishi. 2020. A new insight into isotopic fractionation associated with decarboxylation in organisms: implications for amino acid isotope approaches in biogeoscience. Progress in Earth and Planetary Science 7:50.

Thorp, J. H., and R. E. Bowes. 2017. Carbon sources in riverine food webs: New evidence from amino acid isotope techniques. Ecosystems 20:1029–1041.

Valiela, I., and C. S. Rietsma. 1984. Nitrogen, phenolic acids, and other feeding cues for salt marsh detritus. Oecologia 63:350–356.

Vanni, M. J., D. L. DeAngelis, D. E. Schindler, and G. R. Huxel. 2004. Overview: cross-habitat flux of nutrients and detritus. *Food webs at the landscape level*, 3–11.

Venables, W. N., and B. D. Ripley. 2002. Modern Applied Statistics with S. Fourth Edition. Springer, New York.

Walsh, R. G., S. He, and C. T. Yarnes. 2014. Compound-specific $\delta^{13}C$ and $\delta^{15}N$ analysis of amino acids: a rapid, chloroformate-based method for ecological studies. Rapid Communications in Mass Spectrometry 28:96–108.

Webster, J. R., and E. F. Benfield. 1986. Vascular plant breakdown in freshwater ecosystems. Annual Review of Ecology and Systematics 17:567–594.

Whiteman, J. P., E. A. Elliott Smith, A. C. Besser, and S. D. Newsome. 2019. A guide to using compound-specific stable isotope analysis to study the fates of molecules in organisms and ecosystems. Diversity 11:8.

# Chapter 3: Global Analysis of Temperate Steppe Headwater Streams Reveals Consistent Autochthonous Trophic Basis of Production for Fishes


## Abstract

Quantifying the trophic bases of production supporting metazoan consumers in freshwater food webs has been a research priority for many decades. Conceptual models have hypothesized that the relative proportions of autochthonous versus allochthonous resources supporting consumer production reflect the amount of local canopy shading or the type of valley-scale hydrogeomorphology characterizing a particular stream site. However, accurately estimating patterns of basal resource assimilation at broad scales has previously been limited by both ecoregional coverage and methodological limitations inherent to using bulk-tissue stable isotope analysis to trace carbon in lotic systems. Here, we sampled fishes ($n$=271) from 50 low-order temperate steppe stream sites representing three ecoregions across two continents. At each site, we characterized local canopy cover and light regime as well as valley-scale hydrogeomorphology as defined by the functional process zone (FPZ) concept. We used amino acid compound-specific stable isotope analysis (CSIA-AA) of carbon to estimate basal resources supporting fish production using Bayesian mixing models. Results suggested that autochthonous resources provided overwhelming support across all stream sites (93.1–99.6%), whereas allochthonous sources provided negligible direct support for fish food webs. At the valley scale, FPZ type was not predictive of differences in resource use. At the local scale, we observed significant relationships between multiple site characteristics and autochthony that differed by ecoregion, but canopy cover was not found to correlate significantly with basal resource use. These findings indicate the widespread importance of carbon of autochthonous origin for supporting fish production in temperate steppe rivers, despite large variability among sites.

## Introduction

Characterizing the trophic bases of production supporting metazoan consumers in freshwater food webs is a central part of describing stream ecosystem functions, with headwater streams serving as important study sites for this undertaking. In particular, quantifying the relative proportions of autochthonous (in-stream aquatic) versus allochthonous (terrestrial) resources supporting consumer production is an important aspect of our conceptual understanding of lotic ecosystems because these are the dominant carbon pathways upon which whole food webs rely. Historically, headwater streams in forested watersheds were thought to be characterized by trophic bases of production primarily allochthonous in origin because of the simultaneous light limitation on in-stream algal production and high inputs of terrestrial organic matter that result from riparian canopy shade over narrow stream channels (i.e., river continuum concept; Vannote et al. 1980).

Some empirical tests have provided support for this hypothesis in forested watersheds of temperate (Hawkins and Sedell 1981, Haggerty et al. 2002, Rosi-Marshall and Wallace 2002, Grubaugh et al. 2003, Curtis et al. 2018) and tropical (Greathouse and Pringle 2006, Tomanova et al. 2007, Jiang et al. 2011) ecosystems. However, streams draining watersheds of climatically different ecoregions with hydrogeomorphically unique characteristics, such as such as grassland, mountain, and xeric ecoregions of the temperate steppe biome, often do not fit into conceptual models based on forested headwaters (Dodds et al. 2015). While Vannote et al. (1980) noted that autochthonous resources may be more important than allochthonous resources in headwater streams with open canopies, streams located outside of northern forested watersheds lack research attention despite their widespread global occurrence (González-Bergonzoni et al. 2019).

Furthermore, most previous support for allochthonous resource use in headwater streams has been found by classifying invertebrates into functional feeding group designations or by identifying diet items in invertebrate guts, neither of which provide information about carbon assimilated into consumer tissues.

Therefore, while a well-developed framework is important for our ability to contextualize empirical observations, robust tools and techniques are also essential for accurate interpretation of consumer resource use. Although early studies of resource use in lotic systems relied on behavioral or gut content observations, which provide short-term snapshots of ingested (not necessarily assimilated) diet components, the more recent onset of stable isotope analysis has been pivotal for advancing understanding of consumer resource use in streams (Guo et al. 2016). Still, limitations inherent to the stable isotope analysis of bulk-tissues can raise obstacles for interpretation, such as overlapping signatures among materials of terrestrial and algal origin, widespread changes in algal signatures even over small spatiotemporal scales, and issues with collecting sufficient quantities of desirable food sources present at very low standing stocks (Finlay et al. 1999, Finlay 2001, Phillips et al. 2014). These problems may be particularly pronounced in low-order streams (Trudeau and Rasmussen 2003, Estévez et al. 2019).

Fortunately, the recent application and development of compound specific stable isotope analysis of amino acids (CSIA-AA) offers tremendous benefits for understanding complex resource dynamics occurring in stream headwaters (Chapter 1) because carbon isotope values of essential amino acids ($\delta^{13}C_{EAA}$) undergo minimal modification when moving between diet resources and their consumers. Therefore, $\delta^{13}C_{EAA}$ profiles of primary producers can serve as isotopic “fingerprints” (sensu Larsen et al. 2009) that can be traced directly to consumers. This isotopic fingerprinting technique using CSIA-AA can provide more clarity than bulk tissue stable

isotope analysis in studies of complex food webs because these isotopic fingerprints are diagnostic of broad resource groups (e.g., algae, or $C_3$ plants, among others), and they are highly conserved across time and space (e.g., Larsen et al. 2012, 2013, 2015, Chapter 1). Additionally, while bulk-tissue stable isotope analysis provides an integrated $\delta^{13}C$ value for all biomolecular tissue components (i.e., carbohydrate, protein, and lipid fractions), CSIA-AA allows researchers to quantify a unique $\delta^{13}C$ value for each amino acid composing the protein fraction of consumer tissue. Therefore, the high dimensionality of tracers available for CSIA-AA studies can negate issues of overlapping signatures of functionally distinct food sources.

The increasing use of this novel CSIA-AA tool has allowed for further contextualization of a few previous studies that revealed the importance of autochthonous resources not only in grassland or semi-arid reaches (González-Bergonzoni et al. 2018), but also in numerous studies of forested, light-limited headwaters both in temperate and tropical areas (Finlay 2001, McNeely et al. 2007, Lau et al. 2009, Hayden et al. 2016, Neres-Lima et al. 2016, Bellamy et al. 2017, Bellamy et al. 2019) using bulk-tissue isotope analyses. These results suggest that autochthonous algal resources may be preferentially assimilated by consumers even at sites where they are less abundant because they are more labile and of higher quality than detrital matter (Thorp and Delong 1994, 2002, Lau et al. 2009). Therefore, the hydrology and channel morphology that form the physical templates for streams may together provide a better framework than local light regime and canopy cover for predicting basal resource use across diverse headwater systems.

To characterize a stream site based on its integrated hydrology, geology, and morphology (i.e., hydrogeomorphology), we can use the concept of the functional process zone (FPZ; Thorp et al. 2006, 2008). FPZs form physical templates for ecological processes that should share similar patterns among comparable FPZ types (Thoms et al. 2017). Several recent studies have

found evidence for differences in the assemblage or trait structure of invertebrate communities (Godoy et al. 2016, Maasri et al. 2019), fish assemblages (Elgueta et al. 2019, Maasri et al. 2021b, Robbins and Pyron 2021), and food chain length (Thoms et al. 2017) based on FPZ type. Therefore, one might also expect that the underlying hydrogeomorphic template of an FPZ may have the ability to explain differences in resource use. For example, primary productivity is expected to vary by FPZ based on characteristic hydrology (i.e., retention and connectivity), geomorphology (i.e., channel complexity), and riparian influences that include light availability and riparian inputs, and FPZs with high lateral complexity are expected to retain more organic matter over longer periods of time (Thorp et al. 2006, 2008). However, only a few studies have been conducted to assess the FPZ concept as it relates to basal resource use. In a study of the Kanawha River Basin (USA), Thoms et al. (2017) found that basal resources were assimilated differently by invertebrate primary consumers based on their relative availabilities across FPZs. Additionally, González-Bergonzoni et al. (2019) found support for the FPZ concept in the tropical Uraguay River, with apparent differences in the relative proportion of allochthonous and autochthonous resource use between upstream anabranch FPZs and lowland wide FPZ sites.

Here, we quantify the trophic basis of production for fish consumers in understudied temperate steppe headwaters of grassland, mountain steppe, and semi-arid terminal basin regions across continents. In addition, we evaluated potential influential drivers on the trophic basis of production for fish consumers at both local (site), valley (FPZ), and ecoregional scales. We hypothesized that: (1) autochthonous resources would provide the dominant support of fish food webs in temperate steppe headwater streams; (2) hydrogeomorphic variation among FPZs would explain more variation in the trophic basis of production than variation among sites within an FPZ; and (3) at the ecoregion level, allochthonous versus autochthonous basal resource use will

be more highly correlated with local site influences of channel canopy cover in mountain steppe headwaters, but more highly correlated with differences in valley-scale hydrogeomorphology in sites representing understudied grassland and semi-arid terminal basin ecoregions. To test these hypotheses, we quantified the trophic bases of production at low-order (1-4) stream sites of each of three temperate steppe ecoregions on two continents (Mongolia and the United States) using carbon CSIA-AA.

## Methods

### *Study Sites*

We sampled a total of 50 sample sites (2016-2019) within headwater reaches distributed over 10 drainages together representing three types of ecoregions (grassland, mountain steppe, and semi-arid terminal basins) located within two globally significant stretches of temperate steppe biome (United States Great Plains and the Eurasian Steppes of Mongolia; Olson et al. 2001; Figure 3-1; Figure 3-2;
Supplemental Table **C-**1). Mountain steppe sites in the United States (Tensleep and Tongue Rivers, Wyoming, both ultimately tributaries of the Mississippi River) and Mongolia (Delgermörön River, a tributary of the Selenge River) were represented by high-elevation sites that ranged from high-gradient forested sites to meandering streams located in mountain meadows. Grassland steppe rivers sampled included the Kherlen River of Mongolia (a tributary of the Amur River), which is mostly precipitation-fed and therefore controlled by flashy hydrological regimes that alternate periods of flooding and drying, and tributaries of the Niobrara River (Nebraska, USA, a tributary of the Missouri and Mississippi Rivers), which are fed by a combination of precipitation and groundwater inputs from the Ogallala Aquifer. Finally, semi-

arid terminal basin sites, represented by the Bear, Carson, and Humboldt Rivers (flowing from the mountains surrounding the United States Great Basin) and the Khovd and Zavkhan Rivers of northwestern Mongolia (flowing from the Altai and Khangai Mountains), are endorheic streams that are sourced by melting from high-elevation snowpack and glaciers, and then ultimately flow to a terminal lake or dry basin, rather than into the ocean.

### *FPZ Delineation and Site Characterization*

Study sites were selected *a priori* to maximize representation of a wide range of hydrogeomorphic conditions using the GIS-based tool RESonate, which assigns functional process zone (FPZ) designations to river segments within a drainage (Thoms and Parsons 2003, Williams et al. 2013, Maasri et al. 2021a). First, river network models were established using several geospatial datasets, including WorldClim mean annual precipitation (30 arc-second), the Shuttle Radar Topography Mission digital elevation model (DEM; 30 m), the Northern circumpolar soils map from the National Snow and Ice Data Center, and streamline data. Then, rivers were delineated into FPZ segments based on nine hydrogeomorphic variables (mean annual precipitation (WorldClim), elevation, valley width, valley floor width, ratio of valley width to valley floor width, left valley slope, right valley slope, down valley slope, and channel sinuosity), which were extracted at the 10 km scale. Separately for each river, we then constructed a Gower dissimilarity matrix based on normalized (0-1 scale) data representing these nine FPZ variables. To group segments into zones of unique hydrogeomorphology (i.e., FPZs), we then used a hierarchical clustering method using the *cluster* package in R (Maechler et al. 2021). Finally, FPZ segments were mapped, and study sites were selected to represent a variety of FPZ types (Maasri et al. 2021a).

A total of 14 unique FPZ types were represented by the headwater 50 sites sampled: three FPZs in the Mongolia grassland (M_G1, M_G5, and M_G6), one FPZ in the Mongolia mountain steppe (M_M1), two FPZs in the Mongolia semi-arid terminal basin (M_T1 and M_T3), two FPZs in the United States grassland (U_G6 and U_G7), two FPZs in the United States mountain steppe (U_M2 and U_M6), and four FPZs in the United States semi-arid terminal basin (U_T2, U_T3, U_T4, and U_T5; Figure 3-1, Figure 3-2). FPZs are comparable only within their respective ecoregional boundaries.

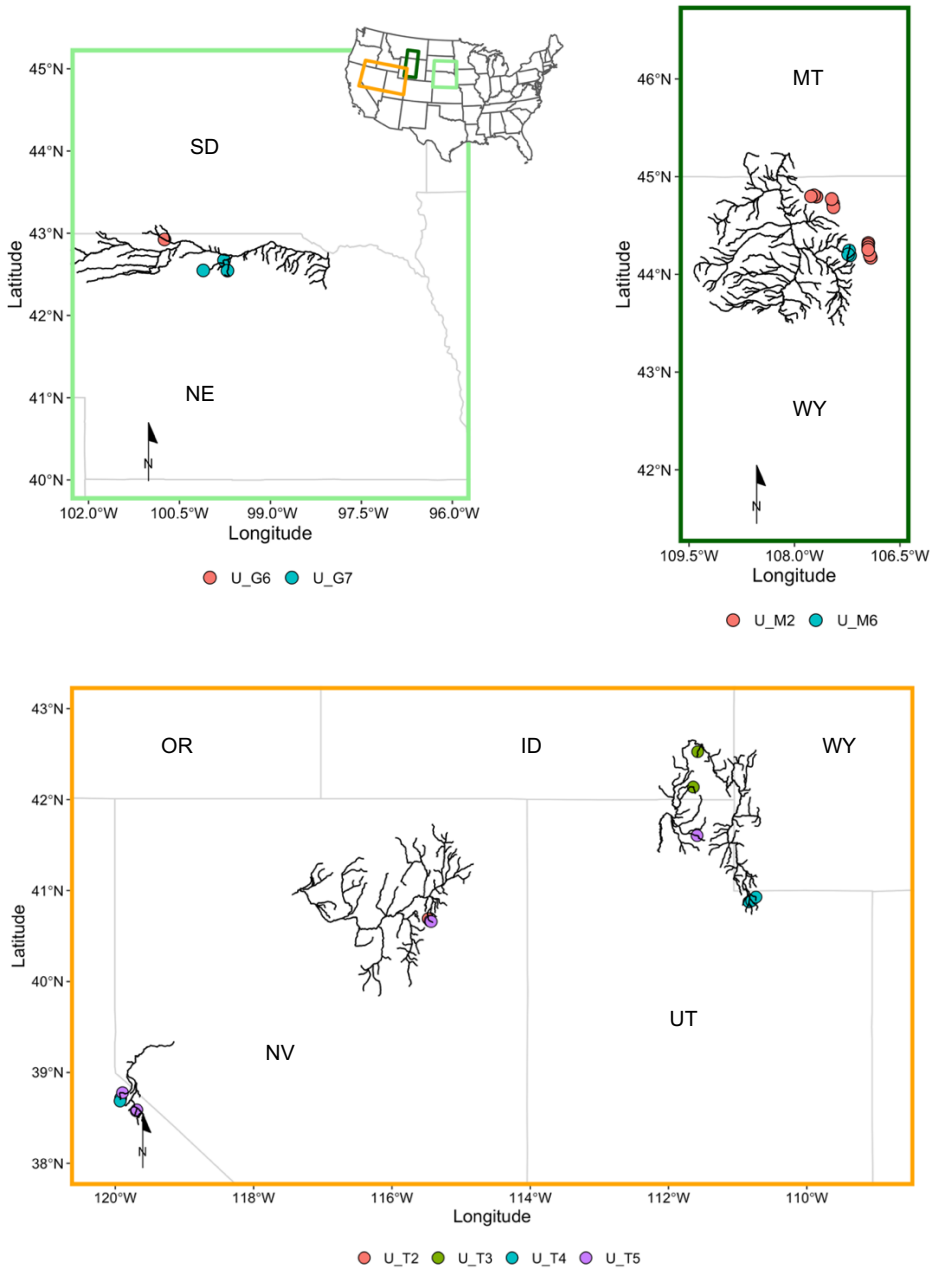


**Figure 3-1.** Map of United States study sites, with panels corresponding to areas located on map by color (light green and top left=grassland, dark green and top right=mountain steppe, and orange and bottom=semi-arid terminal basin). A total of eight functional process zones (FPZs) were sampled across the three ecoregions, together representing a total of 33 sample sites. Point colors represent distinct FPZs sampled within each ecoregion. Colors are not comparable across plots.

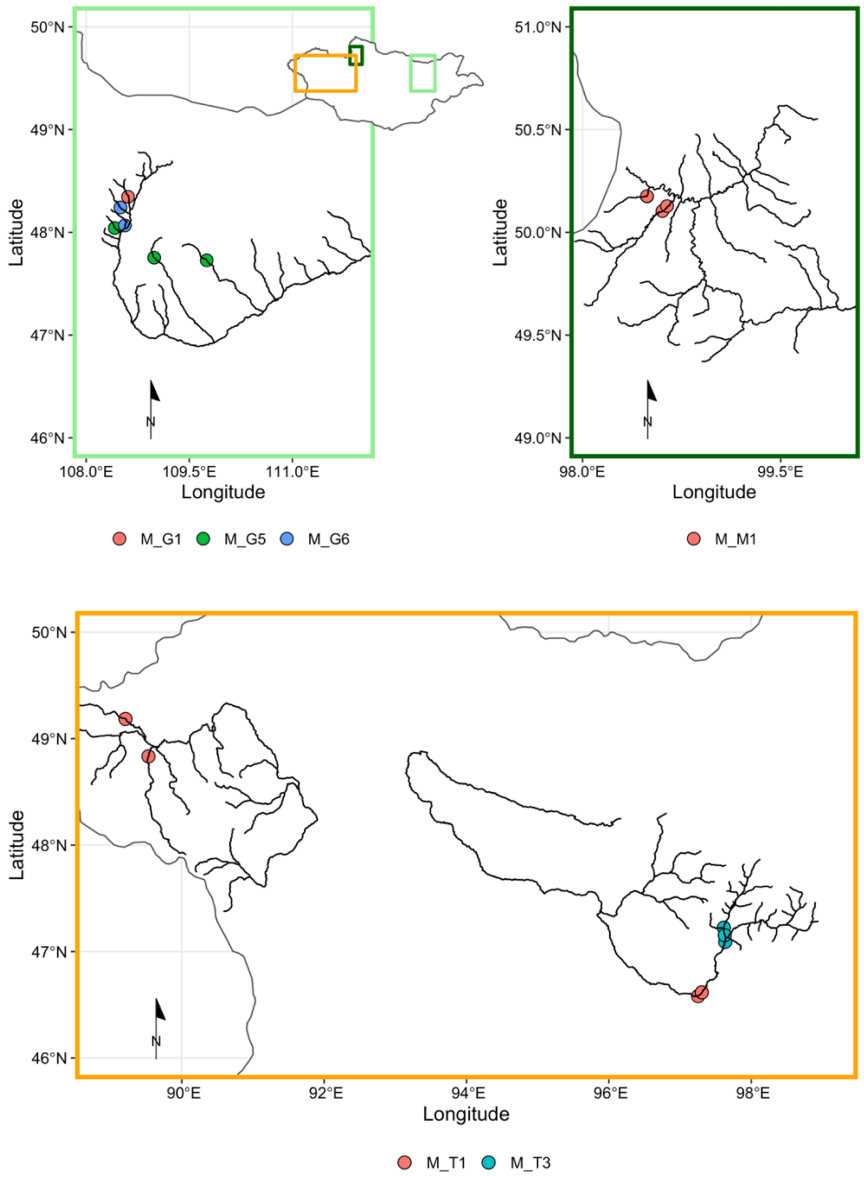


**Figure 3-2.** Map of Mongolia study sites, with panels corresponding to areas located on map by color (light green and top left=grassland, dark green and top right=mountain steppe, and orange and bottom= semi-arid terminal basin). A total of six functional process zones and 17 individual sites were sampled. Point colors represent distinct FPZs sampled within each ecoregion. Colors are not comparable across plots.

In addition to characterized sites based on valley-scale hydrogeomorphology (FPZ type), we also measured site variables at the local scale to analyze sites by canopy cover and light regime. Using Environmental Monitoring and Assessment Program (EMAP) standard methods (Lazorchak et al. 1998), mean canopy cover was estimated using a convex spherical densiometer at both mid-stream and left and right bank positions at evenly spaced transect positions. Average wetted width (m) of the stream channel was estimated at each site by taking the mean of the wetted widths measured along these same equidistant transects. Additionally, we calculated Strahler stream order for each site using the National Hydrology Dataset Plus algorithm according to Pierson et al. (2008; Supplemental Table C-2).

***Fish Collections***

Fishes were handled ethically and collected under Ball State University IACUC permit #126193 to M. Pyron. All necessary field sampling permits and permissions were obtained. Fish samples were collected during the summer season (July-September) during 2016, 2017, 2018, or 2019, depending on ecoregion. We collected a representative fish community sample at each of the 50 sites using single-pass backpack electrofishing (ETS model ABP-2), supplemented by seining, gill netting, and angling, following guidelines of the American Fisheries Society standard methods (Bonar et al. 2009). Fishes were collected from a reach length measuring a minimum of 20x the average wetted stream width. All fishes were weighed to the nearest 0.1 g and measured to standard length to the nearest 1.0 mm. To characterize fish communities in a way that was comparable across geographically dispersed sites, we collected fish tissue samples from three individuals of similar size of the most dominant species representing at least two unique feeding groups when possible. In instances where three species were equally dominant

within the reach, three replicates of an additional species were also analyzed. Fishes were identified to species in the field and later assigned into functional feeding groups based on species and size according to FishBase (Froese and Pauly 2000) or Mendsaikhan et al. (2017). We extracted muscle samples from the area between the dorsal fin and the caudal peduncle using a clean scalpel and then stored them in 70% ethanol until our return to the lab. In the lab, we prepared fish samples for CSIA-AA by rinsing with distilled water, drying in a gravity oven at 60°C for 48 hours, homogenizing using a Wig-L-Bug mixer/amalgamator, and weighing powders into pre-combusted (400°C for 8 hr) glass vials in quantities of ~2 mg. Samples were then sent to the Louisiana State University Stable Isotope Ecology Laboratory for CSIA-AA.

***Resource Collections***

In addition to consumer samples, we sampled representative primary producers, including terrestrial $C_3$ plants (*Salix* spp. and *Pinus* sp.; *n*=21), terrestrial $C_4$ plants (*Zea* sp. and *Panicum* sp.; *n*=3), microalgae (*Chlorella* sp., and a diatom-dominated biofilm; *n*=6), filamentous algae (*Spirogyra* sp.; n=3), cyanobacteria (*Spirulina* sp.; *n*=3), and aquatic macrophytes (*Hydrilla* sp.; *n*=3). Primary producers were either collected *in situ* (diatom-dominated biofilm, *Spirogyra* sp., *Hydrilla* sp., *Salix* spp., *Pinus* sp., *Zea* sp., and *Panicum* sp.) or purchased from commercial suppliers (*Chlorella* sp., and *Spirulina* sp.). Diatom-dominated biofilms and *Spirogyra* sp. were harvested *in situ* from the Zavkhan River, Mongolia, separated and sorted in stream water under a microscope to remove invertebrates and coarse organic material, and air-dried. Diatoms were also filtered to further improve sample purity prior to drying. All other field-collected samples, including *Hydrilla* sp., *Salix* spp., *Pinus* sp., *Zea* sp., and *Panicum* sp. were rinsed with distilled water and examined for purity in the laboratory after collection.

We also supplemented the primary producer resource samples collected in the present study with resource samples collected previously but analyzed for CSIA-AA at the same analytical laboratory (*n*=5; Moyo et al. 2020). From this dataset, we added samples of epiphytic macroalgae (*n*=2) and filamentous algae (*n*=3). All source samples were dried in a laboratory oven at 60ºC for 48 hours or until completely dry, and then homogenized to a fine powder using a Wig-L-Bug mixer/amalgamator. Homogenized samples were then weighed into quantities of 20-30 mg and placed into glass vials that were pre-combusted at 400ºC for 8 hours. Samples were then sent to the Louisiana State University Stable Isotope Ecology Laboratory for CSIA-AA of carbon.

***Carbon Isotope Analysis of Amino Acids***

Samples of fish muscle tissue and resources were analyzed for $\delta^{13}C_{AA}$ at the Louisiana State University Stable Isotope Ecology Laboratory using gas chromatography-combustion-isotope ratio mass spectrometry. Briefly, samples were acid hydrolyzed, derivatized with methyl chloroformate following Walsh et al. (2014) and injected in duplicate onto a constant flow column on a Trace 1310 GC gas chromatograph for amino acid separation. Then, $\delta^{13}C_{AA}$ values were obtained using a Thermo Delta V Advantage isotope ratio mass spectrometer. For primary producer samples, amino acid hydrolysates were cleaned and columned using a Dowex 50WX8-400 cation exchange resin prior to GC/C/IRMS runs. Raw isotope signatures of samples were corrected based on internal standards of L-Norleucine and two reference material mixtures of pure amino acids, in addition to a natural reference material (red drum fish muscle), which were included with all sample runs. Isotope signatures are expressed in delta (δ) per mil (‰) notation according to the following formula, as calculated for each amino acid in the sample tissue:

$\delta^{13}C_{AA}$ (‰) = ([($^{13}C/^{12}C)_{sample}$ / ($^{13}C/^{12}C)_{standard}$) – 1])*1000. Amino acids alanine (Ala), aspartic acid (Asp), glutamic acid (Glu), glycine (Gly), isoleucine (Ile), leucine (Leu), proline (Pro), threonine (Thr), and valine (Val) were recovered for all samples, with a mean analytical error (SD) of 0.25‰ for all amino acids in samples and 0.45‰ for all amino acids in reference materials.

***Statistical Analysis***

All statistical analyses were conducted in R version 3.6.3 (R Core Team 2020). Following the isotopic "fingerprinting" approach, we only used $\delta^{13}C$ data for amino acids that are essential for fishes to trace basal diets (Larsen et al. 2009, 2013). These amino acids were isoleucine (Ile), leucine (Leu), phenylalanine (Phe), threonine (Thr), and valine (Val). We normalized (mean-centered) resource $\delta^{13}C_{EAA}$ values by subtracting the mean $\delta^{13}C$ of all essential amino acids ($n$=5) for a particular sample from each $\delta^{13}C_{EAA}$ in that sample. This method of normalization allows comparison and aggregation of source data across wide spatiotemporal scales by maximizing the biomolecular differences among amino acids, and reducing the noise introduced by environmental variability (Larsen et al. 2020).

We visualized resource data using principal component analysis (PCA) based on normalized $\delta^{13}C_{EAA}$ values, using the *prcomp* package in R (Supplemental Figure C-1). Then, we used an isotopic fingerprinting approach following Larsen et al. (2009, 2013) to classify samples into food source categories that were pre-determined based on PCA visualization with linear discriminant analysis (LDA) using the *MASS* package in R, using non-normalized data. We used a leave-one-out cross validation approach to test whether the three resource groups were

statistically distinguishable from one another, as indicated by a high (>80%) classification accuracy.

To quantify the relative proportions of basal resources composing the trophic base of production for fish consumers, we first plotted normalized consumer $\delta^{13}C_{EAA}$ profiles along with normalized resource $\delta^{13}C_{EAA}$ profiles by ecoregional type as a preliminary visualization of consumer diet sources using PCA. Then, we used two different Bayesian mixing models to estimate the relative proportions of different food sources composing the diet of temperate steppe headwater stream fishes using the *MixSIAR* package in R (Stock and Semmens 2016), each run separately for each ecoregion studied. We parameterized the first model (Model 1) using primary producer resource $\delta^{13}C_{EAA}$ profiles characterized in the present study. Because these resources were analyzed for CSIA-AA at the same analytical laboratory, they can be compared quantitatively with a high level of confidence. The second model (Model 2) was parameterized with published, normalized $\delta^{13}C_{EAA}$ values for autochthonous and allochthonous sources from Liew et al. (2019). Model 2 was used to contextualize Model 1 to ensure that results were retained when resource categories were characterized by a much larger aggregated $\delta^{13}C_{EAA}$ dataset. However, results from Model 2 were more qualitative, because $\delta^{13}C_{EAA}$ values cannot yet be compared among analytical laboratories with complete confidence (Chapter 1).

Prior to running Bayesian models, source and consumer data were examined for normality using Q-Q plots and Shapiro-Wilk tests. For both Model 1 and Model 2, separate mixing models were run for each ecoregional type, with each model set to run for 100,000 iterations (burn-in=50,000) on three parallel Monte Carlo chains with a thinning interval of 50 (i.e. a "normal" run in *MixSIAR*), and non-informative (generalist) priors. For all mixing models, the multiplicative error method was used as recommended by Stock and Semmens (2016), by

incorporating both process and residual error into models. To account for any minimal trophic discrimination between diet and consumer $\delta^{13}C_{EAA}$, we set a small, non-zero value for trophic discrimination (0.1 ± 0.1; McMahon et al. 2010, 2016). Model convergence was assessed using both Geweke and Gelman-Rubin statistics, and when necessary, models were re-run with more iterations until converged (i.e., a "long" run in *MixSIAR*). Mixing model posterior distributions outputs for Model 1 were used for within- and among-FPZ valley-scale site comparisons, and outputs from Model 2 were used to test local site-level differences by ecoregion.

To compare the trophic basis of production among sites, we visualized posterior distributions across three dimensions in ternary plots using the R package, *ggtern* (Hamilton and Ferry 2018), with each axis representing the relative proportion of algal, other autochthonous (i.e., cyanobacteria and macrophytes), and terrestrial resources (Model 1) used as a basal resource by fish consumers at each site. Then, we generated three dimensional hypervolumes (point clouds) using a Gaussian kernel density estimation algorithm for each site using the *hypervolume* package in R (Blonder et al. 2014, Blonder et al. 2018). Hypervolumes were set to include 95% of the total probability density of the Bayesian mixing model posterior distributions (Lesser et al. 2020). We compared hypervolumes across sites by calculating the Sørensen overlap (similarity) between each pair of sites. We then compared overlaps between sites within and among FPZ categories for each ecoregion. Welch's t-tests were used to determine whether similarities in basal resource use were higher within or among FPZs, with higher within-FPZ differences suggesting the importance of local variables and higher among-FPZ differences suggesting the importance of valley-scale drivers on the trophic base of production. One-way ANOVAs were also used to determine differences in resource use by fish feeding guild across all studied sites.

Finally, we ran Pearson's correlations to identify relationships between both local- and valley-scale characteristics and average basal resource use across sites. We used Model 2 mean results for these calculations to identify potential relationships between local and valley-scale stream characteristics and autochthonous versus allochthonous resource use broadly. Local-scale variables were chosen to represent riparian canopy cover characteristics and light regime and included Strahler stream order, average wetted channel width, and canopy cover at both mid-stream and stream bank. Valley-scale variables represented the nine variables used to delineate FPZ segments (mean annual precipitation, elevation, valley width, valley floor width, ratio of valley width to valley floor width, left valley slope, right valley slope, down valley slope, and channel sinuosity).

## Results

### *Basal Resource Estimation*

A principal component analysis (PCA) showed distinct qualitative differences among resource categories, with terrestrial $C_3$ and $C_4$ plants showing distinct signatures from autochthonous resources (Figure 3-3, Supplemental Figure C-1). Within a larger group of autochthonous primary producers, an algae-specific group comprised of samples of field-collected diatoms, filamentous algae (*Spirogyra* sp.), epiphytic macroalgae, and commercially harvested *Chlorella* sp. formed a distinct group that set them apart from other autochthonous resources aquatic macrophytes (*Hydrilla* sp.) and cyanobacteria (*Spirulina* sp.), which formed an intermediate cluster between algal and terrestrial resources. Based on PCA clustering, we identified three potential basal resource categories: algal resources (hereafter referred to as A; $n$=14), other autochthonous resources (hereafter referred to as O; $n$=6), and terrestrial resources

(hereafter referred to as T; *n*=24). Additionally, for all six ecoregional types, fish consumers tended to cluster tightly with autochthonous sources, with PC1 explaining 71.69-77.83% of variation and PC2 explaining an additional 9.41-14.06%.

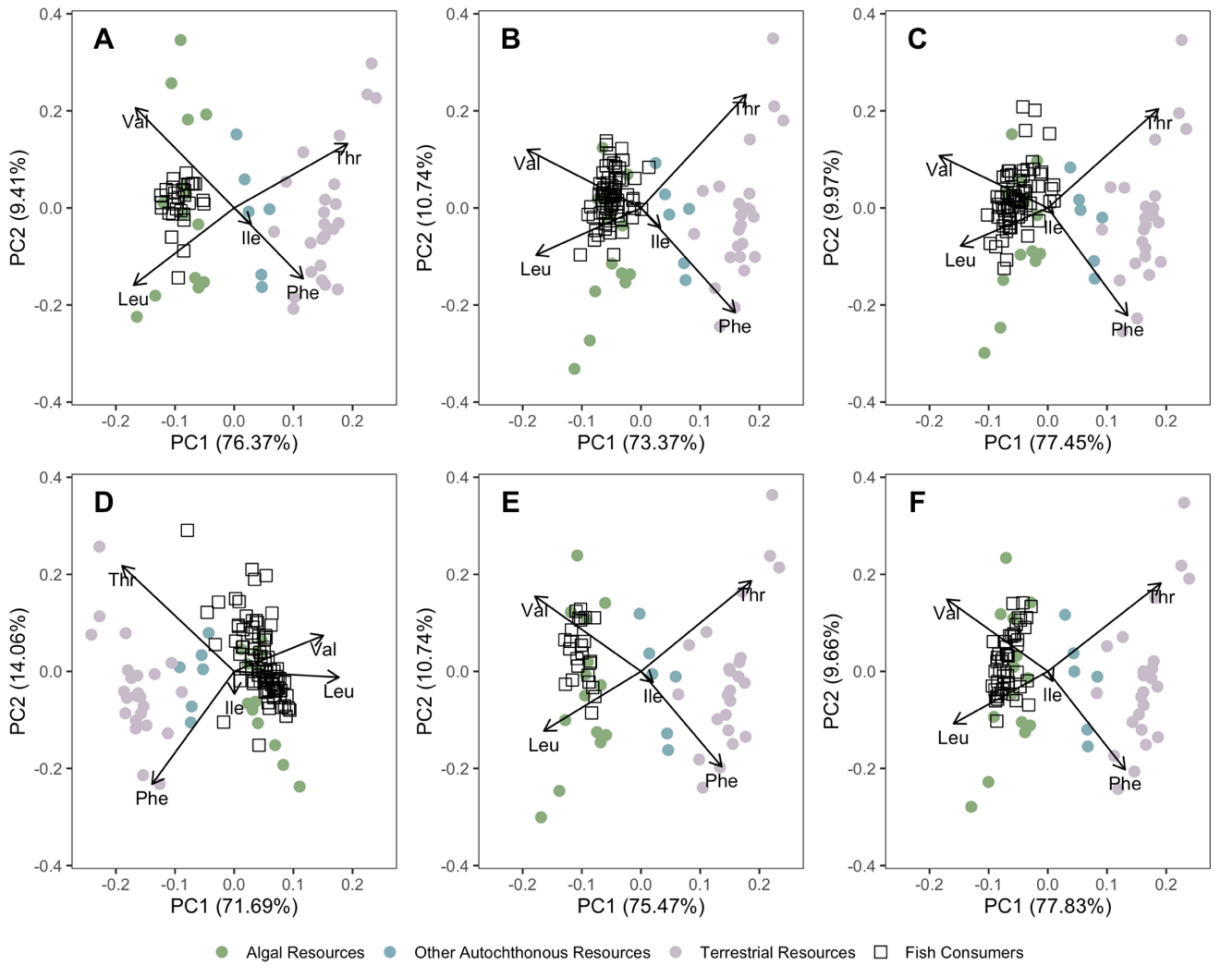


**Figure 3-3.** Principal component analysis showing normalized $\delta^{13}C_{AA}$ profiles of essential amino acids isoleucine (Ile), leucine (Leu), phenylalanine (Phe), threonine (Thr), and valine (Val) for six ecoregional types in two countries (A = United States grassland, B = United States mountain steppe, C = United States semi-arid terminal basin, D = Mongolia grassland, E = Mongolia mountain steppe, and F = Mongolia semi-arid terminal basin). Solid points represent potential basal carbon resources for freshwater systems, categorized as algal, other autochthonous, and

terrestrial, and fish consumers collected in each ecoregion are represented by open boxes. Overlap between sources and consumers indicates likely basal dietary contribution

A linear discriminant analysis (LDA) explained variation among algal (*n*=14), other autochthonous (*n*=6), and terrestrial (*n*=24) food source categories, with LD1 explaining 94.82% of the variance among groups (Supplemental Figure C-2). Of the five essential amino acids used as biotracers in this study, the LDA indicated that Phe explained most variation among groups, followed by Leu, Val, Thr, and Ile, as determined using the absolute values of the coefficients of linear discriminants. LDA with leave-one-out cross validation approach classified source samples into their correct groups with 100% accuracy, which means that sources could be reliably distinguished from one another by group.

Bayesian mixing models met convergence standards with Gelman-Rubin diagnostic values falling under 1.05 for all variables. Mixing model results suggest that algal resources provided the dominant support to fish production in temperate steppe headwater streams overall. Model 1 estimates of consumer reliance on algal resources ranged from 82.5–95.1% across sites representing three ecoregional types in Mongolia and the United States, with other autochthonous food sources ranging from 3.9–16.1% (Table 3-1). Assimilation of terrestrial basal resources by fish consumers was minimal, with terrestrial support ranging from 0.6–2.6% (Table 3-1). Model 2 supported Model 1 results, showing that autochthonous and allochthonous resources provided 93.1–99.7% and 0.4–6.9% support across all sites, respectively (Table 3-1).

**Table 3-1.** Mixing model outputs (mean ± SD) showing the proportional importance of basal carbon resources in supporting fish production in different functional process zones (FPZs) representing three ecoregions grassland, mountain steppe, and semi-arid terminal basin) of the United States and Mongolia. Results are presented for Model 1 (based on putative resources of Algal, Other Autochthonous (Other Auto.), and Terrestrial origin collected in the present study) and Model 2 (based on normalized $\delta^{13}C_{AA}$ resource profiles of autochthonous (Auto.) and allochthonous (Allo.) resources published in Liew et al. (2019).

| | | Model 1 | | | Model 2 | |
|---|---|---|---|---|---|---|
| | **n** | **Algal** | **Other Auto.** | **Terrestrial** | **Allo.** | **Auto.** |
| Mongolia | | | | | | |
| *Grassland* | 44 | 0.864 ± 0.178 | 0.116 ± 0.153 | 0.020 ± 0.037 | 0.056 ± 0.138 | 0.944 ± 0.138 |
| FPZ M_G1 | 7 | 0.951 ± 0.018 | 0.039 ± 0.013 | 0.010 ± 0.005 | 0.011 ± 0.005 | 0.989 ± 0.005 |
| FPZ M_G5 | 23 | 0.829 ± 0.232 | 0.152 ± 0.209 | 0.018 ± 0.029 | 0.069 ± 0.173 | 0.931 ± 0.173 |
| FPZ M_G6 | 14 | 0.825 ± 0.167 | 0.149 ± 0.134 | 0.026 ± 0.044 | 0.057 ± 0.104 | 0.943 ± 0.104 |
| *Mountain Steppe* | 24 | 0.894 ± 0.019 | 0.089 ± 0.017 | 0.017 ± 0.002 | 0.016 ± 0.006 | 0.984 ± 0.006 |
| FPZ M_M1 | 24 | 0.894 ± 0.019 | 0.089 ± 0.017 | 0.017 ± 0.002 | 0.016 ± 0.006 | 0.984 ± 0.006 |
| *Terminal Basin* | 29 | 0.942 ± 0.009 | 0.041 ± 0.006 | 0.017 ± 0.003 | 0.004 ± 0.001 | 0.996 ± 0.001 |
| FPZ M_T1 | 15 | 0.944 ± 0.007 | 0.040 ± 0.005 | 0.017 ± 0.003 | 0.004 ± 0.001 | 0.996 ± 0.001 |
| FPZ M_T3 | 14 | 0.941 ± 0.006 | 0.042 ± 0.004 | 0.017 ± 0.002 | 0.004 ± 0.001 | 0.996 ± 0.001 |
| United States | | | | | | |
| *Grassland* | 29 | 0.878 ± 0.016 | 0.102 ± 0.014 | 0.019 ± 0.003 | 0.012 ± 0.004 | 0.988 ± 0.004 |
| FPZ U_G6 | 8 | 0.884 ± 0.012 | 0.098 ± 0.010 | 0.019 ± 0.002 | 0.011 ± 0.002 | 0.989 ± 0.002 |
| FPZ U_G7 | 21 | 0.876 ± 0.018 | 0.104 ± 0.015 | 0.020 ± 0.003 | 0.013 ± 0.005 | 0.987 ± 0.005 |
| *Mountain Steppe* | 73 | 0.846 ± 0.087 | 0.148 ± 0.086 | 0.006 ± 0.002 | 0.007 ± 0.003 | 0.993 ± 0.004 |
| FPZ U_M2 | 56 | 0.833 ± 0.094 | 0.161 ± 0.093 | 0.007 ± 0.002 | 0.008 ± 0.003 | 0.992 ± 0.003 |
| FPZ U_M6 | 17 | 0.889 ± 0.036 | 0.105 ± 0.035 | 0.006 ± 0.001 | 0.006 ± 0.001 | 0.994 ± 0.001 |

| | | | | | | |
|---|---|---|---|---|---|---|
| *Terminal Basin* | 72 | 0.890 ± 0.098 | 0.088 ± 0.083 | 0.022 ± 0.019 | 0.020 ± 0.036 | 0.980 ± 0.036 |
| FPZ U_T2 | 6 | 0.896 ± 0.068 | 0.085 ± 0.060 | 0.019 ± 0.009 | 0.013 ± 0.009 | 0.987 ± 0.009 |
| FPZ U_T3 | 11 | 0.907 ± 0.049 | 0.071 ± 0.034 | 0.022 ± 0.016 | 0.010 ± 0.006 | 0.990 ± 0.006 |
| FPZ U_T4 | 27 | 0.909 ± 0.066 | 0.071 ± 0.054 | 0.020 ± 0.013 | 0.012 ± 0.012 | 0.988 ± 0.012 |
| FPZ U_T5 | 28 | 0.864 ± 0.134 | 0.111 ± 0.115 | 0.025 ± 0.027 | 0.033 ± 0.055 | 0.967 ± 0.055 |

At the ecoregion level, we observed differences in the relative proportions of algal resources among ecoregions. Algal resources provided the highest support to fish consumers in the semi-arid terminal basin ecoregions of both Mongolia (94.2 ± 0.9%) and the United States (89.0 ± 9.8%). In the United States, algal resources composed a higher proportion of basal carbon use in grassland ecoregion sites (87.8 ± 1.6%) compared to mountain steppe ecoregion sites (84.6 ± 8.7%), while the opposite was true in Mongolia (Table 3-1). Overall, basal resources supporting fish consumers were overwhelmingly autochthonous in origin across all ecoregions studied, and support of terrestrial resources was negligible (Figure 3-4, Figure 3-5).

M_G1

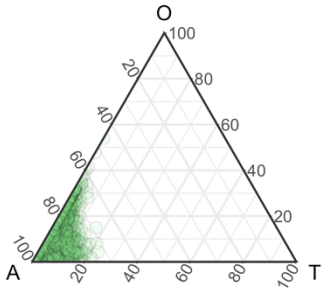


M_G5_a

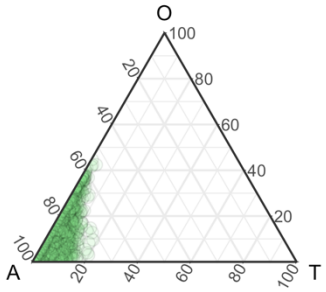


M_G5_b

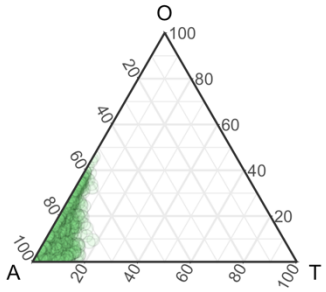


M_G5_c

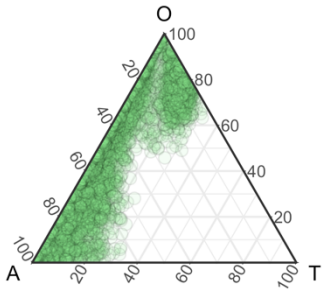


M_G6_a

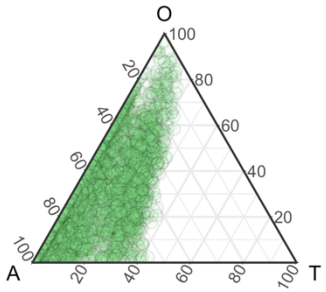


M_G6_b

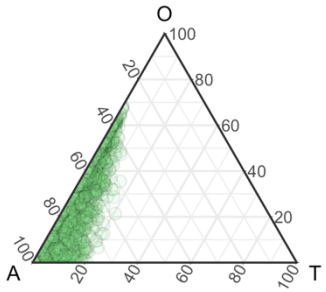


M_M1_a

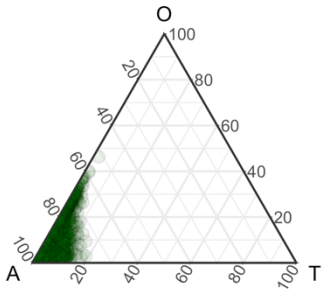


M_M1_b

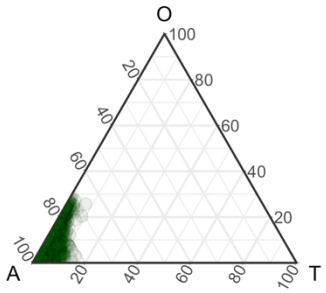


M_M1_c

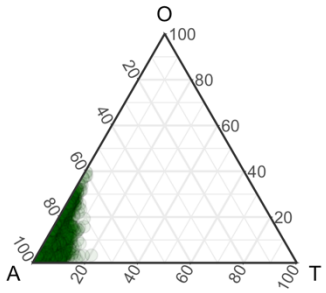


M_M1_d

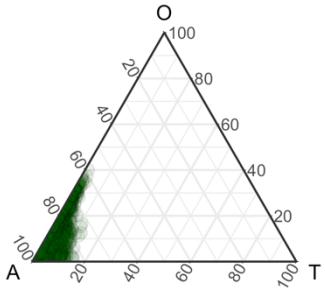


M_T1_b

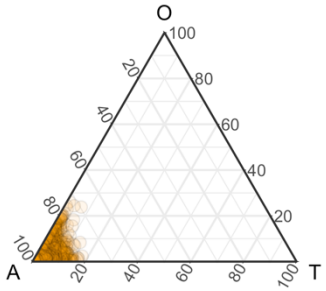


M_T1_c

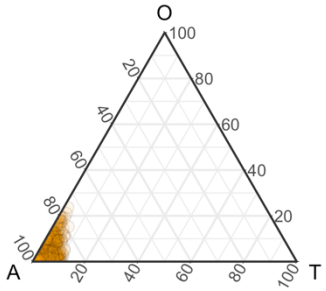

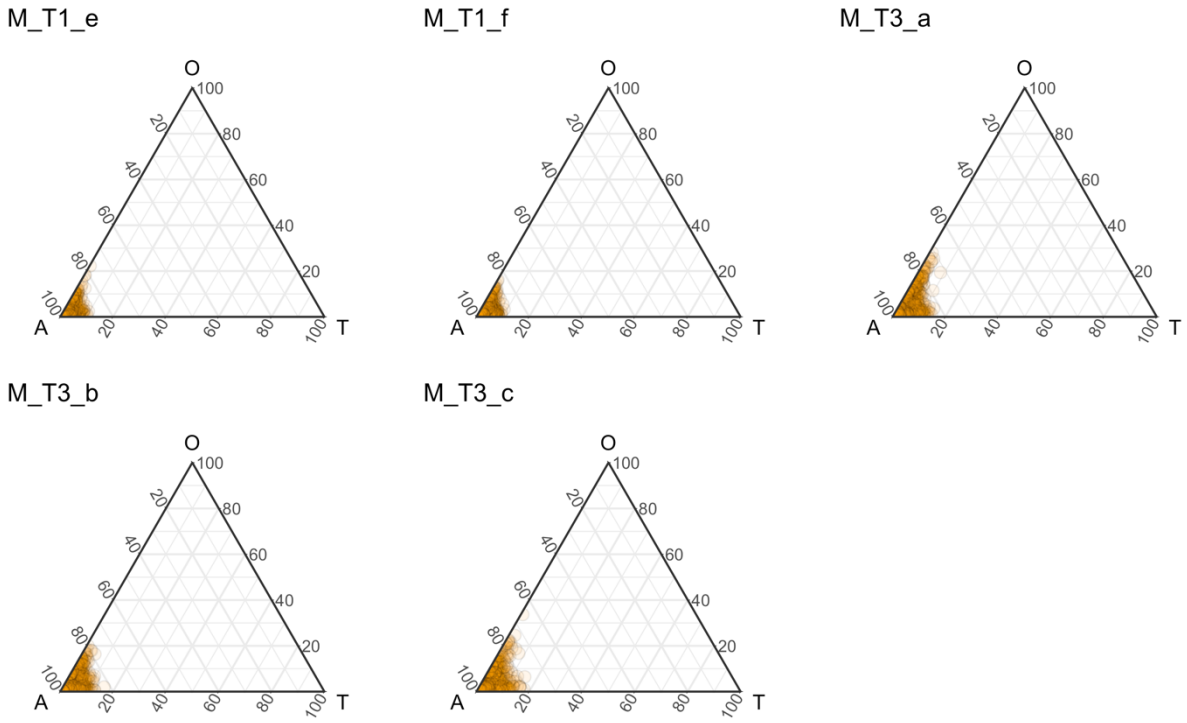


**Figure 3-4.** Ternary plots showing the basal resources contributing to the trophic basis of production for fishes in Mongolia, based on Bayesian mixing model posterior distributions describing the probable contributions of algal (A), other autochthonous (O), and terrestrial (T) resources contributing to the trophic basis of production for fish consumers collected in each ecoregional type (grassland=light green, mountain steppe=dark green, and semi-arid terminal basin=brown). Each plot represents a different study site. Sites are categorized into their respective functional process zones (U_G6, U_G7, U_M2, U_M6, U_T2, U_T3, U_T4, and U_T5), with lowercase letters indicating site replicates.

U_G6_a

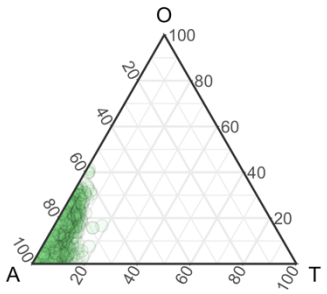


U_G7_a

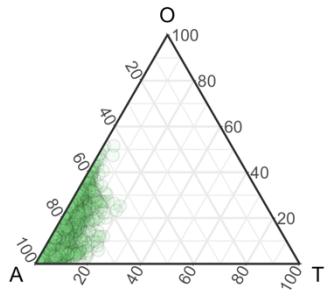


U_G7_b

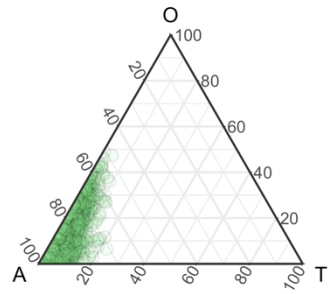


U_G7_c

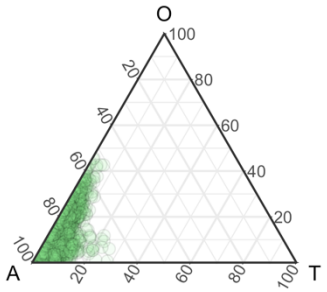


U_M2_a

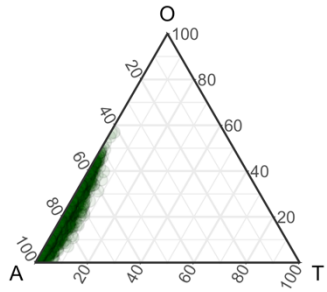


U_M2_b

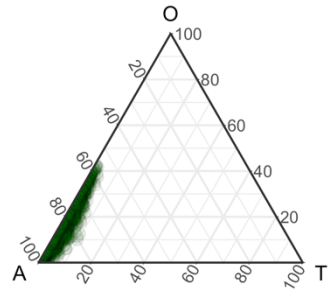


U_M2_c

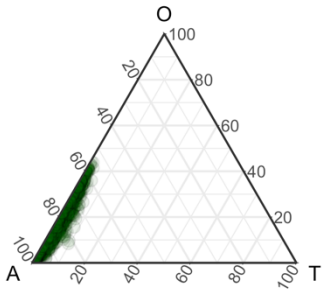


U_M2_d

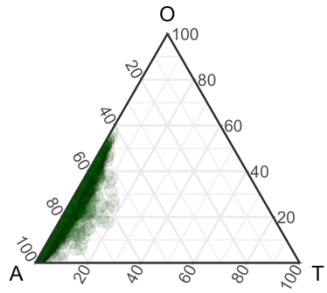


U_M2_e

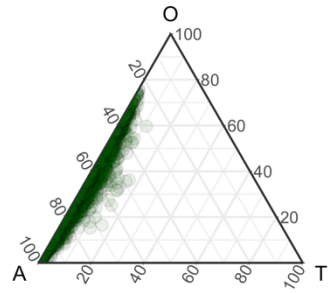


U_M2_f

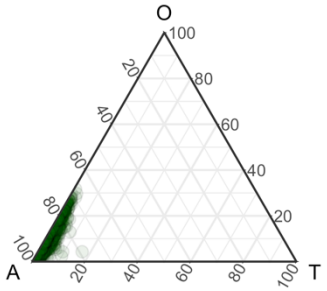


U_M2_g

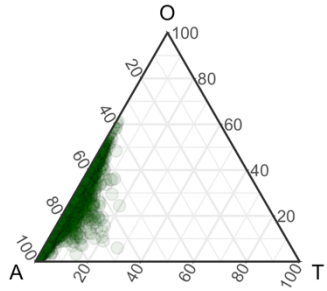


U_M2_h

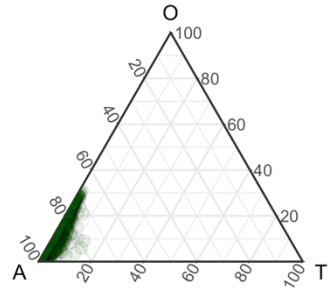

U_M2_i

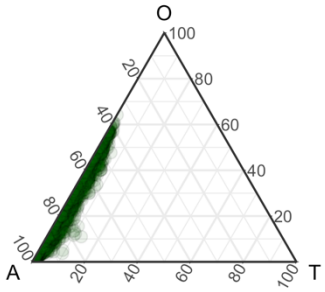


U_M2_j

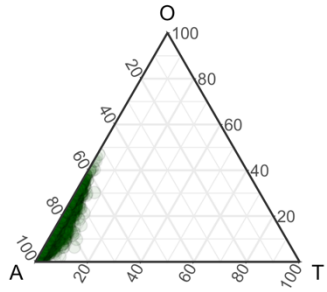


U_M2_k

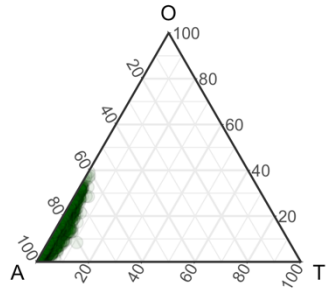


U_M2_l

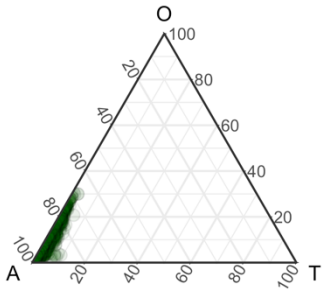


U_M6_a

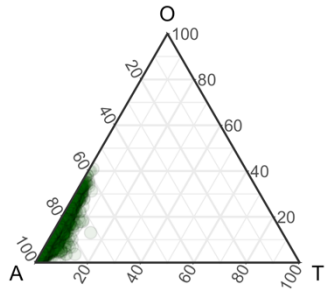


U_M6_b

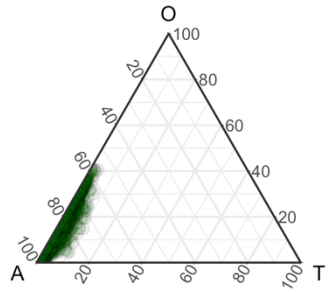


U_M6_c

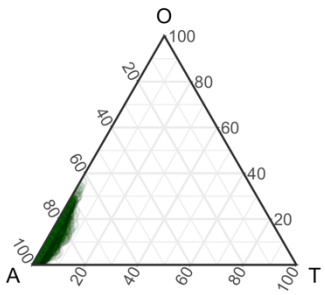


U_T2_a

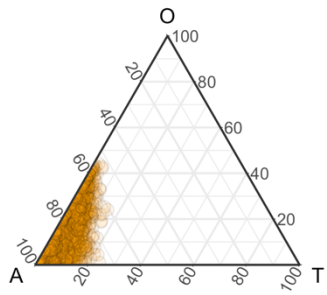


U_T3_a

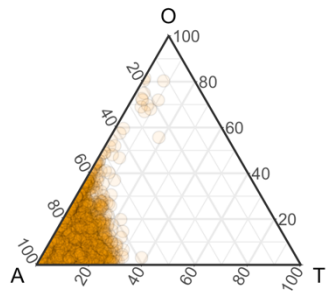


U_T3_b

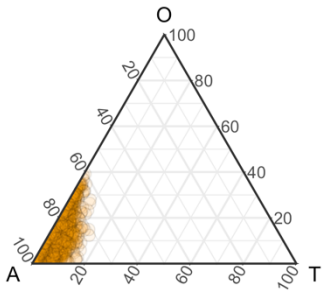


U_T4_a

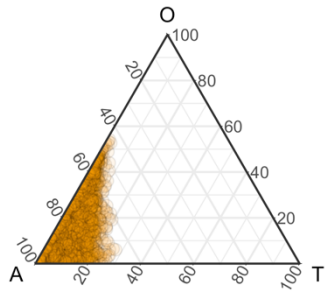


U_T4_b

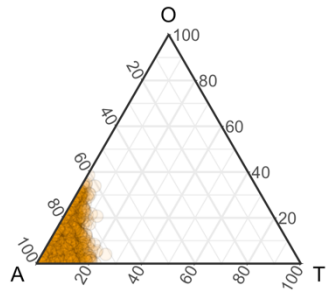

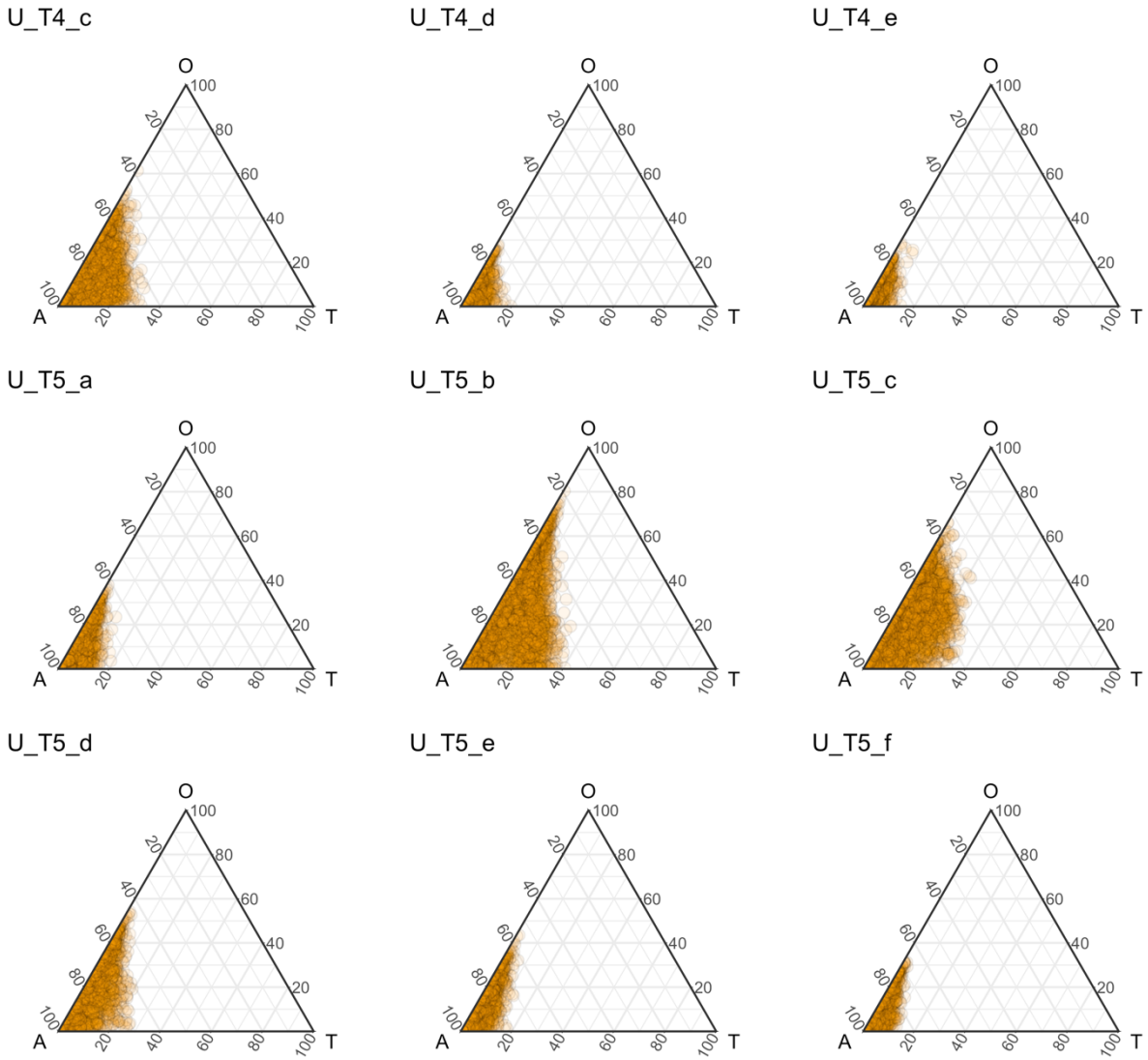


**Figure 3-5.** Ternary plots showing the basal resources contributing to the trophic basis of production for fishes at United States sites, based on Bayesian mixing model posterior distributions describing the probable contributions of algal (A), other autochthonous (O), and terrestrial (T) resources contributing to the trophic basis of production for fish consumers collected in each ecoregional type (grassland=light green, mountain steppe=dark green, and semi-arid terminal basin=brown). Each plot represents a different study site. Sites are categorized into their respective functional process zones (U_G6, U_G7, U_M2, U_M6, U_T2, U_T3, U_T4, and U_T5), with lowercase letters indicating site replicates.

### *Fish Community*

We analyzed a total of 271 individual fishes representing three ecoregional types in two countries: United States grassland (*n*=29), United States mountain steppe (*n*=73), United States terminal basin (*n*=72), Mongolia grassland (*n*=44), Mongolia mountain steppe (*n*=24), and Mongolia terminal basin (*n*=29; Supplemental Table C-4). Of the 27 unique species collected, three feeding groups were represented: piscivores (*n*=49), invertivores (*n*=175), and omnivores (*n*=47). United States fish assemblages included 10 native species, 6 species that were nonnative within at least one part of their collected range, and one hybrid (*Salmo trutta* x *Salvelinus fontinalis*). Mongolia was represented only by native species (*n*=11; Supplemental Table C-4).

Across all sampled sites, we observed some differences in the proportion of algal resources (df=2, F=4.72, p=0.010), other autochthonous resources (df=2, F=3.54, p=0.030), and terrestrial resources (df=2, F=6.55, p=0.002) by fish feeding guild. For omnivorous fishes, the trophic basis of production was characterized by a significantly lower proportion of algal resources (p=0.007) and significantly higher proportions of both other autochthonous (p=0.023) and terrestrial resources (p=0.001) than invertivorous fishes, and omnivores also assimilated a significantly higher proportion of terrestrial resources than piscivorous fishes (p=0.031).

### *Local- and Valley-Scale Comparisons*

Comparisons of hypervolumes based on Sørensen overlap values revealed variability across sites by ecoregion, but no consistent patterns were observed (Supplemental Table C-6, Supplemental Table C-7, Supplemental Table C-8, Supplemental Table C-9, Supplemental Table C-10, Supplemental Table C-11). Sørensen overlaps were higher among sites within FPZs than sites among different FPZs for Mongolia grassland sites and United States grassland sites, and

Sørensen overlaps were higher across different FPZs than they were among sites within an FPZ for the United States mountain steppe sites and for the semi-arid terminal basin sites in both Mongolia and the United States (Figure 3-4, Figure 3-5). However, no statistically significant differences in Sørensen overlap values were observed when comparing within-FPZ and among-FPZ Sørensen overlap values for any studied ecoregions. The highest Sørensen overlap values occurred between sites within FPZs in the United States grassland ecoregion (0.814 ± 0.115), and the lowest (and most variable) Sørensen overlap values occurred among different FPZs in the Mongolia grassland ecoregion (0.285 ± 0.367; Table 3-2).

**Table 3-2.** Mean ± SD Sørensen overlaps (similarity) occurring within and among functional process zone (FPZ) categories for each ecoregion. Among-FPZ Sørensen overlaps were not calculated for Mongolia mountain steppe sites, because sites studied were all replicates of the same FPZ type.

| Ecoregion | Within-FPZ Sørensen | Among-FPZ Sørensen |
|---|---|---|
| Mongolia Grassland | 0.285 ± 0.367 | 0.323 ± 0.318 |
| Mongolia Mountain Steppe | 0.806 ± 0.119 | NA |
| Mongolia Semi-Arid Terminal Basin | 0.726 ± 0.150 | 0.755 ± 0.140 |
| United States Grassland | 0.814 ± 0.115 | 0.712 ± 0.177 |
| United States Mountain Steppe | 0.534 ± 0.232 | 0.585 ± 0.242 |
| United States Semi-Arid Terminal Basin | 0.409 ± 0.260 | 0.476 ± 0.255 |

When examined as a whole, no significant correlations were observed between local nor valley-scale site characteristics and autochthony. However, when analyzed by ecoregion, several trends emerged. For local factors, we observed a significant negative correlation between bank canopy cover and autochthony ($r_2$=-0.97, p=0.030) for Mongolia mountain steppe sites, but no

relationship was observed between mid-stream canopy cover and autochthony at these sites. At United States mountain steppe sites, marginally significant relationships were found between autochthony and Strahler stream order ($r_{13}$=0.47, p=0.076) and wetted width ($r_{13}$=0.47, p=0.080). Finally, autochthony increased with increasing Strahler stream order ($r_{12}$=0.60, p=0.023) at United States terminal basin sites. Valley-scale variables that showed significant relationships with autochthonous resource assimilation included the ratio of valley width to valley floor width ($r_4$=-0.90, p=0.014), down valley slope ($r_4$=0.90, p=0.015), and channel sinuosity ($r_4$=0.88, p=0.021) in the Mongolia grassland ecoregion, elevation in the United States grassland ($r_2$=0.99, p=0.009), valley floor width ($r_{13}$=0.52, p=0.046) and left valley slope ($r_{13}$=-0.74, p=0.002) within the United States mountain steppe, and finally down valley slope at United States terminal basin sites ($r_{12}$=0.79, p<0.001).

**Discussion**

In this study, we present multiple lines of evidence that carbon of autochthonous origin was the dominant resource providing the trophic basis of production for fish in headwater streams of the temperate steppe biomes across continents. This result provided strong support for our first hypothesis that autochthonous resources would provide the ultimate dominant support for fish food webs in temperate steppe headwaters. This result also contradicts the commonly supported idea that local canopy cover is the primary control for resource use in headwater streams (Vannote et al. 1980). We found negligible direct support of allochthonous resource use in our sampled sites, even for those characterized by high canopy cover, and even at mountain steppe sites that provided the most similar comparisons to the forested headwater streams that established the foundational ideas of the river continuum concept (Vannote et al. 1980). Across

ecoregions, we found no consistent relationships between canopy cover measured at mid-stream or stream bank and resource use. However, we did observe the most significant relationships between local site variables and basal resource use at mountain steppe sites of both the United States and Mongolia and terminal basin sites of the United States, all of which were characterized by relatively high canopy cover overall. Our study did not provide evidence that the FPZs we examined were important in influencing food sources. We did not find evidence to support the FPZ concept, because sites representing different FPZs within an ecoregion did not have significantly different degrees of overlap in their resource bases when compared to site replicates of the same FPZ type within an ecoregion. We did observe significant relationships between certain valley-scale variables and resource use, but these variables differed according to site and no broad-scale explanatory patterns emerged.

The emerging method of CSIA-AA allows users to trace and quantify assimilated, rather than merely ingested, basal resources with a high level of accuracy (Chapter 1). Relatively recent developments in biochemical methods in diet tracing have challenged the commonly held idea that detritus plays a dominant role in supporting headwater stream consumers based on its availability in these systems (Brett et al. 2017). This is because organisms have been found to preferentially assimilate high-quality resources even when present in low biomass (Marcarelli et al. 2011, Brett et al. 2017). Support for allochthonous resource use in headwaters has been based largely on observations of invertebrate functional feeding group proportions in the stream environment (Jiang et al. 2011) or on gut contents of invertebrates (Rosi-Marshall et al. 2016). Both observations merely provide snapshots of feeding behaviors rather than integrated diet, and they do not differentiate between presence and assimilation of food in the fish intestinal tract. Because CSIA-AA allows evaluation of the basal diet through the lens of fish consumer tissues,

it enables researchers to accurately and specifically quantify the basal resources that have actually been assimilated (and thus are important to growth), rather than those resources that have been ingested but hold minimal nutritional value.

Here, both Model 1 and Model 2 provided evidence for autochthonous resources providing the dominant support for fish food webs overall. We also observed some site-level differences in the relative proportions of algal versus other autochthonous resources (i.e., macrophytes and cyanobacteria) comprising the trophic basis of production. However, these differences could not be explained universally by valley-scale FPZ categorizations, and overlap in resource use did not differ when comparing within-FPZ site overlaps or among-FPZ site overlaps for any ecoregions studied. This result does not support previous studies that suggested that valley-scale hydrogeomorphology may be an important driver of basal resource use (Thoms et al. 2017, González-Bergonzoni et al. 2019). However, these previous studies both had greater coverage of single river networks, rather than broad spatial coverage across headwater sites of many different streams. Therefore, hydrogeomorphic differences among FPZs in the present study were likely not as distinct because they focused on only low-order segments of these stream networks and did not make comparisons to downstream sites. Additionally, limited replication of certain FPZ types (e.g., M_G1, U_G6, U_T2) may have obscured potential differences in basal resource use at the valley scale.

While fishes representing different feeding guilds did show some statistically significant differences in basal resource assimilation, the magnitude of these differences was not particularly ecologically meaningful because algal resources were dominant over both other autochthonous resources and terrestrial resources for all sites. However, omnivorous fishes were more likely to be supported by a more variable mixture of algal, other autochthonous, and terrestrial resources

than other feeding groups, which relied on mostly algae across sites. This also suggests that terrestrial insects were not a common food source for invertivores at these sites during the time of sampling, which supports findings from two studies of gut contents for fishes collected at some of the same sites sampled as part of the present study (Minder et al. 2020, 2021). As generalists, omnivorous fishes may be supported by some proportion of less desirable food resources when compared to invertivores and piscivores. Many of the omnivores collected were small-bodied minnows that may rely on macrophyte cover for shelter and could be more likely to feed on invertebrates associated with aquatic plants, as well as the aquatic plants themselves (Mendsaikhan et al. 2017). Still, because CSIA-AA relies on amino acid tracers in the protein fraction of consumer diets specifically, using CSIA-AA to quantify diets of omnivorous fishes that rely on a more diverse range of resources than just animal protein may introduce some uncertainty. Studies by Newsome et al. (2011) and Kelly and Martínez del Rio (2010) demonstrated evidence that CSIA-AA may be most accurate in diet tracing of carnivorous metazoans that are characterized by high protein diets. Therefore, further study may uncover new ways to better interpret mixing model results from omnivorous fishes included in this study.

While results presented here show strong evidence for autochthonous basal support of fish food webs, more methodological work is needed to completely rule out the role of fungi or other heterotrophic microorganisms in providing support for temperate steppe stream food webs. Developments toward the appropriate treatment of fungi in CSIA-AA studies of natural systems suggest that current fungal $\delta^{13}C_{EAA}$ profile characterizations may not accurately represent fungi for studies focused on the ultimate sources of carbon (i.e., autochthonous versus allochthonous) fueling consumer food webs (Chapter 2). However, a review by Brett et al. (2017) highlighted the nutritional importance of algal resources for fish food webs, even in cases when availability

of fungal resources is high. Previous studies have shown that diets consisting of purely heterotrophic bacteria were insufficient for the survival of freshwater zooplankton and that these zooplankton preferentially assimilated algal diet components when fed a mixture of heterotrophic bacteria and algae (Martin-Creuzburg et al. 2011, Beck and Freese 2011, Taipale et al. 2012, Taipale 2014, Wenzel et al. 2012). Nevertheless, the results presented here strongly indicate that terrestrial vegetation did not directly support food webs at any sampled sites, even at sites where canopy cover and channel shading were high.

Our findings that autochthonous resources provide important basal support for consumers in lotic systems support a growing number of studies using bulk tissue (Bunn et al. 2003, McNeely et al. 2007, Hayden et al. 2016, Neres-Lima et al., 2016) and compound specific (Lau et al. 2009, Guo et al. 2017, Thorp and Bowes 2017, Liew et al. 2019, Ebm et al. 2020) stable isotope analyses. These studies have found evidence for the primary, ultimate dependence by fish consumers on autochthonous resources. Thorp and Bowes (2017) found carbon of algal origin to be the dominant source of support for fishes for the Mississippi and Ohio rivers over many decades. Additionally, Liew et al. (2019) found predominantly autochthonous support for an endangered fish in the freshwater cave system using CSIA-AA. In a study of subalpine headwater stream fishes, Ebm et al. (2020) reported that polyunsaturated fatty acids from algal resources were vital for the development of neural organs across species groups, suggesting that important algal resources may be selectively retained within fish biomass (Guo et al. 2016, Brett et al. 2017). Therefore, because algal resources are highly nutritious, labile, and contain essential compounds needed for metazoan growth (Thorp and Delong 1994, 2002, Brett et al. 2017), carbon of autochthonous origin is likely of widespread importance as an energy pathway for lotic food webs (Mayer and Likens 1987). Future studies that identify basal resources for both fishes

and their invertebrate intermediates may be useful to further contextualize the movement and assimilation of autochthonous carbon in temperate steppe stream systems.

**Conclusion**

In the largest study to date quantifying basal resources in headwater streams using CSIA-AA, we found evidence for widespread autochthonous support of fish production in headwater streams of three ecoregions of two globally significant regions of the temperate steppe biome across two continents. Basal carbon sources supporting fish production at a highly diverse range of low-order stream sites sampled at the global scale were overwhelmingly autochthonous in origin. Local and valley-scale (FPZ) drivers of this finding were variable by site, and we did not identify environmental predictors that could explain the consistency of this result among sites, suggesting that autochthony may be more ubiquitous than previously thought. Quantifying the relative proportions of basal resources that provide the trophic basis of production for fish consumers is critical because these resources form the template onto which entire food webs are built in ecosystems.

**References**

Bellamy, A. R., J. E. Bauer, and A. G. Grottoli. 2019. Contributions of autochthonous, allochthonous, and aged carbon and organic matter to macroinvertebrate nutrition in the Susquehanna River basin. Freshwater Science 38:616–628.

Bellamy, A. R., J. E. Bauer, and A. G. Grottoli. 2017. Influence of land use and lithology on sources and ages of nutritional resources for stream macroinvertebrates: a multi-isotopic approach. Aquatic Sciences 79:925–939.

Blonder, B., C. Lamanna, C. Violle, and B. J. Enquist. 2014. The n-dimensional hypervolume. Global Ecology and Biogeography 23:595–609.

Blonder, B., C. B. Morrow, B. Maitner, D. J. Harris, C. Lamanna, C. Violle, B. J. Enquist, and A. J. Kerkhoff. 2018. New approaches for delineating n-dimensional hypervolumes. Methods in Ecology and Evolution 9:305–319.

Bonar, S. A., W. A. Hubert, and D. W. Willis. 2009. Standard methods for sampling North American freshwater fishes.

Brett, M. T., S. E. Bunn, S. Chandra, A. W. E. Galloway, F. Guo, M. J. Kainz, P. Kankaala, D. C. P. Lau, T. P. Moulton, M. E. Power, J. B. Rasmussen, S. J. Taipale, J. H. Thorp, and J. D. Wehr. 2017. How important are terrestrial organic carbon inputs for secondary production in freshwater ecosystems? Freshwater Biology 62:833–853.

Bunn, S. E., P. M. Davies, and M. Winning. 2003. Sources of organic carbon supporting the food web of an arid zone floodplain river. Freshwater Biology 48:619–635.

Curtis, W. J., A. E. Gebhard, and J. S. Perkin. 2018. The river continuum concepts predicts prey assemblage structure for an invertivorous fish along a temperate riverscape. Freshwater Science 37:618–630.

Dodds, W. K., K. Gido, M. R. Whiles, M. D. Daniels, and B. P. Grudzinski. 2015. The Stream Biome Gradient Concept: factors controlling lotic systems across broad biogeographic scales. Freshwater Science 34:1–19.

Ebm, N., F. Guo, M. T. Brett, S. E. Bunn, and M. J. Kainz. 2020. Polyunsaturated fatty acids in fish tissues more closely resemble algal than terrestrial diet sources. Hydrobiologia 848:371–383.

Elgueta, A., M. C. Thoms, K. Górski, G. Díaz, and E. M. Habit. 2019. Functional process zones and their fish communities in temperate Andean river networks. River Research and Applications 35:1702–1711.

Estévez, E., J. M. Álvarez-Martínez, M. Álvarez-Cabria, C. T. Robinson, T. J. Battin, and J. Barquin. 2019. Catchment land cover influences macroinvertebrate food-web structure and energy flow pathways in mountain streams. Freshwater Biology 64:1557–1571.

Finlay, J. C. 2001. Stable-carbon-isotope ratios of river biota: implications for energy flow in lotic food webs. Ecology 82:1052–1064.

Finlay, J. C., M. E. Power, and G. Cabana. 1999. Effects of water velocity on algal carbon isotope ratios: Implications for river food web studies. Limnology and Oceanography 44:1198–1203.

Froese, R., D. Pauly (Eds.). 2000. FishBase 2000: concepts designs and data sources (Vol. 1594). WorldFish.

Godoy, B. S., J. Simião-Ferreira, S. Lodi, and L. G. Oliveira. 2016. Functional process zones characterizing aquatic insect communities in streams of the Brazilian Cerrado. Neotropical Entomology 45:159–169.

González-Bergonzoni, I., P. B. Kristensen, A. Baattrup-Pedersen, E. A. Kristensen, A. B. Alnoee, and T. Riis. 2018. Riparian forest modifies fueling sources for stream food webs but not food-chain length in lowland streams of Denmark. Hydrobiologia 805:291–310.

González-Bergonzoni, I., A. D'Anatro, N. Vidal, S. Stebniki, G. Tesitore, I. Silva, and F. T. de Mello. 2019. Origin of fish biomass in a diverse subtropical river: An allochthonic-supported biomass increase following flood pulses. Ecosystems 22:1736–1753.

Greathouse, E. A., and C. M. Pringle. 2006. Does the river continuum concept apply on a tropical island? Longitudinal variation in a Puerto Rican stream. Canadian Journal of Fisheries and Aquatic Sciences 63:134–152.

Grubaugh, J., B. Wallace, and E. Houston. 2003. Production of benthic macroinvertebrate communities along a southern Appalachian river continuum. Freshwater Biology 37:581–596.

Guo, F., M. J. Kainz, F. Sheldon, and S. E. Bunn. 2016. The importance of high-quality algal food sources in stream food webs – current status and future perspective. Freshwater Biology 61:815–831.

Guo, F. S. E. Bunn, M. T. Brett, M. J. Kainz. 2017. Polyunsaturated fatty acids in streams food webs – high dissimilarity among producers and consumers. Freshwater Biology 62:1325–1334.

Haggerty, S. M., D. P. Batzer, and C. R. Jackson. 2002. Macroinvertebrate assemblages in perennial headwater streams of the Coastal Mountain range of Washington, U.S.A. Hydrobiologia 479:143–154.

Hamilton N. E., and M. Ferry. 2018. ggtern: Ternary Diagrams Using ggplot2. Journal of Statistical Software, Code Snippets 87:1–17.

Hawkins, C. P., and J. R. Sedell. 1981. Longitudinal and seasonal changes in functional organization of macroinvertebrate communities in four Oregon streams. Ecology 62:387–397.

Hayden, B., S. M. McWilliam-Hughes, and R. A. Cunjak. 2016. Evidence for limited trophic transfer of allochthonous energy in temperate river food webs. Freshwater Science 35:544–558.

Jiang, X., J. Xiong, Z. Xie, and Y. Chen. 2011. Longitudinal patterns of macroinvertebrate functional feeding groups in a Chinese river system: A test for river continuum concept (RCC). Quaternary International 244:289–295.

Kelly, L. J., and C. Martínez del Rio. 2010. The fate of carbon in growing fish: an experimental study of isotopic routing. In Review. Physiological and Biochemical Zoology 83: 473–480.

Larsen, T., D. E. Taylor, M. B. Leigh, D. M. O'Brien. 2009. Stable isotope fingerprinting: a novel method for identifying plant, fungal, or bacterial origins of amino acids. Ecology 90:3526–3535.

Larsen, T., M. J. Wooller, M. L. Fogel, D. M. O'Brien. 2012. Can amino acid carbon isotope ratios distinguish primary producers in a mangrove ecosystem? Rapid Communications in Mass Spectrometry 26:1541–1548.

Larsen, T., M. Ventura, N. Andersen, D. M. O'Brien, U. Piatkowski, and M. D. McCarthy. 2013. Tracing carbon sources through aquatic and terrestrial food webs using amino acid stable isotope fingerprinting. PLoS ONE 8:e73441.

Larsen, T., L. T. Bach, R. Salvatteci, Y. V. Wang, N. Andersen, M. Ventura, M. D. McCarthy. 2015. Assessing the potential of amino acid $^{13}C$ patterns as a carbon source tracer in

marine sediments: effects of algal growth conditions and sedimentary diagenesis. Biogeosciences Discussions 12:4979–4992.

Larsen, T., T. Hansen, and J. Dierking. 2020. Characterizing niche differentiation among marine consumers with amino acid $\delta^{13}C$ fingerprinting. Ecology and Evolution 10:7768–7782.

Lau, D. C., P. Leung, M. Y. Kenneth, and D. Dudgeon. 2009. Are autochthonous foods more important than allochthonous resources to benthic consumer in tropical headwater streams? Journal of the North American Benthological Society 28:426–439.

Lazorchak, J. M., D. J. Klemm, and D. V. Peck (Eds.). 1998. Environmental monitoring and assessment program surface waters: field operations and methods for measuring the ecological condition of wadeable streams.

Lesser, J. S., W. R. James, C. D. Stallings, R. M. Wilson, J. A. Nelson. 2020. Trophic niche size and overlap decreases with increasing ecosystem productivity. Oikos 129:1303–1313.

Liew, J. H., K. W. J. Chua, E. R. Arsenault, J. H. Thorp, A. Suvarnaraksha, A. Amirrudin, and D. C. J. Yeo. 2019. Quantifying terrestrial carbon in freshwater food webs using amino acid isotope analysis: Case study with an endemic cavefish. Methods in Ecology and Evolution 10:1594–1605.

Maasri, A., J. H. Thorp, J. K. Gelhaus, F. Tromboni, S. Chandra, and S. J. Kenner. 2019. Communities associated with the Functional Process Zone scale: A case study of stream macroinvertebrates in endorheic drainages. Science of the Total Environment 677:184–193.

Maasri, A., J. H. Thorp, N. Kotlinski, J. Kiesel, B. Erdenee, and S. C. Jähnig. 2021a. Variation in macroinvertebrate community structure of functional process zones along the river

continuum: New elements for the interpretation of the river ecosystem synthesis. River Research and Applications 37:665–674.

Maasri, A., M. Pyron, E. R. Arsenault, J. H. Thorp, B. Mendsaikhan, F. Tromboni, M. Minder, S. J. Kenner, J. Costello, S. Chandra, A Otgonganbat, and B. Boldgiv. 2021b. Valley-scale hydrogeomorphology drives river fish assemblage variation in Mongolia. Ecology and Evolution *In press*.

Maechler M., P. Rousseeuw, A. Struyf, M. Hubert, K. Hornik. 2021. cluster: Cluster Analysis Basics and Extensions. R package version 2.1.2.

Marcarelli, A. M., C. V. Baxter, M. M. Mineau, and R. O. Hall, Jr. 2011. Quantity and quality: unifying food web and ecosystem perspectives on the role of resource subsidies in freshwaters. Ecology 92:1215–1225.

Martin-Creuzburg, D., B. Beck, and H. M. Freese. 2011. Food quality of heterotrophic bacteria for *Daphnia magna*: Evidence for a limitation by sterols. FEMS Microbiology Ecology 76:592–601.

Mayer, M. S., and G. E. Likens. 1987. The importance of algae in a shaded headwater stream as food for an abundant caddisfly (Trichoptera). Journal of the North Americal Benthological. Society 6:262–269.

McMahon, K. W., M. L. Fogel, T. S. Elsdon, S. R. Thorrold. 2010. Carbon isotope fractionation of amino acids in fish muscle reflects biosynthesis and isotopic routing from dietary protein. Journal of Animal Ecology 79:1132–1141.

McMahon, K. W., S. R. Thorrold, L. A. Houghton, and M. L. Berumen. 2016. Tracing carbon flow through coral reef food webs using a compound-specific stable isotope approach. Oecologia 180:809–821.

McNeely, C., J. C. Finlay, and M. E. Power. 2007. Grazer traits, competition, and carbon sources to a headwater stream food web. Ecology 88:391–401.

Mendsaikhan, B., Y. Y. Dgebuadze, and P. Surenkhorloo. 2017. Guide Book to Mongolian Fishes. World Wildlife Fund for Nature (WWF) Mongolia Programme.

Minder, M., E. R. Arsenault, B. Erdenee, and M. Pyron. 2020. Dietary specificity and overlap in endorheic river fishes: how do native and nonnative species compare? Journal of Fish Biology 97:453–464.

Minder, M., E. R. Arsenault, B. Erdenee, A. Maasri, and M. Pyron. 2021. Diet overlap among non-native trout species and native cutthroat trout (*Oncorhynchus clarkii*) in two U.S. ecoregions. Ecology and Evolution 11:2782–2795.

Moyo, S., J. Olin, J. Johnson, P. Lopez-Duarte, B. J. Roberts, L. Hooper-Bui, H. Bennadji, and M. J. Polito. 2020. Southern Louisiana Marsh Food Webs: 2016 Amino Acid Compound-Specific Stable Isotope Data. Distributed by: Gulf of Mexico Research Initiative Information and Data Cooperative (GRIIDC), Harte Research Institute, Texas A&M University–Corpus Christi. doi:10.7266/n7-fx66-gp35

Neres-Lima, V., E. F. Brito, F. A. M. Krsulović, A. M. Detweiler, A. E. Hershey, and T. P. Moulton. 2016. High importance of autochthonous basal food source for the food web of a Brazilian tropical stream regardless of shading. International Review of Hydrobiology 101:132–142.

Newsome, S. D., M. L. Fogel, L. Kelly, C. Martinez del Rio. 2011. Contributions of direct incorporation from diet and microbial amino acids to protein synthesis in Nile tilapia. Functional Ecology 25:1051–1062.

Olson, D. M., E. Dinerstein, E. D. Wikramanayake, N. D. Burgess, G. V. N. Powell, E. C. Underwood, J. A. D'Amico, I. Itoua, H. E. Strand, J. C. Morrison, C. J. Loucks, T. F. Allnutt, T. H. Ricketts, Y. Kura, J. F. Lamoreux, W. W. Wettengel, P. Hedao, and K. R. Kassem. 2001. Terrestrial ecoregions of the world: a new map of life on Earth. Bioscience 51:933–938.

Phillips, D. L., R. Inger, S. Bearhop, A. L. Jackson, J. W. Moore, A. C. Parnell, B. X. Semmens, and E. J. Ward. 2014. Best practices for use of stable isotope mixing models in food-web studies. Canadian Journal of Zoology 92:823–835.

Pierson, S. M., B. J. Rosenbaum, L. D. McKay, and T. G. Dewald. 2008. Strahler stream order and Strahler calculator values in NHD*Plus*. *SOSC Technical Paper*, 11.

R Core Team. 2020. R: A language and environment for statistical computing. R Foundation for Statistical Computing, Vienna, Austria. https://www.R-project.org/

Robbins, J., and M. Pyron. 2021. Geomorphological characteristics of the Wabash River, USA: Influence on fish assemblages. Ecology and Evolution 11**:**4542–4549.

Rosi-Marshall, E. J., and B. Wallace. 2002. Invertebrate food webs along a stream resource gradient. Freshwater Biology 47:129–141.

Rosi-Marshall, E. J., K. L. Vallis, C. V. Baxter, and J. M. Davis. 2016. Retesting a prediction of the River Continuum Concept: autochthonous versus allochthonous resources in the diets of invertebrates. Freshwater Science 35:534–543.

Stock, C., and B. X. Semmens. 2016. MixSIAR GUI User Manual. Version 3.1. https://github.com/brianstock/MixSIAR.

Taipale, S. J., M. T. Brett, K. Pulkkinen, and M. J. Kainz. 2012. The influence of bacteria-dominated diets on *Daphnia magna* somatic growth, reproduction, and lipid composition. FEMS Microbiology Ecology 82:50–62.

Taipale, S. J., M. T. Brett, M. W. Hahn, D. Martin-Creuzburg, S. Yeung, M. Hiltunen, et al. 2014. Differing *Daphnia magna* assimilation efficiencies for terrestrial, bacterial and algal carbon and fatty acids. Ecology 95:563–576.

Thoms, M. C., and M. Parsons. 2003. Identifying spatial and temporal patterns in the hydrological character of Condamine-Balonne River, Australia, using multivariate statistics. River Research and Applications 19:443–457.

Thoms, M., M. Delong, J. Flotemersch, and S. Collins. 2017. Physical heterogeneity and aquatic community function in river networks: A case study from the Kanawha River Basin, USA. Geomorphology 290:277–287.

Thorp, J. H., and M. D. Delong. 1994. The riverine productivity model: an heuristic view of carbon sources and organic processing in large river ecosystems. Oikos 70:305–308.

Thorp, J. H., and M. D. Delong. 2002. Dominance of autochthonous autotrophic carbon in food webs of heterotrophic rivers. Oikos 96:543–550.

Thorp, J. H., M. C. Thoms, and M. D. Delong. 2006. The riverine ecosystem synthesis: biocomplexity in river networks across space and time. River Research and Applications, 22:123–147.

Thorp, J. H., M. C. Thoms, and M. D. Delong. 2008. The riverine ecosystem synthesis: toward conceptual cohesiveness in river science. Elsevier, Amsterdam.

Thorp, J. H., and R. E. Bowes. 2017. Carbon sources in riverine food webs: new evidence from amino acid isotope techniques. Ecosystems 20:1029–1041.

Trudeau, V., and J. Rasmussen. 2003. The effect of water velocity on stable carbon and nitrogen isotope signatures of periphyton. Limnology and Oceanography 48:2194–2199.

Vannote, R. L., G. W. Minshall, K. W. Cummins, J. R. Sedell, and C. E. Cushing. 1980. The river continuum concept. Canadian Journal of Fisheries and Aquatic Sciences 37:130–137.

Walsh, R. G., S. He, and C. Yarnes. 2014. Compound-specific $\delta^{13}C$ and $\delta^{15}N$ analysis of amino acids: A rapid, chloroformate-based method for ecological studies. Rapid Communications in Mass Spectrometry 28:96–108.

Wenzel, A., A.-K. Bergström, M. Jansson, and T. Vrede. 2012. Survival, growth and reproduction of *Daphnia galeata* feeding on single and mixed *Pseudomonas* and *Rhodomonas* diets. Freshwater Biology 57:835–846.

Williams, B. S., E. D'Amico, J. H. Kastens, J. H. Thorp, J. E. Flotemersch, and M. C. Thoms. 2013. Automated riverine landscape characterization: GIS-based tools for watershed-scale research, assessment, and management. Environmental Monitoring and Assessment 185:7485–7499.

# Appendix A: Chapter 1 Supplemental Information

**Supplemental Methods A-1:** We obtained source signature data from 42 total basal resources, including terrestrial $C_3$ plants (N=21), terrestrial $C_4$ plants (N=3), algae (N=9), cyanobacteria (N=3), aquatic macrophytes (N=3), and fish pellet food (N=3) to rule out potential dietary contributions from hatchery-raised fishes. Food sources were either collected *in situ* (Diatom-dominated biofilm, *Spirogyra* sp., *Hydrilla* sp., *Salix* spp., *Pinus* sp., *Zea* sp., and *Panicum* sp.) or purchased from commercial suppliers (*Chlorella* sp., *Spirulina* sp., and Skretting brand trout pellet feed). Field-collected diatoms were harvested from the Zavkhan River, Mongolia, separated and sorted under a field microscope directly after collection, filtered for purity, and air-dried. All other field-collected samples, including *Spirogyra* sp., *Hydrilla* sp., *Salix* spp., *Pinus* sp., *Zea* sp., and *Panicum* sp. examined for purity under a microscope in the field or laboratory after collection. All source samples were rinsed with distilled water and dried in a gravity oven at 60ºC for 48 hours or until completely dry and then homogenized to a fine powder using a Wig-L-Bug mixer/amalgamator. Homogenized samples were then weighed into quantities of 20-30 mg and placed into pre-combusted glass vials. Samples were delivered to the Louisiana State University Stable Isotope Ecology Laboratory for amino acid compound specific stable isotope analysis of carbon.

Homogenized resource samples were analyzed for $\delta^{13}C_{AA}$ at the Louisiana State University Stable Isotope Ecology Laboratory using the methyl chloroformate derivatization method described by Walsh et al. (2014). Briefly, samples were acid hydrolyzed, derivatized with methyl chloroformate, and injected in duplicate for gas chromatography/combustion/isotope ratio mass spectrometry (GC/C/IRMS). All food source samples were cleaned using Dowex

column purification. Raw isotope signatures of samples were corrected based on norleucine and individual L-amino acid standards of known isotopic composition, which were included with all sample runs. Isotope signatures are expressed in delta (δ) per mil (‰) notation according to the following formula, as calculated for each amino acid in the sample tissue: $\delta^{13}C_{AA}$ (‰) = $([(^{13}C/^{12}C)_{sample} / (^{13}C/^{12}C)_{standard}) - 1])*1000$

All statistical analyses were conducted in R version 3.6.3 (R Core Team 2020). Amino acids used in analyses were isoleucine (Ile), leucine (Leu), phenylalanine (Phe), threonine (Thr), and valine (Val). Raw carbon stable isotope signatures of essential amino acids for source samples were normalized by subtracting the mean $\delta^{13}C$ of all essential amino acids (N=5) for a particular sample from each $\delta^{13}C_{AA}$. Food sources were visualized in a principal component analysis (PCA) based on normalized, essential amino acid $\delta^{13}C$ data (Supplemental Figure A-).

**Supplemental Table A-1.** Food source amino acid carbon isotope signature library for each of five essential amino acids in mean ± standard deviation $\delta^{13}C_{AA}$ per mil (‰). Asterisks (*) represent samples of culture or commercial origin; all other samples were collected *in situ* (MN=Mongolia). Samples collected after the onset of senescence are indicated by †. Amino acids are abbreviated as Ala (alanine), Asp (aspartic acid), Glu (glutamic acid), Gly (glycine), Ile (isoleucine), Leu (leucine), Phe (phenylalanine), Pro (proline), Thr (threonine), and Val (valine).

| Sample | Location | n | Ile | Leu | Phe | Thr | Val |
|---|---|---|---|---|---|---|---|
| Algae | | | | | | | |
| *Chlorella* sp.* | NA | 3 | -35.7 ± 0.6 | -44.1 ± 0.8 | -40.1 ± 0.6 | -29.1 ± 0.7 | -37.0 ± 0.9 |
| Diatom-dominated biofilm | Zavkhan River, MN | 3 | -26.7 ± 0.3 | -36.9 ± 0.1 | -33.8 ± 0.3 | -19.7 ± 0.7 | -29.4 ± 1.6 |
| *Spirogyra* sp. | Zavkhan River, MN | 3 | -26.7 ± 0.4 | -32.0 ± 0.2 | -31.6 ± 0.3 | -17.1 ± 0.2 | -29.7 ± 0.5 |
| Cyanobacteria | | | | | | | |
| *Spirulina* sp.* | NA | 3 | -24.0 ± 0.8 | -29.2 ± 0.8 | -24.8 ± 0.1 | -10.3 ± 0.5 | -25.4 ±1.7 |
| Macrophyte | | | | | | | |
| *Hydrilla* sp. | Niobrara River, USA | 3 | -28.3 ± 0.6 | -35.6 ± 0.5 | -31.2 ± 0.3 | -17.9 ± 0.9 | -33.6 ± 1.1 |
| $C_3$ Plant | | | | | | | |
| *Salix* sp. | Kherlen River, MN | 3 | -24.9 ± 0.8 | -34.8 ± 0.5 | -27.0 ± 0.3 | -13.3 ± 1.1 | -32.5 ± 1.5 |
| *Salix* sp. | Zavkhan River, MN | 3 | -24.4 ± 0.3 | -35.6 ± 0.3 | -28.2 ± 0.3 | -13.7 ± 0.6 | -32.7 ± 0.3 |
| *Salix* sp. | Carson River, USA | 3 | -23.3 ± 0.2 | -35.2 ± 0.4 | -25.9 ± 0.5 | -12.6 ± 0.3 | -30.2 ± 0.3 |
| *Salix* sp. | Little Missouri River, USA | 3 | -26.1 ± 0.3 | -37.0 ± 0.3 | -30.3 ± 0.6 | -16.9 ± 1.1 | -35.3 ± 0.2 |
| *Salix* sp. | Tensleep River, USA | 3 | -24.3 ± 0.5 | -34.3 ± 0.5 | -24.8 ± 0.5 | -14.2 ± 1.0 | -30.2 ± 0.1 |
| *Pinus* sp. | Lawrence, KS, USA | 3 | -26.3 ± 0.8 | -37.4 ± 0.5 | -29.3 ± 0.1 | -14.7 ± 0.6 | -33.1 ± 1.6 |
| *Pinus* sp.† | Lawrence, KS, USA | 3 | -25.0 ± 0.4 | -38.2 ± 0.8 | -28.9 ± 0.7 | -12.0 ± 0.7 | -32.1 ± 0.2 |
| $C_4$ Plant | | | | | | | |
| *Zea* sp. | Lawrence, KS, USA | 2 | -12.4 ± 0.2 | -22.2 ± 0.4 | -16.7 ± 0.1 | -2.3 ± 0.7 | -18.6 ± 0.4 |
| *Panicum* sp. | Lawrence, KS, USA | 1 | -9.8 ± NA | -22.3 ± NA | -15.4 ± NA | 5.3 ± NA | -17.4 ± NA |
| Fish Pellet Food | | | | | | | |
| Skretting Brand Classic Trout* | NA | 3 | -20.7 ± 0.8 | -27.3 ± 0.9 | -27.3 ± 0.4 | -11.0 ± 1.0 | -26.1 ± 0.4 |

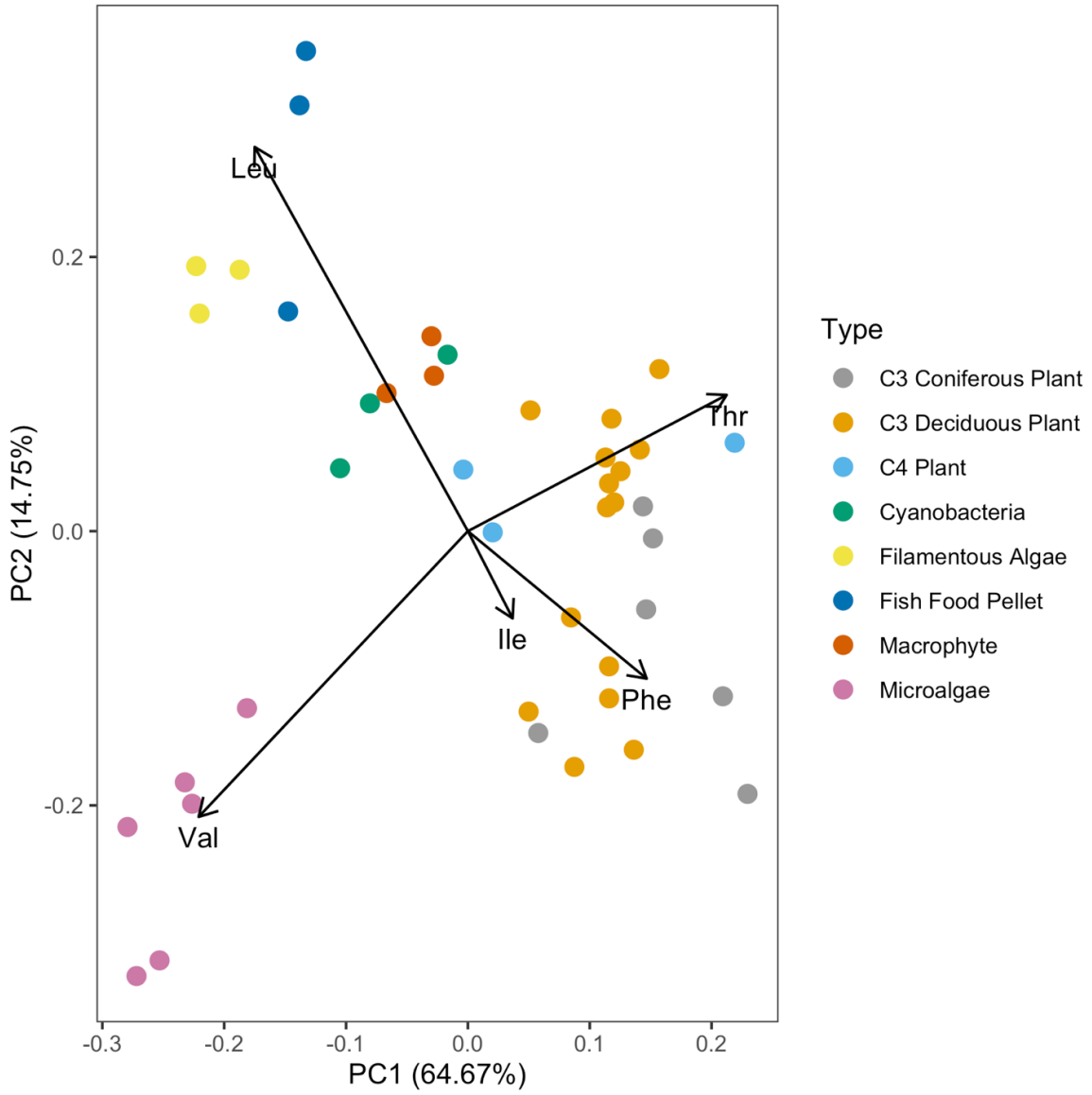


**Supplemental Figure A-1.** PCA of food source groups based on essential amino acid isotope signatures of carbon ($\delta^{13}C_{EAA}$) from the amino acids isoleucine (Ile), leucine (Leu), phenylalanine (Phe), threonine (Thr), and valine (Val). Food sources are labeled as different source groups as indicated in the figure legend (*n*=42). PCA visualization suggested good separation of food source groupings, with 64.67% of variance explained by PC1 and 14.75% of variance explained by PC2.

**Supplemental Table A-2.** Literature search and summary of carbon CSIA-AA basal resource tracing data analysis methods (AA=amino acid, EAA=essential amino acid, NEAA=non-essential amino acid, PCA=principal component analysis, and LDA=linear discriminant analysis). We summarized the common approaches taken in this fingerprinting step of carbon CSIA-AA data analysis by conducting a comprehensive literature search of original research articles employing the method in the last ten years (2010-2020). We then reviewed the methods of each study and highlighted where data analysis steps typical of carbon CSIA-AA were employed.

| Citation | AA Selection | Data Normalized | PCA | LDA | Mixing Model |
|---|---|---|---|---|---|
| Elliott Smith et al. 2021 | EAAs | - | - | Yes | - |
| Martinez et al. 2020 | EAAs | - | Yes | - | - |
| Pollierer et al. 2020 | EAAs | - | - | Yes | - |
| Phillips et al. 2020 | EAAs | - | - | Yes | - |
| Liew et al. 2019 | EAAs and NEAAs | Yes | Yes | Yes | simmr |
| Potapov et al. 2019 | EAAs | Yes | - | Yes | FRUITS |
| Elliott Smith et al. 2018 | EAAs | Yes | | CAP | MixSIAR |
| Mora et al. 2018 | EAAs and NEAAs | - | - | - | FRUITS |
| Gómez et al. 2018 | EAAs | Yes | - | Yes | FRUITS |
| McMahon et al. 2018 | EAAs | Yes | Yes | - | SIAR |
| Pomerleau et al. 2017 | EAAs and NEAAs | - | - | - | - |
| Jarman et al. 2017 | EAAs | Yes | Yes | - | FRUITS |
| Thorp and Bowes 2017 | EAAs and NEAAs | Yes | Yes | Yes | FRUITS |

| | | | | | |
|---|---|---|---|---|---|
| Mora et al. 2017 | EAAs and NEAAs | - | Yes | - | FRUITS |
| McMahon et al. 2016 | EAAs | - | Yes | - | SIAR |
| Ayayee et al. 2016 | EAAs | - | - | Yes | - |
| McMahon et al. 2015 | EAAs | Yes | - | Yes | - |
| Arthur et al. 2014 | EAAs | Yes | Yes | Yes | - |
| Ellis et al. 2014 | EAAs and NEAAs | Yes | - | - | - |
| Vokhshoori et al. 2014 | EAAs | Yes | - | Yes | - |
| Larsen et al. 2013 | EAAs and NEAAs | Yes | Yes | Yes | FRUITS |
| Choy et al. 2010 | EAAs and NEAAs | - | - | - | - |

**Supplemental References A-1:**

Arthur, K. E., S. Kelez, T. Larsen, A. A. Choy, and B. N. Popp. 2014. Tracing the biosynthetic source of essential amino acids in marine turtles using $\delta^{13}C$ fingerprints. Ecology 95:1285–1293.

Ayayee, P. A., T. Larsen, Z. Sabree. 2016. Symbiotic essential amino acids provisioning in the American cockroach, *Periplaneta americana* (Linnaeus) under various dietary conditions. PeerJ 4:e2046.

Choy, K., C. I. Smith, B. T. Fuller, and M. P. Richards. 2010. Investigation of amino acid $\delta^{13}C$ signatures in bone collagen to reconstruct human palaeodiets using liquid chromatography–isotope ratio mass spectrometry. Geochimica et Cosmochimica Acta 74:6093–6111.

Elliott Smith, E.A., C. Harrod, F. Docmac, and S. D. Newsome. 2021. Intraspecific variation and energy channel coupling within a Chilean kelp forest. Ecology 102:e03198.

Elliott Smith, E. A., C. Harrod, S. D. Newsome. 2018. The importance of kelp to an intertidal ecosystem varies by trophic level: insights from amino acid delta C-13 analysis. Ecosphere 9:e02516.

Ellis, G. S., G. Herbert, and D. Hollander. 2014. Reconstructing carbon sources in a dynamic estuarine ecosystem using oyster amino acid $\delta^{13}C$ values from shell and tissue. Journal of Shellfish Research 33:217–225.

Gómez, C., T. Larsen, B. Popp, K. A. Hobson, and C. D. Cadena. 2018. Assessing seasonal changes in animal diets with stable-isotope analysis of amino acids: a migratory boreal songbird switches diet over its annual cycle. Oecologia 187:1–13.

Jarman, C. L., T. Larsen, T. Hunt, C. Lipo, R. Solsvik, N. Wallsgrove, C. Ka'apu-Lyons, H. G. Close, B. N. Popp. 2017. Diet of the prehistoric population of Rapa Nui (Easter Island, Chile) shows environmental adaptation and resilience. Americal Journal of Physical Anthropology 164:343–361.

Larsen, T., M. Ventura, N. Andersen, D. M. O'Brien, U. Piatkowski, and M. D. McCarthy. 2013. Tracing carbon sources through aquatic and terrestrial food webs using amino acid stable isotope fingerprinting. PLoS ONE 8:e73441.

Larsen, T., D. L. Taylor, M. B. Leigh, and D. M. O'Brien. 2009. Stable isotope fingerprinting: a novel method for identifying plant, fungal, or bacterial origins of amino acids. Ecology 90:3526–3535.

Liew, J. H., K. W. J. Chua, E. R. Arsenault, J. H. Thorp, A. Suvarnaraksha, A. Amirrudin, and D. C. J Yeo. 2019. Quantifying terrestrial carbon in freshwater food webs using amino acid isotope analysis: Case study with an endemic cavefish. Methods in Ecology and Evolution. 10:1594–1605.

Martinez, S., Y. Kolodny, E. Shemesh, F. Scucchia, R. Nevo, S. Levin-Zaidman, Y. Paltiel, N. Keren, D. Tchernov, and T. Mass. 2021. Energy sources of the depth-generalist mixotrophic coral *Stylophora pistillata*. Frontiers in Marine Science 7:988.

McMahon, K. W., M. J. Polito, S. Abel, M. D. McCarthy, and S. R. Thorrold. 2015. Carbon and nitrogen isotope fractionation of amino acids in an avian marine predator, the gentoo penguin (*Pygoscelis papua*). Ecology and Evolution 5:1278–1290.

McMahon, K. W., S. R. Thorrold, L. A. Houghton, and M. L. Berumen. 2016. Tracing carbon flow through coral reef food webs using a compound-specific stable isotope approach. Oecologia 180:809–821.

McMahon, K. W., B. Williams, T. P. Guilderson, D. S. Glynn, and M. D. McCarthy. 2018. Calibrating amino acid $\delta^{13}C$ and $\delta^{15}N$ offsets between polyp and protein skeleton to develop proteinaceous deep-sea corals as paleoceanographic archives. Geochimica et Cosmochimica Acta 220:261–275.

Mora, A., B. T. Arriaza, V. G. Standen, C. Valdiosera, A. Salim, and C. Smith. 2017. High-resolution palaeodietary reconstruction: Amino acid $\delta^{13}C$ analysis of keratin from single hairs of mummified human individuals. Quaternary International 436:96–113.

Mora, A., A. Pacheco, C. Roberts, C. Smith. 2018. Pica 8: Refining dietary reconstruction through amino acid delta C-13 analysis of tendon collagen and hair keratin. Journal of Archaeological Science 93:94–109.

Phillips, N. D., E. A. Elliott Smith, S. D. Newsome, J. D. R. Houghton, C. D. Carson, J. Alfaro-Shigueto, J. C. Mangel, L. E. Eagling, L. Kubicek, and C. Harrod. 2020. Bulk tissue and amino acid stable isotope analyses reveal global ontogenetic patterns in ocean sunfish trophic ecology and habitat use. Marine Ecology Progress Series 633:127–140.

Pollierer, M. M., S. Scheu, and A. V. Tiunov. 2020. Isotope analyses of amino acids in fungi and fungal feeding Diptera larvae allow differentiating ectomycorrhizal and saprotrophic fungi-based food chains. Functional Ecology 34:2375–2388.

Pomerleau, C., M. P. Heide-Jørgensen, S. H. Ferguson, H. L. Stern, J. L. Høyer, and G. A. Stern. Reconstructing variability in West Greenland ocean biogeochemistry and bowhead whale (*Balaena mysticetus*) food web structure using amino acid isotope ratios. Polar Biology 40:2225–2238.

Potapov, A. M., A. V. Tiunov, S. Scheu, T. Larsen, and M. M. Pollierer. 2019. Combining bulk and amino acid stable isotope analyses to quantify trophic level and basal resources of detritivores: a case study on earthworms. Oecologia 189:447–460.

Thorp, J. H., and R. E. Bowes. 2017. Carbon sources in riverine food webs: new evidence from amino acid isotope techniques. Ecosystems 20:1029–1041.

Vokhshoori, N. L., T. Larsen, and M. D. McCarthy. 2014. Reconstructing $\delta^{13}C$ isoscapes of phytoplankton production in a coastal upwelling system with amino acid isotope values of littoral mussels. Marine Ecology Progress Series 504:59–72.

# Appendix B: Chapter 2 Supplemental Information

**Supplemental Table B-1.** Mean ± SD $\delta^{13}C_{AA}$ for seven amino acids used to supplement yeast growth media, bulk $\delta^{13}C$ and $\delta^{15}N$, and C:N ratio for media substrate and yeast cultured under four experimental media conditions (*C=Control*, *L=Low*, *R=Reference*, and *H=High* amounts of amino acid supplements).

| | CSIA-AA | | | | | | | BSIA | | C:N |
|---|---|---|---|---|---|---|---|---|---|---|
| | $\delta^{13}C_{Asp}$ | $\delta^{13}C_{Glu}$ | $\delta^{13}C_{Ile}$ | $\delta^{13}C_{Leu}$ | $\delta^{13}C_{Phe}$ | $\delta^{13}C_{Thr}$ | $\delta^{13}C_{Val}$ | $\delta^{13}C$ | $\delta^{15}N$ | |
| Substrate | -20.6 ± 0.2 | -11.2 ± 0.1 | -11.9 ± 0.1 | -11.2 ± 0.1 | -11.5 ± 0.1 | -10.6 ± 0.1 | -11.4 ± 0.1 | NA | NA | NA |
| Yeast *C* | -5.4 ± 1.2 | 6.2 ± 1.8 | -7.7 ± 0.4 | -13.3 ± 0.4 | -13.8 ± 0.1 | -1.9 ± 1.6 | -7.9 ± 0.6 | -8.2 ± 0.4 | -4.5 ± 0.4 | 6.6 ± 0.1 |
| Yeast *L* | -7.1 ± 0.6 | 4.3 ± 1.2 | -9.4 ± 0.4 | -14.3 ± 0.2 | -13.5 ± 0.3 | -3.6 ± 0.4 | -9.7 ± 0.4 | -8.8 ± 0.5 | -4.0 ± 1.0 | 6.4 ± 0.3 |
| Yeast *R* | -9.4 ± 0.6 | -1.3 ± 3.2 | -7.1 ± 0.7 | -11.1 ± 0.8 | -13.4 ± 0.8 | -2.2 ± 0.4 | -11.6 ± 1.2 | -9.0 ± 0.3 | -4.9 ± 1.1 | 6.5 ± 0.3 |
| Yeast *H* | -12.4 ± 0.7 | 0.2 ± 1.7 | -6.6 ± 0.2 | -9.9 ± 1.2 | -13.1 ± 0.7 | -3.1 ± 1.1 | -9.6 ± 0.7 | -9.2 ± 0.1 | -5.1 ± 0.8 | 5.8 ± 0.2 |

**Supplemental Table B-2.** Pairwise differences in $\delta^{13}C_{AA}$ for each amino acid and experimental treatment (Control, Low, Reference, and High). P-values are from Tukey HSD tests. Shaded boxes indicate non-significant differences.

| | **Asp** | **Glu** | **Ile** | **Leu** | **Phe** | **Thr** | **Val** |
|---|---|---|---|---|---|---|---|
| *Control-Low* | 0.023 | 0.505 | <0.001 | 0.146 | 0.794 | 0.063 | 0.011 |
| *Control-Reference* | <0.001 | <0.001 | 0.261 | 0.002 | 0.735 | 0.969 | <0.001 |
| *Control-High* | <0.001 | 0.002 | 0.011 | <0.001 | 0.208 | 0.230 | 0.019 |
| *Low-Reference* | 0.002 | 0.004 | <0.001 | <0.001 | 1.000 | 0.143 | 0.009 |
| *Low-High* | <0.001 | 0.038 | <0.001 | <0.001 | 0.672 | 0.879 | 0.992 |
| *Reference-High* | <0.001 | 0.697 | 0.351 | 0.087 | 0.735 | 0.435 | 0.005 |

**Supplemental Table B-3.** Relative abundances of amino acids in natural aquatic and terrestrial primary producers in mg/100 mg total amino acid. Data aggregated by Bowen (1987) from Bowen (1980), Sigleo et al. (1983), De la Cruz and Poe (1975), and Boyd (1970, 1973).

| Sample | Asp | Thr | Ser | Glu | Pro | Gly | Ala | Val | Met | Ile | Leu | Tyr | Phe | His | Lys | Arg |
|---|---|---|---|---|---|---|---|---|---|---|---|---|---|---|---|---|
| Periphytic detritus (Bowen 1980) | 14.5 | 5.8 | 6.2 | 15.9 | 5.6 | 7.6 | 8.9 | 4.2 | 1.5 | 3.2 | 7.2 | 3.1 | 2.7 | 1.7 | 5.4 | 6.9 |
| Benthic detritus (Bowen, *unpubl*) | 16.7 | 7.4 | 6.0 | 16.5 | 5.2 | 8.9 | 8.5 | 5.1 | 1.6 | 3.3 | 5.9 | 2.0 | 2.1 | 1.3 | 5.5 | 4.1 |
| Estuarine colloids (Sigleo et al. 1983) | 11.6 | 7.3 | 6.4 | 11.4 | 3.0 | 7.9 | 9.3 | 6.3 | 1.6 | 4.5 | 7.9 | 3.6 | 5.4 | 4.3 | 4.6 | 5.0 |
| Estuarine seston (Sigleo et al. 1983) | 10.7 | 4.9 | 4.4 | 12.2 | 2.7 | 6.3 | 7.2 | 5.5 | 2.1 | 4.4 | 7.7 | 2.6 | 5.0 | 3.0 | 6.1 | 5.9 |
| Salt marsh plants (De la Cruz and Poe 1975) | 15.6 | 4.9 | 5.1 | 14.3 | 9.8 | 4.8 | 6.0 | 6.2 | 1.9 | 4.3 | 7.3 | 2.7 | 7.8 | 2.3 | 5.4 | 4.9 |
| Salt marsh detritus (De la Cruz and Poe 1975) | 12.1 | 6.7 | 5.9 | 12.3 | 5.9 | 7.9 | 7.8 | 6.7 | 2.2 | 4.8 | 8.2 | 2.0 | 5.0 | 1.6 | 4.5 | 4.9 |
| Freshwater algae (Boyd 1973) | 12.2 | 5.0 | 5.0 | 13.3 | 4.4 | 6.1 | 8.7 | 5.8 | 1.8 | 4.5 | 8.6 | 3.8 | 4.9 | 2.1 | 7.0 | 8.2 |
| Aquatic vascular plants (Boyd, 1970) | 13.1 | 5.2 | 5.4 | 12.2 | 5.1 | 6.4 | 6.5 | 6.0 | 1.4 | 5.1 | 9.8 | 3.9 | 5.7 | 2.3 | 5.5 | 6.1 |

# Appendix C: Chapter 3 Supplemental Information

**Supplemental Table C-1.** Coordinates for each study site sampled as part of this study (*n*=50). Ecoregions sampled include: Mongolia grassland (MNGR), Mongolia mountain steppe (MNMS), Mongolia semi-arid terminal basin (MNTB), United States grassland (USGR), United States mountain steppe (USMS), and United States semi-arid terminal basin (USTB).

| Ecoregion | Site | Lat. | Long. |
|---|---|---|---|
| MNGR | M_G1_a | 48.3466 | 108.6083 |
| | M_G5_a | 47.7535 | 108.9890 |
| | M_G5_b | 47.7281 | 109.7534 |
| | M_G5_c | 48.0420 | 108.4160 |
| | M_G6_a | 48.2422 | 108.4984 |
| | M_G6_b | 48.0675 | 108.5629 |
| MNMS | M_M1_a | 50.1748 | 98.4884 |
| | M_M1_b | 50.1760 | 98.4874 |
| | M_M1_c | 50.1038 | 98.6047 |
| | M_M1_d | 50.1280 | 98.6397 |
| MNTB | M_T1_b | 48.8336 | 89.5313 |
| | M_T1_c | 49.1852 | 89.2085 |
| | M_T1_e | 46.5816 | 97.2542 |
| | M_T1_f | 46.6165 | 97.3066 |
| | M_T3_a | 47.0914 | 97.6352 |
| | M_T3_b | 47.2247 | 97.6156 |
| | M_T3_c | 47.1538 | 97.6278 |
| USGR | U_G6_a | 42.9240 | -100.7469 |
| | U_G7_a | 42.6716 | -99.7661 |
| | U_G7_b | 42.5450 | -99.7099 |
| | U_G7_c | 42.5473 | -100.1077 |
| USMS | U_M2_a | 44.3211 | -106.9503 |
| | U_M2_b | 44.3030 | -106.9534 |

| | | | |
|---|---|---|---|
| | U_M2_c | 44.2763 | -106.9526 |
| | U_M2_d | 44.1692 | -106.9153 |
| | U_M2_e | 44.1948 | -106.9279 |
| | U_M2_f | 44.7944 | -107.6886 |
| | U_M2_g | 44.8087 | -107.7208 |
| | U_M2_h | 44.7986 | -107.7651 |
| | U_M2_i | 44.2521 | -106.9533 |
| | U_M2_j | 44.7217 | -107.4493 |
| | U_M2_k | 44.6866 | -107.4460 |
| | U_M2_l | 44.7709 | -107.4710 |
| | U_M6_a | 44.1925 | -107.2101 |
| | U_M6_b | 44.2438 | -107.2224 |
| | U_M6_c | 44.2045 | -107.2370 |
| USTB | U_T2_a | 40.6898 | -115.4770 |
| | U_T3_a | 42.1373 | -111.6434 |
| | U_T3_b | 42.5268 | -111.5781 |
| | U_T4_a | 40.8743 | -110.8365 |
| | U_T4_b | 40.8867 | -110.7982 |
| | U_T4_c | 40.9283 | -110.7363 |
| | U_T4_d | 38.7180 | -119.9219 |
| | U_T4_e | 38.6852 | -119.9297 |
| | U_T5_a | 41.6042 | -111.5872 |
| | U_T5_b | 40.6642 | -115.4477 |
| | U_T5_c | 40.6582 | -115.4330 |
| | U_T5_d | 38.7762 | -119.8956 |
| | U_T5_e | 38.5773 | -119.6967 |
| | U_T5_f | 38.5875 | -119.6882 |

**Supplemental Table C-2.** Valley-scale functional process zone (FPZ) characteristics describing each study site sampled as part of this study (*n*=50). Ecoregions sampled include: Mongolia grassland (MNGR), Mongolia mountain steppe (MNMS), Mongolia semi-arid terminal basin (MNTB), United States grassland (USGR), United States mountain steppe (USMS), and United States semi-arid terminal basin (USTB). The nine variables used to delineate FPZs were: mean annual precipitation in mm (MAP), elevation in m (Elev.), valley width in m (VW), valley floor width in m (VFW), ratio of valley width to valley floor width (Ratio), left valley slope (LVS), right valley slope (RVS), down valley slope (DVS), and channel sinuosity (Sinu.). Values are calculated at the FPZ scale, which means that sites located within the same FPZ segment will share the same characteristic values.

| Ecoregion | Site | MAP | Elev. | VW | VFW | Ratio | LVS | RVS | DVS | Sinu. |
|---|---|---|---|---|---|---|---|---|---|---|
| MNGR | M_G1_a | 37.0 | 1424 | 6972 | 4901 | 1.423 | 0.016 | 0.032 | -0.004 | 1.271 |
| | M_G5_a | 32.0 | 1407 | 2710 | 1145 | 2.368 | 0.075 | 0.091 | -0.003 | 1.301 |
| | M_G5_b | 30.0 | 1225 | 2986 | 1190 | 2.510 | 0.042 | 0.157 | -0.002 | 1.379 |
| | M_G5_c | 34.5 | 1394 | 5139 | 153 | 33.519 | 0.087 | 0.141 | -0.008 | 1.133 |
| | M_G6_a | 36.0 | 1423 | 9925 | 6715 | 1.478 | 0.060 | -0.001 | -0.005 | 1.273 |
| | M_G6_b | 34.0 | 1357 | 7501 | 3926 | 1.911 | 0.068 | 0.098 | -0.001 | 1.304 |
| MNMS | M_M1_a | 32.9 | 1319 | 11690 | 6708 | 1.743 | 0.017 | -0.001 | -0.004 | 1.299 |
| | M_M1_b | 32.9 | 1319 | 11690 | 6708 | 1.743 | 0.017 | -0.001 | -0.004 | 1.299 |
| | M_M1_c | 24.6 | 1650 | 7528 | 375 | 20.085 | 0.139 | 0.165 | -0.006 | 1.251 |
| | M_M1_d | 24.6 | 1650 | 7528 | 375 | 20.085 | 0.139 | 0.165 | -0.006 | 1.251 |
| MNTB | M_T1_b | 11.4 | 1769 | 15852 | 10300 | 1.539 | 0.127 | 0.034 | -0.004 | 1.143 |
| | M_T1_c | 12.0 | 1817 | 9094 | 4263 | 2.133 | 0.109 | 0.246 | -0.004 | 1.249 |
| | M_T1_e | 13.0 | 1783 | 3840 | 471 | 8.156 | 0.124 | 0.020 | -0.002 | 1.172 |
| | M_T1_f | 11.0 | 1858 | 8231 | 3068 | 2.683 | 0.041 | 0.046 | -0.018 | 1.159 |
| | M_T3_a | 15.5 | 2116 | 6695 | 255 | 26.253 | 0.152 | 0.169 | -0.002 | 1.225 |
| | M_T3_b | 16.0 | 2143 | 7599 | 1098 | 6.923 | 0.125 | 0.102 | -0.002 | 1.199 |
| | M_T3_c | 15.0 | 2128 | 13000 | 3621 | 3.590 | 0.110 | 0.168 | -0.002 | 1.174 |
| USGR | U_G6_a | 523.4 | 808 | 1819 | 558 | 3.262 | 0.086 | 0.030 | -0.001 | 1.731 |
| | U_G7_a | 595.1 | 612 | 1326 | 277 | 4.794 | 0.179 | 0.082 | -0.004 | 1.674 |
| | U_G7_b | 601.2 | 670 | 672 | 103 | 6.544 | 0.500 | 0.084 | -0.004 | 1.356 |
| | U_G7_c | 595.2 | 768 | 5804 | 2520 | 2.304 | -0.001 | 0.061 | -0.002 | 1.412 |
| USMS | U_M2_a | 465 | 2038 | 4342 | 176 | 24.605 | 0.124 | 0.088 | -0.036 | 1.290 |
| | U_M2_b | 457 | 2201 | 4029 | 176 | 22.889 | 0.059 | 0.055 | -0.020 | 1.559 |
| | U_M2_c | 495 | 2104 | 1697 | 143 | 11.881 | 0.178 | 0.193 | -0.041 | 1.462 |
| | U_M2_d | 440 | 1933 | 2308 | 121 | 19.000 | 0.226 | 0.562 | -0.048 | 1.365 |

| | | | | | | | | | | |
|---|---|---|---|---|---|---|---|---|---|---|
| | U_M2_e | 440 | 1933 | 2308 | 121 | 19.000 | 0.226 | 0.562 | -0.048 | 1.365 |
| | U_M2_f | 719 | 2453 | 2469 | 66 | 37.238 | 0.132 | 0.415 | -0.023 | 1.147 |
| | U_M2_g | 725 | 2579 | 1683 | 70 | 24.184 | 0.249 | 0.178 | -0.014 | 1.158 |
| | U_M2_h | 680 | 2470 | 2645 | 141 | 18.809 | 0.163 | 0.267 | -0.024 | 1.269 |
| | U_M2_i | 508 | 2246 | 2232 | 150 | 14.886 | 0.177 | 0.214 | -0.027 | 1.163 |
| | U_M2_j | 631 | 2359 | 2467 | 290 | 8.493 | 0.071 | 0.128 | -0.020 | 1.497 |
| | U_M2_k | 657 | 2555 | 4628 | 350 | 13.234 | 0.160 | 0.034 | -0.017 | 1.315 |
| | U_M2_l | 637 | 2143 | 5788 | 211 | 27.376 | 0.131 | 0.150 | -0.022 | 1.457 |
| | U_M6_a | 25 | 2374 | 852 | 329 | 2.592 | 0.105 | 0.162 | -0.040 | 1.152 |
| | U_M6_b | 27 | 2707 | 1561 | 300 | 5.207 | 0.112 | 0.190 | -0.017 | 1.186 |
| | U_M6_c | 25 | 2458 | 1351 | 294 | 4.594 | 0.130 | 0.141 | -0.025 | 1.216 |
| USTB | U_T2_a | 369 | 1815 | 1145 | 597 | 1.917 | 0.005 | 0.015 | -0.027 | 1.110 |
| | U_T3_a | 460 | 1362 | 10247 | 182 | 56.164 | 0.002 | 0.015 | -0.001 | 1.258 |
| | U_T3_b | 365 | 768 | 3477 | 443 | 7.856 | 0.019 | 0.072 | -0.003 | 2.524 |
| | U_T4_a | 679 | 2554 | 2097 | 119 | 17.614 | 0.060 | 0.059 | -0.010 | 1.354 |
| | U_T4_b | 570 | 2412 | 1053 | 264 | 3.986 | 0.041 | 0.025 | -0.014 | 1.118 |
| | U_T4_c | 705 | 2632 | 1180 | 230 | 5.125 | 0.067 | 0.052 | -0.028 | 1.239 |
| | U_T4_d | 1134 | 2171 | 1783 | 595 | 2.996 | 0.103 | 0.101 | -0.011 | 1.239 |
| | U_T4_e | 1134 | 2171 | 1783 | 595 | 2.996 | 0.103 | 0.101 | -0.011 | 1.239 |
| | U_T5_a | 638 | 1610 | 1391 | 61 | 22.728 | 0.398 | 0.440 | -0.011 | 1.306 |
| | U_T5_b | 469 | 1950 | 1760 | 38 | 45.491 | 0.491 | 0.360 | -0.053 | 1.147 |
| | U_T5_c | 469 | 1950 | 1760 | 38 | 45.491 | 0.491 | 0.360 | -0.053 | 1.147 |
| | U_T5_d | 939 | 1966 | 5478 | 75 | 72.832 | 0.567 | 0.082 | -0.020 | 1.852 |
| | U_T5_e | 686 | 1851 | 2295 | 172 | 13.349 | 0.333 | 0.285 | -0.026 | 1.199 |
| | U_T5_f | 686 | 1851 | 2295 | 172 | 13.349 | 0.333 | 0.285 | -0.026 | 1.199 |

**Supplemental Table C-3.** Local-scale site attributes for sites sampled as part of this study (*n*=50). Ecoregional types include Mongolia Grassland (MNGR), Mongolia mountain steppe (MNMS), Mongolia semi-arid terminal basin (MNTB), United States Grassland (USGR), United States mountain steppe (USMS), and United States semi-arid terminal basin (USTB). Local variables measured included Strahler stream order (Order), average wetted width (WW), average canopy cover at stream bank (BC), and average canopy cover at mid-stream (MC).

| Ecoregion | Site | Order | WW (m) | BC (%) | MC (%) |
|---|---|---|---|---|---|
| MNGR | M_G1_a | 3 | 5.2 | 35.3 | 6.5 |
| | M_G5_a | 3 | 3.6 | 0.0 | 0.0 |
| | M_G5_b | 4 | 1.8 | 0.0 | 0.0 |
| | M_G5_c | 3 | 1.5 | 21.5 | 4.4 |
| | M_G6_a | 3 | 2.2 | 20.9 | 2.2 |
| | M_G6_b | 2 | 1.2 | 0.0 | 0.0 |
| MNMS | M_M1_a | 2 | 1.0 | 33.5 | 26.2 |
| | M_M1_b | 3 | 4.0 | 5.9 | 1.6 |
| | M_M1_c | 4 | 7.6 | 8.8 | 1.3 |
| | M_M1_d | 4 | 6.2 | 0.0 | 0.0 |
| MNTB | M_T1_b | 4 | 5.0 | 0.0 | 0.0 |
| | M_T1_c | 1 | 6.4 | 0.6 | 0.0 |
| | M_T1_e | 4 | 19.1 | 7.4 | 2.5 |
| | M_T1_f | 4 | 11.9 | 0.0 | 0.0 |
| | M_T3_a | 4 | 20.3 | 0.0 | 0.0 |
| | M_T3_b | 3 | 25.4 | 0.0 | 0.0 |
| | M_T3_c | 3 | 12.1 | 0.0 | 0.0 |
| USGR | U_G6_a | 4 | 1.9 | 40.9 | 10.7 |
| | U_G7_a | 3 | 3.0 | 27.8 | 2.0 |
| | U_G7_b | 2 | 1.8 | 42.7 | 8.8 |
| | U_G7_c | 3 | 2.0 | 37.1 | 19.7 |
| USMS | U_M2_a | 2 | 2.0 | 88.5 | 67.2 |
| | U_M2_b | 2 | 1.9 | 87.6 | 74.2 |
| | U_M2_c | 3 | 2.6 | 83.4 | 47.7 |

| | | | | | |
|---|---|---|---|---|---|
| | U_M2_d | 2 | 1.9 | 2.4 | 0.0 |
| | U_M2_e | 1 | 1.0 | 2.4 | 0.0 |
| | U_M2_f | 2 | 1.0 | 0.0 | 0.0 |
| | U_M2_g | 1 | 1.0 | 3.2 | 1.9 |
| | U_M2_h | 1 | 0.7 | 0.6 | 0.0 |
| | U_M2_i | 1 | 1.5 | 37.4 | 6.5 |
| | U_M2_j | 3 | 3.6 | 77.7 | 22.9 |
| | U_M2_k | 3 | 2.6 | 23.8 | 13.7 |
| | U_M2_l | 3 | 4.0 | 32.1 | 6.2 |
| | U_M6_a | 1 | 0.9 | 37.6 | 17.2 |
| | U_M6_b | 1 | 3.3 | 18.2 | 9.6 |
| | U_M6_c | 2 | 4.6 | 29.4 | 7.1 |
| USTB | U_T2_a | 2 | 2.6 | 43.1 | 7.6 |
| | U_T3_a | 3 | 2.6 | 84.8 | 28.7 |
| | U_T3_b | 3 | 1.3 | 45.6 | 25.0 |
| | U_T4_a | 3 | 3.3 | 36.8 | 7.4 |
| | U_T4_b | 3 | 4.5 | 28.9 | 11.3 |
| | U_T4_c | 2 | 1.2 | 45.6 | 3.7 |
| | U_T4_d | 3 | 2.3 | 73.0 | 51.2 |
| | U_T4_e | 3 | 2.2 | 24.6 | 0.4 |
| | U_T5_a | 4 | 2.4 | 58.8 | 8.3 |
| | U_T5_b | 2 | 2.4 | 64.2 | 19.9 |
| | U_T5_c | 2 | 1.9 | 51.0 | 25.0 |
| | U_T5_d | 3 | 3.8 | 75.4 | 19.3 |
| | U_T5_e | 3 | 2.5 | 54.6 | 20.1 |
| | U_T5_f | 3 | 2.9 | 25.5 | 13.0 |

**Supplemental Table C-4.** Fish samples (*n*=271) collected from low-order streams in three temperate steppe ecoregions of Mongolia and the United States (Mongolia grassland=MNGR, Mongolia mountain steppe=MNMS, Mongolia semi-arid terminal basin=MNTB, United States grassland=USGR, United States mountain steppe=USMS, and United States semi-arid terminal basin=USTB). Feeding guild (FG) designations are omnivores (O), invertivores (I), and piscivores (P). Standard lengths (SL) and masses are presented as means ± standard deviations. Sample size (n) indicates the number of replicates of each species at each site that were analyzed for carbon compound specific amino acid stable isotope analysis.

| Ecoregion | FPZ | Species | FG | SL (mm) | Mass (g) | n |
|---|---|---|---|---|---|---|
| MNGR | M_G1_a | *Rhynchocypris lagowskii* | O | 37.5 ± 13.4 | 1.0 ± 0.8 | 2 |
| | | *Barbatula toni* | I | 73.7 ± 6.8 | 4.0 ± 0.7 | 3 |
| | | *Brachymystax lenok* | I | 437.5 ± 137.9 | 813.6 ± 725.8 | 2 |
| | M_G5_a | *Barbatula toni* | I | 85.0 ± 0.0 | 6.3 ± 0.6 | 3 |
| | | *Gobio gobio cynocephalus* | I | 78.0 ± 17.6 | 8.5 ± 4.5 | 3 |
| | | *Rhynchocypris lagowskii* | O | 84.7 ± 0.6 | 7.9 ± 0.8 | 3 |
| | M_G5_b | *Gobio gobio cynocephalus* | I | 64.0 ± 0.0 | 4.5 ± 0.0 | 1 |
| | | *Barbatula toni* | I | 80.3 ± 0.6 | 4.0 ± 0.1 | 3 |
| | | *Rhynchocypris lagowskii* | O | 85.0 ± 0.0 | 9.8 ± 3.1 | 3 |
| | M_G5_c | *Gobio gobio cynocephalus* | I | 72.0 ± 0.0 | 5.2 ± 0.0 | 1 |
| | | *Barbatula toni* | I | 65.3 ± 1.5 | 2.7 ± 0.2 | 3 |
| | | *Rhynchocypris lagowskii* | O | 63.3 ± 0.6 | 3.0 ± 0.1 | 3 |
| | M_G6_a | *Thymallus grubei* | I | 208.0 ± 0.0 | 91.6 ± 0.0 | 1 |

| | | | | | | |
|---|---|---|---|---|---|---|
| | | *Rhynchocypris lagowskii* | O | 57.3 ± 1.2 | 2.4 ± 0.5 | 3 |
| | | *Barbatula toni* | I | 95.3 ± 2.5 | 6.7 ± 0.7 | 3 |
| | M_G6_b | *Lota lota* | P | 255 ± 0.0 | 131.5 ± 0.0 | 1 |
| | | *Barbatula toni* | I | 54.0 ± 0.0 | 1.8 ± 0.1 | 3 |
| | | *Rhynchocypris lagowskii* | O | 72.7 ± 2.1 | 5.0 ± 1.0 | 3 |
| MNMS | M_M1_a | *Phoxinus phoxinus* | O | 65.3 ± 2.3 | 3.0 ± 0.6 | 3 |
| | | *Brachymystax lenok* | I | 146.0 ± 7.2 | 24.7 ± 3.4 | 3 |
| | M_M1_b | *Phoxinus phoxinus* | O | 69.7 ± 2.1 | 2.7 ± 0.2 | 3 |
| | | *Brachymystax lenok* | I | 151.7 ± 11.0 | 46.0 ± 30.2 | 3 |
| | M_M1_c | *Phoxinus phoxinus* | O | 73.7 ± 5.8 | 4.1 ± 1.1 | 3 |
| | | *Brachymystax lenok* | I | 82.3 ± 1.2 | 5.5 ± 0.9 | 3 |
| | M_M1_d | *Phoxinus phoxinus* | O | 83.7 ± 0.6 | 5.2 ± 0.6 | 3 |
| | | *Brachymystax lenok* | I | 85.0 ± 2.7 | 5.3 ± 0.5 | 3 |
| MNTB | M_T1_b | *Barbatula golubtsovi* | I | 77.0 ± 12.7 | 6.0 ± 2.9 | 2 |
| | | *Thymallus brevirostris* | P | 154.3 ± 73.0 | 69.2 ± 85.0 | 3 |
| | M_T1_c | *Barbatula barbatula* | I | 45.3 ± 5.1 | 1.2 ± 0.2 | 3 |
| | | *Oreoleuciscus potanini* | O | 23.0 ± 0.0 | 0.2 ± 0.0 | 1 |
| | M_T3_a | *Oreoleuciscus potanini* | O | 155.5 ± 75.7 | 441.5 ± 603.2 | 2 |
| | | *Thymallus brevirostris* | P | 205.2 ± 35.1 | 146.7 ± 15.3 | 3 |
| | M_T1_e | *Oreoleuciscus potanini* | O | 205.0 ± 0.0 | 110.0 ± 0.0 | 1 |
| | | *Thymallus brevirostris* | P | 120.0 ± 0.0 | 29.0 ± 0.0 | 1 |
| | M_T3_b | *Thymallus brevirostris* | P | 285.0 ± 42.4 | 350.5 ± 194.7 | 2 |
| | | *Barbatula barbatula* | I | 58.3 ± 5.7 | 1.8 ± 0.6 | 3 |
| | M_T3_c | *Oreoleuciscus potanini* | O | 145.0 ± 80.6 | 11.1 ± 0.2 | 2 |

| | | | | | | |
|---|---|---|---|---|---|---|
| | | *Barbatula barbatula* | I | 113.5 ± 6.4 | 5.6 ± 0.8 | 2 |
| | M_T1_f | *Thymallus brevirostris* | P | 55.3 ± 1.5 | 4.3 ± 1.5 | 3 |
| | | *Barbatula barbatula* | I | 45.0 ± 0.0 | 1.0 ± 0.0 | 1 |
| USGR | U_G7_a | *Semotilus atromaculatus* | O | 39.3 ± 2.1 | 1.1 ± 0.5 | 3 |
| | | *Rhinichthys cataractae* | I | 66.7 ± 0.6 | 4.5 ± 0.2 | 3 |
| | U_G7_b | *Salmo trutta* | I | 167.3 ± 13.3 | 77.3 ± 12.5 | 3 |
| | | *Catostomus commersonii* | O | 153.3 ± 122.3 | 148.1 ± 236.3 | 3 |
| | U_G6_a | *Esox lucius* | P | 256.5 ± 3.5 | 159.8 ± 20.1 | 2 |
| | | *Notropis stramineus* | O | 58.7 ± 1.2 | 2.3 ± 1.5 | 3 |
| | | *Moxostoma macrolepidotum* | I | 211.7 ± 7.6 | 157.9 ± 17.8 | 3 |
| | U_G7_c | *Salmo trutta* | P | 259.0 ± 30.0 | 243.0 ± 64.7 | 3 |
| | | *Lepomis cyanellus* | I | 59.3 ± 20.0 | 7.6 ± 7.4 | 3 |
| | | *Catostomus commersonii* | O | 146.7 ± 6.5 | 58.7 ± 10.5 | 3 |
| USMS | U_M2_a | *Salvelinus fontinalis* | I | 119.7 ± 28.0 | 22.8 ± 13.3 | 3 |
| | | *Oncorhynchus mykiss* | I | 212.7 ± 8.6 | 101.4 ± 5.6 | 3 |
| | U_M2_b | *Salmo trutta* | I | 171.0 ± 23.1 | 55.1 ± 22.6 | 3 |
| | | *Oncorhynchus mykiss* | I | 183.7 ± 16.4 | 69.9 ± 9.7 | 3 |
| | U_M2_c | *Salmo trutta* | I | 189.3 ± 1.2 | 64.5 ± 1.4 | 3 |
| | U_M2_d | *Salvelinus fontinalis* | I | 172.0 ± 6.6 | 57.7 ± 7.1 | 3 |
| | | *Oncorhynchus mykiss* | I | 201 ± 0.0 | 73.1 ± 0.0 | 1 |
| | U_M2_e | *Salvelinus fontinalis* | I | 174.3 ± 20.2 | 64.9 ± 24.4 | 3 |
| | | *Oncorhynchus mykiss* | I | 195.5 ± 7.8 | 73.8 ± 5.7 | 2 |
| | U_M6_a | *Salvelinus fontinalis* | I | 168.0 ± 1.7 | 50.5 ± 0.6 | 3 |
| | | *Oncorhynchus clarki bouvieri* | I | 191.0 ± 17.4 | 73.6 ± 22.8 | 3 |

| | | | | | | |
|---|---|---|---|---|---|---|
| | U_M2_f | *Oncorhynchus clarki bouvieri* | I | 276.5 ± 23.5 | 225.9 ± 79.2 | 3 |
| | U_M2_g | *Oncorhynchus clarki bouvieri* | I | 250.7 ± 17.9 | 163.6 ± 46.4 | 3 |
| | U_M2_h | *Salvelinus fontinalis* | P | 217.5 ± 4.9 | 126.0 ± 0.6 | 2 |
| | | *Oncorhynchus clarki bouvieri* | I | 135.7 ± 4.7 | 24.1 ± 1.7 | 3 |
| | U_M2_i | *Salvelinus fontinalis* | P | 223.0 ± 9.2 | 124.6 ± 9.6 | 3 |
| | | *Oncorhynchus mykiss* | I | 202.7 ± 3.2 | 73.8 ± 3.4 | 3 |
| | U_M6_b | *Salvelinus fontinalis* | P | 227.7 ± 13.6 | 115.6 ± 24.5 | 3 |
| | | *Salmo trutta* × *Salvelinus fontinalis* | P | 172.5 ± 4.9 | 48.6 ± 0.2 | 2 |
| | U_M6_c | *Salvelinus fontinalis* | P | 210.3 ± 6.8 | 88.1 ± 10.2 | 3 |
| | | *Salmo trutta* | P | 273.7 ± 7.5 | 190.1 ± 24.2 | 3 |
| | U_M2_j | *Salvelinus fontinalis* | I | 163.0 ± 22.9 | 44.1 ± 21.1 | 3 |
| | | *Salmo trutta* | I/P | 196.3 ± 4.0 | 75.9 ± 5.5 | 3 |
| | U_M2_k | *Salvelinus fontinalis* | I/P | 193.3 ± 21.5 | 80.2 ± 23.6 | 3 |
| | | *Salmo trutta* | P | 230.3 ± 1.2 | 126.3 ± 8.1 | 3 |
| | U_M2_l | *Salmo trutta* | P | 237.7 ± 7.6 | 128.2 ± 23.1 | 3 |
| USTB | U_T3_a | *Oncorhynchus clarki utah* | I | 233.0 ± 6.2 | 181.6 ± 5.4 | 3 |
| | | *Oncorhynchus mykiss* | I | 243.7 ± 21.8 | 291.6 ± 123.0 | 3 |
| | U_T4_a | *Cottus beldingii* | I | 76.7 ± 7.1 | 9.7 ± 1.5 | 3 |
| | | *Catostomus platyrhynchus* | I | 123 ± 0.0 | 28.3 ± 0.0 | 1 |
| | | *Oncorhynchus mykiss* | I | 275.7 ± 24.0 | 352.3 ± 111.5 | 3 |
| | U_T4_b | *Cottus beldingii* | I | 84.3 ± 7.1 | 11.2 ± 1.9 | 3 |
| | | *Salvelinus fontinalis* | I | 105.0 ± 7.2 | 17.9 ± 5.5 | 3 |
| | | *Oncorhynchus clarki utah* | I | 209.5 ± 0.7 | 132.8 ± 12.3 | 2 |
| | U_T3_b | *Cottus beldingii* | I | 92.0 ± 14.1 | 16.0 ± 4.3 | 2 |
| | | *Salvelinus fontinalis* | I | 136.7 ± 25.1 | 44.4 ± 25.1 | 3 |

| | | | | | |
|---|---|---|---|---|---|
| U_T5_a | *Salmo trutta* | I | 198.0 ± 38.6 | 133.5 ± 75.0 | 3 |
| | *Proposium williamsoni* | I | 319.0 ± 19.7 | 515.6 ± 39.5 | 3 |
| U_T4_c | *Oncorhynchus clarki utah* | I | 198.0 ± 40.8 | 133.7 ± 70.9 | 3 |
| | *Salvelinus fontinalis* | I | 171.0 ± 3.0 | 89.4 ± 6.1 | 3 |
| U_T5_b | *Salmo trutta* × *Salvelinus fontinalis* | P | 220.7 ± 25.1 | 199.7 ± 61.6 | 3 |
| | *Salvelinus fontinalis* | I | 148.7 ± 24.7 | 55.0 ± 30.4 | 3 |
| U_T5_c | *Salvelinus fontinalis* | I | 171.3 ± 13.7 | 88.7 ± 26.3 | 3 |
| | *Salmo trutta* × *Salvelinus fontinalis* | P | 290.7 ± 42.8 | 259.0 ± 130.2 | 3 |
| U_T2_a | *Oncorhynchus mykiss* | I | 113.3 ± 1.5 | 23.5 ± 4.2 | 3 |
| | *Salvelinus fontinalis* | I | 136.3 ± 15.9 | 42.7 ± 10.4 | 3 |
| U_T4_d | *Salvelinus fontinalis* | I | 150.3 ± 23.3 | 60.2 ± 27.6 | 3 |
| U_T5_d | *Salmo trutta* | I | 134.5 ± 2.1 | 36.9 ± 3.0 | 3 |
| | *Oncorhynchus mykiss* | I | 247.0 ± 0.0 | 240.9 ± 0.0 | 1 |
| U_T5_e | *Salmo trutta* | I | 132.0 ± 18.7 | 37.4 ± 15.2 | 3 |
| U_T4_e | *Salvelinus fontinalis* | I | 172.3 ± 22.7 | 92.9 ± 37.8 | 3 |
| U_T5_f | *Salmo trutta* | I | 124.0 ± 3.5 | 35.5 ± 1.0 | 3 |

**Supplemental Table C-5.** Mean ± SD carbon essential amino acid isotope values ($\delta^{13}C_{EAA}$) for fish consumers collected at 50 temperate steppe stream sites (*n*=271).

| Site | Species | n | Ile | Leu | Phe | Thr | Val |
|---|---|---|---|---|---|---|---|
| Mongolia Grassland | | | | | | | |
| M_G1_a | *Barbatula toni* | 3 | -28.9 ± 0.6 | -36.3 ± 0.2 | -35.5 ± 0.3 | -22.0 ± 0.5 | -33.1 ± 0.4 |
| | *Brachymystax lenok* | 2 | -26.0 ± 0.1 | -33.0 ± 0.4 | -30.8 ± 2.1 | -18.2 ± 1.3 | -28.3 ± 0.1 |
| | *Rhynchocypris lagowskii* | 2 | -29.8 ± 0.4 | -35.7 ± 1.3 | -35.7 ± 1.0 | -22.6 ± 0.7 | -33.0 ± 0.6 |
| M_G5_a | *Barbatula toni* | 3 | -29.2 ± 0.7 | -36.9 ± 0.6 | -36.3 ± 0.8 | -22.0 ± 0.9 | -32.9 ± 0.5 |
| | *Gobio gobio cynocephalus* | 3 | -27.8 ± 0.3 | -33.8 ± 0.5 | -33.2 ± 0.4 | -20.3 ± 0.6 | -31.1 ± 0.4 |
| | *Rhynchocypris lagowskii* | 3 | -28.1 ± 0.6 | -34.8 ± 0.8 | -34.6 ± 0.3 | -21.1 ± 0.6 | -32.0 ± 0.3 |
| M_G5_b | *Barbatula toni* | 3 | -29.7 ± 1.9 | -35.9 ± 1.6 | -35.3 ± 1.5 | -21.8 ± 1.6 | -32.9 ± 1.8 |
| | *Gobio gobio cynocephalus* | 1 | -28.7 ± 0.0 | -34.1 ± 0.0 | -32.8 ± 0.0 | -20.6 ± 0.0 | -31.1 ± 0.0 |
| | *Rhynchocypris lagowskii* | 3 | -29.1 ± 0.6 | -36.0 ± 0.2 | -35.5 ± 0.4 | -22.0 ± 0.6 | -32.8 ± 0.6 |
| M_G5_c | *Barbatula toni* | 3 | -27.5 ± 0.3 | -33.7 ± 0.3 | -32.1 ± 0.4 | -18.5 ± 0.3 | -30.5 ± 0.3 |
| | *Gobio gobio cynocephalus* | 1 | -25.5 ± 0.0 | -31.4 ± 0.0 | -30.3 ± 0.0 | -15.9 ± 0.0 | -28.1 ± 0.0 |
| | *Rhynchocypris lagowskii* | 3 | -28.2 ± 1.0 | -34.5 ± 1.1 | -33.0 ± 0.8 | -15.4 ± 1.9 | -30.9 ± 1.0 |
| M_G6_a | *Barbatula toni* | 3 | -31.7 ± 1.1 | -38.1 ± 1.3 | -36.4 ± 0.9 | -23.6 ± 0.3 | -34.7 ± 0.8 |
| | *Rhynchocypris lagowskii* | 3 | -28.2 ± 3.3 | -35.2 ± 3.8 | -33.1 ± 3.1 | -18.0 ± 3.0 | -31.5 ± 3.7 |
| | *Thymallus grubei* | 1 | -27.0 ± 0.0 | -34.4 ± 0.0 | -33.4 ± 0.0 | -18.0 ± 0.0 | -30.1 ± 0.0 |
| M_G6_b | *Barbatula toni* | 3 | -26.3 ± 0.3 | -33.0 ± 0.5 | -33.4 ± 0.4 | -19.3 ± 1.6 | -30.3 ± 0.8 |
| | *Lota lota* | 1 | -24.4 ± 0.0 | -32.3 ± 0.0 | -32.6 ± 0.0 | -19.1 ± 0.0 | -29.1 ± 0.0 |
| | *Rhynchocypris lagowskii* | 3 | -24.9 ± 0.5 | -31.8 ± 0.8 | -30.9 ± 1.3 | -16.0 ± 1.4 | -28.4 ± 0.6 |
| Mongolia Mountain Steppe | | | | | | | |
| M_M1_a | *Phoxinus phoxinus* | 3 | -26.9 ± 0.8 | -33.7 ± 0.8 | -32.6 ± 0.6 | -18.2 ± 1.3 | -29.5 ± 0.8 |
| | *Brachymystax lenok* | 3 | -29.5 ± 1.2 | -36.6 ± 1.2 | -36.1 ± 1.4 | -20.8 ± 1.2 | -32.1 ± 1.3 |
| M_M1_b | *Phoxinus phoxinus* | 3 | -28.7 ± 0.9 | -35.4 ± 0.6 | -34.6 ± 0.7 | -20.4 ± 1.0 | -31.5 ± 0.7 |

| | | | | | | | |
|---|---|---|---|---|---|---|---|
| | *Brachymystax lenok* | 3 | -30.2 ± 0.8 | -36.9 ± 1.2 | -36.6 ± 1.2 | -21.8 ± 0.7 | -32.5 ± 1.1 |
| M_M1_c | *Phoxinus phoxinus* | 3 | -27.8 ± 0.5 | -34.5 ± 0.5 | -33.4 ± 0.7 | -19.5 ± 0.8 | -30.9 ± 0.4 |
| | *Brachymystax lenok* | 3 | -27.8 ± 0.6 | -34.4 ± 0.6 | -33.0 ± 1.1 | -19.1 ± 0.4 | -30.2 ± 0.3 |
| M_M1_d | *Phoxinus phoxinus* | 3 | -27.8 ± 0.4 | -34.3 ± 0.2 | -32.0 ± 0.5 | -19.4 ± 0.3 | -30.4 ± 0.1 |
| | *Brachymystax lenok* | 3 | -28.0 ± 0.8 | -34.4 ± 0.5 | -33.9 ± 0.9 | -20.3 ± 0.4 | -30.7 ± 0.4 |
| Mongolia Semi-Arid Terminal Basin | | | | | | | |
| M_T1_b | *Barbatula golubtsovi* | 2 | -24.2 ± 0.6 | -31.9 ± 0.3 | -30.6 ± 1.0 | -17.4 ± 1.1 | -28.2 ± 0.8 |
| | *Thymallus brevirostris* | 3 | -23.4 ± 1.4 | -31.0 ± 1.6 | -29.9 ± 1.6 | -14.9 ± 1.6 | -26.5 ± 1.5 |
| M_T1_c | *Oreoleuciscus potanini* | 1 | -23.4 ± 0.0 | -30.3 ± 0.0 | -29.3 ± 0.0 | -16.5 ± 0.0 | -26.4 ± 0.0 |
| | *Barbatula barbatula* | 3 | -24.3 ± 0.4 | -31.0 ± 0.2 | -29.7 ± 0.7 | -16.8 ± 0.6 | -27.2 ± 0.5 |
| M_T1_e | *Oreoleuciscus potanini* | 1 | -28.8 ± 0.0 | -35.9 ± 0.0 | -34.6 ± 0.0 | -22.4 ± 0.0 | -32.1 ± 0.0 |
| | *Thymallus brevirostris* | 1 | -23.6 ± 0.0 | -30.5 ± 0.0 | -29.4 ± 0.0 | -15.7 ± 0.0 | -26.3 ± 0.0 |
| M_T1_f | *Thymallus brevirostris* | 3 | -23.6 ± 1.2 | -30.5 ± 1.3 | -29.8 ± 1.3 | -16.0 ± 1.5 | -26.3 ± 1.3 |
| | *Barbatula barbatula* | 1 | -22.0 ± 0.0 | -28.6 ± 0.0 | -27.9 ± 0.0 | -15.4 ± 0.0 | -25.4 ± 0.0 |
| M_T3_a | *Oreoleuciscus potanini* | 2 | -25.6 ± 2.6 | -33.2 ± 2.8 | -31.7 ± 2.8 | -17.6 ± 2.8 | -28.6 ± 2.5 |
| | *Thymallus brevirostris* | 3 | -26.1 ± 0.9 | -33.1 ± 0.6 | -31.4 ± 0.5 | -16.4 ± 0.9 | -28.5 ± 0.6 |
| M_T3_b | *Thymallus brevirostris* | 2 | -26.6 ± 0.2 | -33.8 ± 0.1 | -32.5 ± 0.1 | -17.6 ± 0.6 | -29.3 ± 0.3 |
| | *Barbatula barbatula* | 3 | -24.8 ± 0.2 | -31.7 ± 0.2 | -30.8 ± 0.7 | -17.1 ± 0.1 | -27.8 ± 0.5 |
| M_T3_c | *Oreoleuciscus potanini* | 2 | -26.0 ± 3.5 | -33.2 ± 3.3 | -32.6 ± 3.1 | -19.0 ± 3.4 | -29.8 ± 3.8 |
| | *Barbatula barbatula* | 2 | -24.8 ± 0.3 | -31.7 ± 0.7 | -30.5 ± 0.8 | -17.8 ± 1.1 | -28.0 ± 0.8 |
| United States Grassland | | | | | | | |
| U_G7_a | *Semotilus atromaculatus* | 3 | -25.1 ± 0.2 | -31.6 ± 0.1 | -29.4 ± 0.6 | -16.8 ± 0.8 | -27.7 ± 0.2 |
| | *Rhinichthys cataractae* | 3 | -24.7 ± 0.3 | -30.9 ± 0.3 | -29.9 ± 0.9 | -16.8 ± 0.5 | -27.7 ± 1.1 |
| U_G7_b | *Salmo trutta* | 3 | -25.6 ± 0.8 | -32.0 ± 0.5 | -29.8 ± 0.5 | -17.1 ± 0.4 | -27.7 ± 0.5 |

| | | | | | | | |
|---|---|---|---|---|---|---|---|
| | *Catostomus commersonii* | 3 | -25.8 ± 0.6 | -32.2 ± 0.8 | -31.6 ± 0.8 | -17.2 ± 0.7 | -29.1 ± 0.6 |
| U_G6_a | *Esox lucius* | 2 | -27.4 ± 1.2 | -33.1 ± 0.3 | -31.7 ± 1.0 | -19.4 ± 0.7 | -30.0 ± 1.0 |
| | *Notropis stramineus* | 3 | -26.4 ± 1.0 | -33.1 ± 1.4 | -31.4 ± 1.2 | -18.3 ± 1.0 | -29.3 ± 0.9 |
| | *Moxostoma macrolepidotum* | 3 | -26.7 ± 1.4 | -32.7 ± 1.3 | -32.0 ± 1.6 | -19.0 ± 1.4 | -29.6 ± 1.4 |
| U_G7_c | *Salmo trutta* | 3 | -24.8 ± 0.3 | -30.9 ± 0.6 | -29.7 ± 0.7 | -16.0 ± 0.3 | -26.9 ± 0.8 |
| | *Lepomis cyanellus* | 3 | -28.2 ± 0.3 | -33.3 ± 0.2 | -32.9 ± 0.1 | -19.4 ± 0.6 | -29.8 ± 0.1 |
| | *Catostomus commersonii* | 3 | -25.4 ± 0.4 | -32.2 ± 0.4 | -31.3 ± 0.5 | -17.1 ± 0.6 | -29.0 ± 0.6 |
| United States Mountain Steppe | | | | | | | |
| U_M2_a | *Salvelinus fontinalis* | 3 | -23.7 ± 1.7 | -29.7 ± 1.2 | -28.0 ± 0.9 | -14.0 ± 1.2 | -25.5 ± 1.4 |
| | *Oncorhynchus mykiss* | 3 | -22.7 ± 1.1 | -29.1 ± 0.5 | -28.8 ± 0.4 | -13.6 ± 1.5 | -25.2 ± 0.6 |
| U_M2_b | *Salmo trutta* | 3 | -23.5 ± 0.7 | -29.2 ± 0.5 | -27.7 ± 0.7 | -14.3 ± 1.1 | -25.2 ± 0.7 |
| | *Oncorhynchus mykiss* | 3 | -22.9 ± 1.0 | -28.6 ± 0.6 | -28.4 ± 0.8 | -13.4 ± 0.9 | -25.2 ± 0.6 |
| U_M2_c | *Salmo trutta* | 3 | -22.1 ± 0.6 | -27.5 ± 0.4 | -27.4 ± 0.4 | -12.3 ± 0.3 | -25.0 ± 0.4 |
| U_M2_d | *Salvelinus fontinalis* | 3 | -24.8 ± 0.6 | -30.4 ± 0.1 | -29.0 ± 0.5 | -15.2 ± 0.5 | -27.6 ± 1.2 |
| | *Oncorhynchus mykiss* | 1 | -23.0 ± 0.0 | -29.3 ± 0.0 | -28.1 ± 0.0 | -13.9 ± 0.0 | -26.4 ± 0.0 |
| U_M2_e | *Salvelinus fontinalis* | 3 | -27.7 ± 1.2 | -33.2 ± 1.0 | -31.6 ± 1.4 | -16.8 ± 1.1 | -29.8 ± 1.0 |
| | *Oncorhynchus mykiss* | 2 | -30.3 ± 0.7 | -35.2 ± 0.4 | -34.2 ± 0.5 | -19.0 ± 1.9 | -32.8 ± 0.2 |
| U_M6_a | *Salvelinus fontinalis* | 3 | -22.4 ± 0.8 | -28.7 ± 0.6 | -27.7 ± 0.3 | -13.9 ± 0.8 | -25.4 ± 1.4 |
| | *Oncorhynchus clarki bouvieri* | 3 | -23.2 ± 1.9 | -30.2 ± 1.2 | -28.8 ± 2.4 | -14.0 ± 2.3 | -25.5 ± 2.3 |
| U_M2_f | *Oncorhynchus clarki bouvieri* | 3 | -27.8 ± 0.4 | -36.2 ± 0.3 | -34.1 ± 0.6 | -19.1 ± 0.2 | -30.4 ± 0.4 |
| U_M2_g | *Oncorhynchus clarki bouvieri* | 3 | -22.4 ± 0.4 | -29.6 ± 0.4 | -27.1 ± 0.7 | -12.6 ± 0.3 | -25.5 ± 0.5 |
| U_M2_h | *Salvelinus fontinalis* | 2 | -28.0 ± 0.6 | -35.2 ± 0.8 | -34.5 ± 0.1 | -20.2 ± 0.9 | -31.2 ± 0.6 |
| | *Oncorhynchus clarki bouvieri* | 3 | -29.7 ± 0.6 | -37.6 ± 0.8 | -37.0 ± 1.2 | -22.0 ± 0.9 | -33.6 ± 0.8 |
| U_M2_i | *Salvelinus fontinalis* | 3 | -27.6 ± 1.9 | -33.4 ± 1.8 | -32.4 ± 1.1 | -18.0 ± 0.7 | -30.2 ± 2.0 |
| | *Oncorhynchus mykiss* | 3 | -23.8 ± 0.2 | -30.0 ± 0.2 | -29.1 ± 0.3 | -13.7 ± 0.6 | -25.8 ± 0.3 |

| | | | | | | | |
|---|---|---|---|---|---|---|---|
| U_M6_b | *Salvelinus fontinalis* | 3 | -25.2 ± 1.7 | -32.1 ± 2.0 | -31.1 ± 2.8 | -17.4 ± 3.5 | -28.2 ± 2.2 |
| | *Salmo trutta* × *Salvelinus fontinalis* | 2 | -22.2 ± 0.1 | -28.7 ± 0.7 | -28.0 ± 0.4 | -14.0 ± 0.5 | -24.8 ± 0.4 |
| U_M6_c | *Salvelinus fontinalis* | 3 | -21.9 ± 0.8 | -28.9 ± 0.2 | -28.2 ± 1.2 | -13.6 ± 0.6 | -24.5 ± 1.6 |
| | *Salmo trutta* | 3 | -22.1 ± 0.7 | -28.6 ± 0.4 | -27.6 ± 1.0 | -14.0 ± 0.6 | -24.0 ± 0.6 |
| U_M2_j | *Salvelinus fontinalis* | 3 | -27.1 ± 0.6 | -33.5 ± 0.6 | -32.5 ± 0.6 | -18.4 ± 0.6 | -29.7 ± 0.7 |
| | *Salmo trutta* | 3 | -26.7 ± 0.9 | -33.3 ± 0.7 | -32.2 ± 0.8 | -17.2 ± 0.9 | -28.8 ± 1.3 |
| U_M2_k | *Salvelinus fontinalis* | 3 | -27.7 ± 1.0 | -34.6 ± 0.5 | -33.3 ± 0.6 | -18.7 ± 0.7 | -29.8 ± 1.2 |
| | *Salmo trutta* | 3 | -28.0 ± 0.1 | -34.8 ± 0.2 | -33.5 ± 0.2 | -19.4 ± 0.4 | -30.1 ± 0.4 |
| U_M2_l | *Salmo trutta* | 3 | -26.3 ± 0.4 | -33.3 ± 0.6 | -33.4 ± 0.7 | -16.9 ± 0.7 | -29.1 ± 0.7 |
| United States Semi-Arid Terminal Basin | | | | | | | |
| U_T3_a | *Oncorhynchus clarki utah* | 3 | -30.6 ± 1.0 | -37.8 ± 0.8 | -37.7 ± 1.2 | -20.7 ± 1.2 | -33.3 ± 0.9 |
| | *Oncorhynchus mykiss* | 3 | -25.6 ± 2.1 | -33.3 ± 2.0 | -32.0 ± 2.4 | -16.3 ± 3.0 | -29.0 ± 2.3 |
| U_T4_a | *Cottus beldingii* | 3 | -24.5 ± 0.4 | -32.2 ± 0.5 | -31.8 ± 0.6 | -17.1 ± 0.5 | -27.6 ± 0.5 |
| | *Catostomus platyrhynchus* | 1 | -25.0 ± 0.0 | -33.2 ± 0.0 | -32.7 ± 0.0 | -18.5 ± 0.0 | -29.5 ± 0.0 |
| | *Oncorhynchus mykiss* | 3 | -21.0 ± 0.4 | -28.1 ± 0.3 | -26.3 ± 0.4 | -13.0 ± 0.3 | -24.7 ± 0.8 |
| U_T4_b | *Cottus beldingii* | 3 | -26.3 ± 0.3 | -33.3 ± 1.0 | -32.6 ± 0.4 | -18.4 ± 0.3 | -28.9 ± 0.6 |
| | *Salvelinus fontinalis* | 3 | -26.6 ± 0.6 | -34.0 ± 0.3 | -33.4 ± 0.7 | -18.8 ± 1.1 | -29.7 ± 0.3 |
| | *Oncorhynchus clarki utah* | 2 | -25.0 ± 1.6 | -32.1 ± 1.1 | -31.6 ± 0.6 | -17.8 ± 0.2 | -28.5 ± 0.8 |
| U_T3_b | *Cottus beldingii* | 2 | -30.8 ± 1.3 | -37.0 ± 2.3 | -35.8 ± 1.9 | -22.4 ± 0.9 | -33.0 ± 1.8 |
| | *Salvelinus fontinalis* | 3 | -27.0 ± 0.9 | -34.0 ± 0.6 | -33.1 ± 0.8 | -19.9 ± 0.8 | -29.6 ± 0.5 |
| U_T5_a | *Salmo trutta* | 3 | -27.4 ± 2.0 | -34.5 ± 1.5 | -33.5 ± 1.1 | -19.3 ± 1.1 | -29.7 ± 1.7 |
| | *Proposium williamsoni* | 3 | -29.1 ± 0.8 | -36.1 ± 0.8 | -34.8 ± 0.8 | -21.2 ± 0.2 | -31.4 ± 0.7 |
| U_T4_c | *Oncorhynchus clarki utah* | 3 | -28.8 ± 0.4 | -36.4 ± 0.4 | -34.3 ± 0.5 | -21.9 ± 0.7 | -31.4 ± 0.6 |
| | *Salvelinus fontinalis* | 3 | -28.4 ± 0.8 | -36.4 ± 1.4 | -33.9 ± 1.2 | -19.7 ± 2.0 | -31.2 ± 1.0 |
| U_T5_b | *Salmo trutta* × *Salvelinus fontinalis* | 3 | -21.8 ± 0.6 | -29.2 ± 0.1 | -26.4 ± 0.3 | -12.0 ± 0.3 | -25.1 ± 0.5 |
| | *Salvelinus fontinalis* | 3 | -26.1 ± 0.4 | -33.8 ± 0.5 | -32.1 ± 0.5 | -18.8 ± 1.1 | -28.4 ± 0.8 |
| U_T5_c | *Salvelinus fontinalis* | 3 | -26.2 ± 0.4 | -34.0 ± 0.6 | -31.8 ± 1.1 | -18.9 ± 0.9 | -28.3 ± 0.6 |

| | | | | | | | |
|---|---|---|---|---|---|---|---|
| | *Salmo trutta* × *Salvelinus fontinalis* | 3 | -21.7 ± 0.4 | -28.9 ± 0.5 | -26.6 ± 0.7 | -12.4 ± 0.7 | -24.5 ± 0.3 |
| U_T2_a | *Oncorhynchus mykiss* | 3 | -27.0 ± 0.5 | -34.1 ± 0.5 | -32.6 ± 1.0 | -18.9 ± 1.2 | -29.8 ± 0.4 |
| | *Salvelinus fontinalis* | 3 | -25.3 ± 0.3 | -32.3 ± 0.8 | -31.2 ± 0.6 | -18.2 ± 0.5 | -28.0 ± 0.4 |
| U_T4_d | *Salvelinus fontinalis* | 3 | -27.0 ± 0.2 | -34.1 ± 0.8 | -32.9 ± 0.3 | -19.9 ± 0.8 | -29.5 ± 0.1 |
| U_T5_d | *Salmo trutta* | 3 | -25.1 ± 0.5 | -32.3 ± 0.3 | -30.6 ± 0.7 | -18.5 ± 0.6 | -26.8 ± 0.4 |
| | *Oncorhynchus mykiss* | 1 | -21.1 ± 0.0 | -28.9 ± 0.0 | -27.8 ± 0.0 | -13.8 ± 0.0 | -24.1 ± 0.0 |
| U_T5_e | *Salmo trutta* | 3 | -25.3 ± 0.2 | -31.8 ± 0.4 | -30.6 ± 0.6 | -16.9 ± 0.6 | -27.6 ± 0.4 |
| U_T4_e | *Salvelinus fontinalis* | 3 | -28.8 ± 0.7 | -35.6 ± 0.7 | -34.3 ± 0.7 | -22.0 ± 0.5 | -31.0 ± 0.6 |
| U_T5_f | *Salmo trutta* | 3 | -25.6 ± 1.3 | -31.8 ± 0.9 | -30.8 ± 0.9 | -17.3 ± 1.4 | -27.7 ± 1.1 |

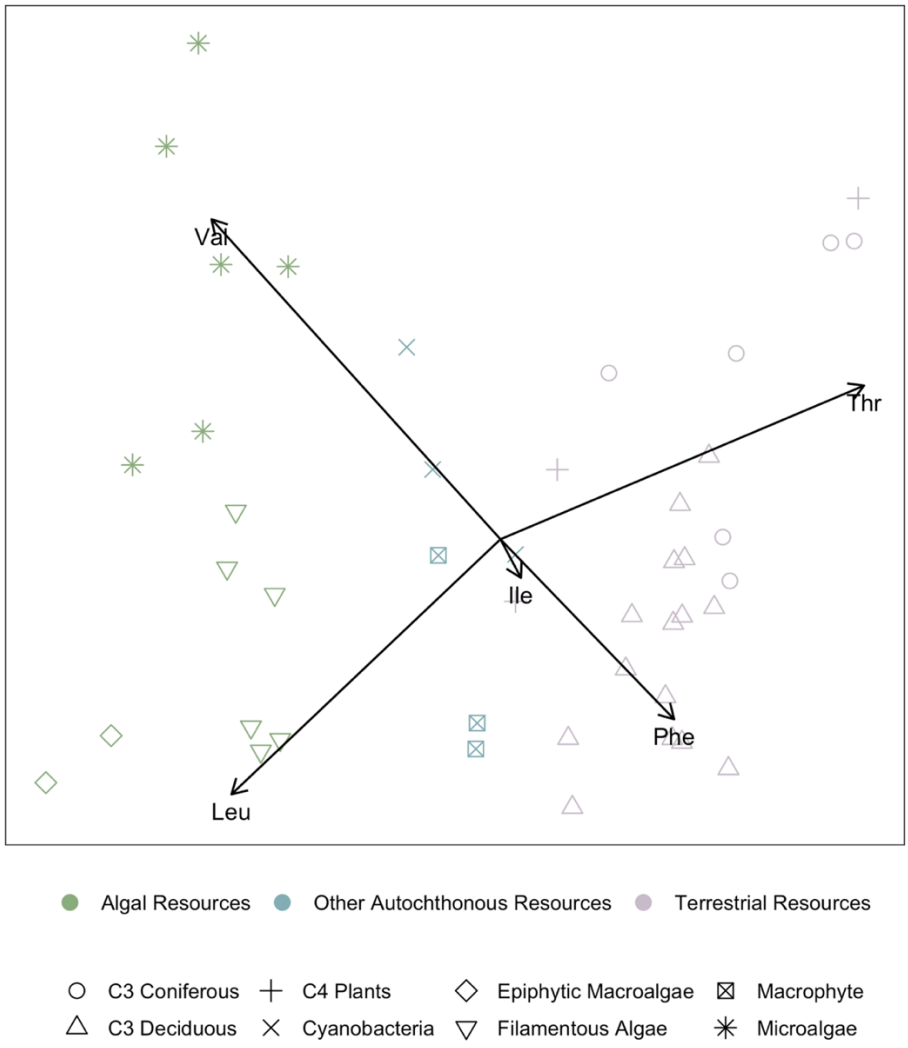


**Supplemental Figure C-1.** Principal component analysis (PCA) showing the distribution of food source samples used as tracers of basal resources in this study. This PCA was plotted based on essential amino acid isotope signatures of carbon ($\delta^{13}C_{EAA}$) from the amino acids isoleucine (Ile), leucine (Leu), phenylalanine (Phe), threonine (Thr), and valine (Val). Food sources were categorized into different functional groups by color, with algal resources in green, other autochthonous resources (cyanobacteria and macrophytes) in blue, and $C_3$ and $C_4$ terrestrial plants in orange ($n$=44). PCA visualization suggested good separation of food source groupings, with 68.5% of variance explained by PC1 and 13.43% of variance explained by PC2.

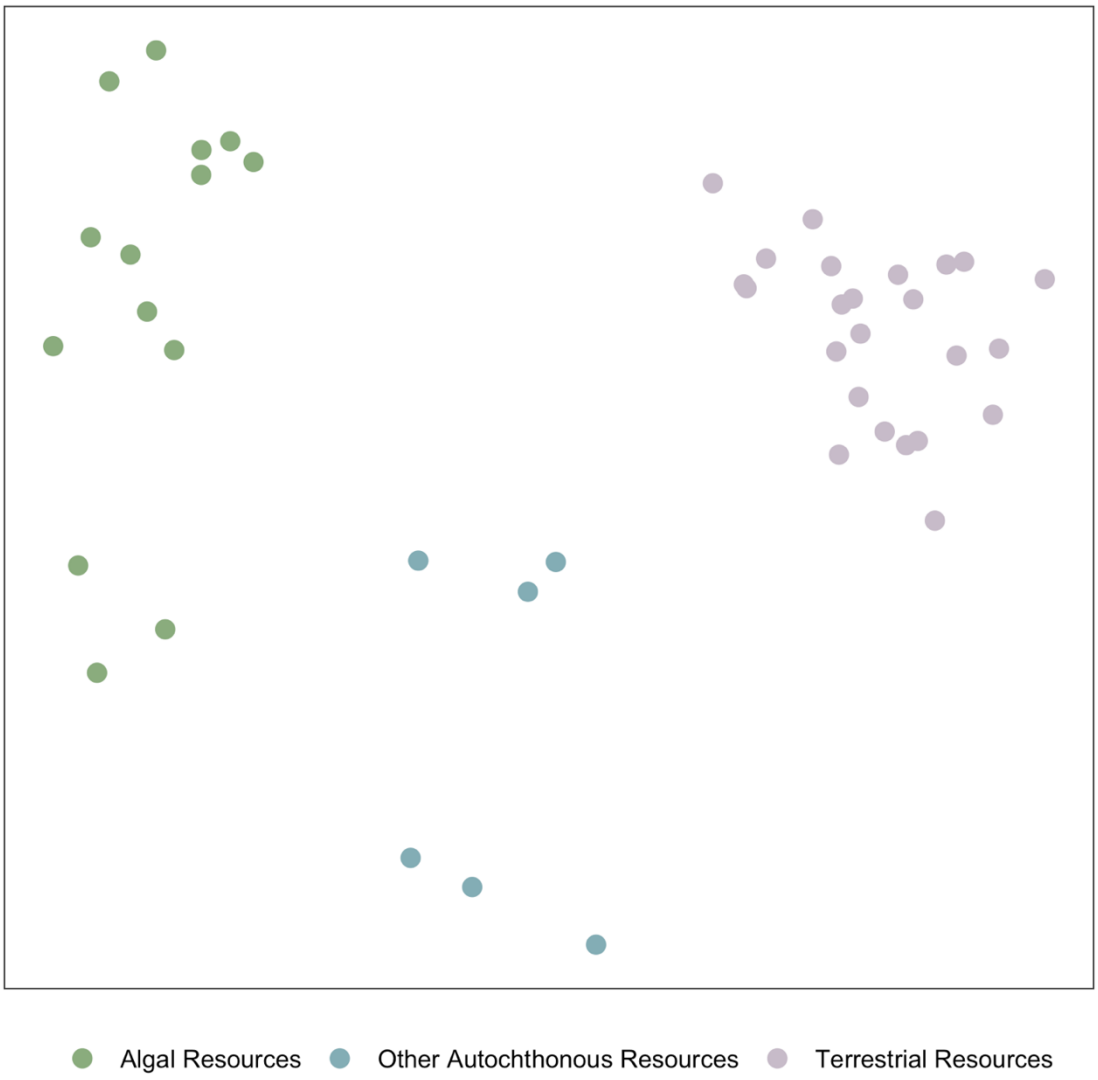


**Supplemental Figure C-2.** A linear discriminant analysis was able to correctly classify food sources into their respective groups (Algal Resources, Other Autochthonous Resources, or Terrestrial Resources) with 100% accuracy using leave-one-out cross validation. LD1 and LD2 explained 94.82% and 5.18% of the variance between groups, respectively. Based on the absolute values of the LD1 loadings, variation between food source groups was best explained by Phe (1.09), followed by Leu (-0.77), Val (-0.59), and Thr (0.26), with Ile being the amino acid that explained the least variation between food source groups (0.17).

**Supplemental Table C-6.** Sørensen overlap values for study sites located in the Mongolia grassland ecoregion. Underlined values represent pairwise overlaps indicating greater than 75% similarity between sites.

| | M_G1_a | M_G5_a | M_G5_b | M_G5_c | M_G6_a | M_G6_b |
|---|---|---|---|---|---|---|
| M_G1_a | – | | | | | |
| M_G5_a | 0.914 | – | | | | |
| M_G5_b | 0.828 | 0.813 | – | | | |
| M_G5_c | 0.033 | 0.030 | 0.043 | – | | |
| M_G6_a | 0.045 | 0.042 | 0.058 | 0.585 | – | |
| M_G6_b | 0.270 | 0.250 | 0.337 | 0.191 | 0.253 | – |

**Supplemental Table C-7.** Sørensen overlap values for study sites located in the Mongolia mountain steppe ecoregion. Underlined values represent pairwise overlaps indicating greater than 75% similarity between sites.

| | M_M1_a | M_M1_b | M_M1_c | M_M1_d |
|---|---|---|---|---|
| M_M1_a | – | | | |
| M_M1_b | 0.694 | – | | |
| M_M1_c | 0.928 | 0.668 | – | |
| M_M1_d | 0.914 | 0.736 | 0.893 | – |

**Supplemental Table C-8.** Sørensen overlap values for study sites located in the Mongolia semi-arid terminal basin ecoregion. Underlined values represent pairwise overlaps indicating greater than 75% similarity between sites.

| | M_T1_b | M_T1_c | M_T1_e | M_T1_f | M_T3_a | M_T3_b | M_T3_c |
|---|---|---|---|---|---|---|---|
| M_T1_b | – | | | | | | |
| M_T1_c | 0.722 | – | | | | | |
| M_T1_e | 0.631 | 0.880 | – | | | | |
| M_T1_f | 0.427 | 0.638 | 0.724 | – | | | |
| M_T3_a | 0.873 | 0.816 | 0.719 | 0.498 | – | | |
| M_T3_b | 0.684 | 0.919 | 0.912 | 0.676 | 0.777 | – | |
| M_T3_c | 0.845 | 0.846 | 0.753 | 0.524 | 0.928 | 0.802 | – |

**Supplemental Table C-9.** Sørensen overlap values for study sites located in the United States grassland ecoregion. Underlined values represent pairwise overlaps indicating greater than 75% similarity between sites.

| | U_G6_a | U_G7_a | U_G7_b | U_G7_c |
|---|---|---|---|---|
| U_G6_a | – | | | |
| U_G7_a | 0.734 | – | | |
| U_G7_b | 0.757 | 0.939 | – | |
| U_G7_c | 0.913 | 0.799 | 0.819 | – |

**Supplemental Table C-10.** Sørensen overlap values for study sites located in the United States mountain steppe ecoregion. Underlined values represent pairwise overlaps indicating greater than 75% similarity between sites.

| | U_M2_a | U_M2_b | U_M2_c | U_M2_d | U_M2_e | U_M2_f | U_M2_g | U_M2_h | U_M2_i | U_M2_j | U_M2_k | U_M2_l | U_M6_a | U_M6_b | U_M6_c |
|---|---|---|---|---|---|---|---|---|---|---|---|---|---|---|---|
| U_M2_a | – | | | | | | | | | | | | | | |
| U_M2_b | 0.766 | – | | | | | | | | | | | | | |
| U_M2_c | 0.933 | 0.780 | – | | | | | | | | | | | | |
| U_M2_d | 0.631 | 0.465 | 0.621 | – | | | | | | | | | | | |
| U_M2_e | 0.451 | 0.323 | 0.443 | 0.749 | – | | | | | | | | | | |
| U_M2_f | 0.450 | 0.615 | 0.462 | 0.245 | 0.159 | – | | | | | | | | | |
| U_M2_g | 0.482 | 0.341 | 0.468 | 0.792 | 0.749 | 0.174 | – | | | | | | | | |
| U_M2_h | 0.427 | 0.588 | 0.439 | 0.228 | 0.152 | 0.920 | 0.162 | – | | | | | | | |
| U_M2_i | 0.683 | 0.505 | 0.666 | 0.867 | 0.687 | 0.271 | 0.715 | 0.255 | – | | | | | | |
| U_M2_j | 0.747 | 0.931 | 0.758 | 0.449 | 0.303 | 0.636 | 0.330 | 0.606 | 0.490 | – | | | | | |

| | U_M2_k | U_M2_l | U_M6_a | U_M6_b | U_M6_c |
|---|---|---|---|---|---|
| U_M2_k | – | | | | |
| U_M2_l | 0.758 | – | | | |
| U_M6_a | 0.856 | 0.649 | – | | |
| U_M6_b | 0.756 | 0.559 | 0.862 | – | |
| U_M6_c | 0.707 | 0.885 | 0.606 | 0.519 | – |
| U_M1_a | 0.555 | 0.707 | 0.885 | 0.606 | 0.519 |
| U_M1_b | 0.229 | 0.555 | 0.707 | 0.885 | 0.606 |
| U_M1_c | 0.909 | 0.229 | 0.555 | 0.707 | 0.885 |
| U_M5_a | 0.146 | 0.909 | 0.229 | 0.555 | 0.707 |
| U_M5_b | 0.868 | 0.146 | 0.909 | 0.229 | 0.555 |
| U_M5_c | 0.598 | 0.356 | 0.570 | 0.526 | 0.914 |
| U_M4_a | 0.689 | 0.297 | 0.657 | 0.442 | 0.904 |
| U_M4_b | 0.914 | 0.162 | 0.936 | 0.251 | 0.597 |
| U_M4_c | 0.149 | 0.227 | 0.407 | 0.277 | 0.225 |
| U_M3_a | 0.225 | 0.336 | 0.602 | 0.484 | 0.333 |
| U_M3_b | 0.789 | 0.241 | 0.763 | 0.369 | 0.801 |
| U_M3_c | 0.135 | 0.208 | 0.399 | 0.208 | 0.135 |

**Supplemental Table C-11.** Sørensen overlap values for study sites located in the United States semi-arid terminal basin ecoregion. Underlined values represent pairwise overlaps indicating greater than 75% similarity between sites.

| | U_T2_a | U_T3_a | U_T3_b | U_T4_a | U_T4_b | U_T4_c | U_T4_d | U_T4_e | U_T5_a | U_T5_b | U_T5_c | U_T5_d | U_T5_e | U_T5_f |
|---|---|---|---|---|---|---|---|---|---|---|---|---|---|---|
| U_T2_a | – | | | | | | | | | | | | | |
| U_T3_a | 0.666 | – | | | | | | | | | | | | |
| U_T3_b | 0.559 | 0.335 | – | | | | | | | | | | | |
| U_T4_a | 0.674 | 0.837 | 0.335 | – | | | | | | | | | | |
| U_T4_b | 0.588 | 0.359 | 0.879 | 0.357 | – | | | | | | | | | |
| U_T4_c | 0.602 | 0.854 | 0.292 | 0.884 | 0.313 | – | | | | | | | | |
| U_T4_d | 0.380 | 0.217 | 0.732 | 0.216 | 0.705 | 0.187 | – | | | | | | | |
| U_T4_e | 0.284 | 0.158 | 0.590 | 0.158 | 0.558 | 0.137 | 0.806 | – | | | | | | |
| U_T5_a | 0.591 | 0.359 | 0.925 | 0.359 | 0.903 | 0.312 | 0.703 | 0.558 | – | | | | | |
| U_T5_b | 0.202 | 0.350 | 0.085 | 0.356 | 0.092 | 0.404 | 0.052 | 0.037 | 0.093 | – | | | | |
| U_T5_c | 0.316 | 0.503 | 0.138 | 0.528 | 0.148 | 0.588 | 0.086 | 0.062 | 0.149 | 0.733 | – | | | |

| | | | | | | | | | | | | | | |
|---|---|---|---|---|---|---|---|---|---|---|---|---|---|---|
| U_T5_d | 0.625 | 0.735 | 0.307 | 0.882 | 0.329 | 0.841 | 0.197 | 0.144 | 0.328 | 0.388 | 0.571 | – | | |
| U_T5_e | 0.873 | 0.588 | 0.637 | 0.586 | 0.636 | 0.521 | 0.441 | 0.336 | 0.668 | 0.170 | 0.266 | 0.546 | – | |
| U_T5_f | 0.557 | 0.335 | 0.922 | 0.332 | 0.855 | 0.291 | 0.731 | 0.590 | 0.909 | 0.085 | 0.138 | 0.305 | 0.637 | – |